Institut für Bodenlandschaftsforschung,

Leibniz-Zentrum für Agrarlandschaftsforschung (ZALF) e.V., Müncheberg

Wind driven soil particle uptake Quantifying drivers of wind erosion across the particle size spectrum

Dissertation

zur Erlangung des akademischen Grades

"doctor rerum naturalium" (Dr. rer. nat.)

in der Wissenschaftsdisziplin "Geoökologie"

eingereicht an der Mathematisch-Naturwissenschaftlichen Fakultät der Universität Potsdam

von Nicole Siegmund

Datum der Disputation
7. Dezember 2022

Betreuer
Prof. Dr. Michael Sommer
Dr. Roger Funk
Prof. Dr. Daniel Buschiazzo

Gutachter/Gutachterinnen
Prof. Dr. Michael Sommer
Dr. Roger Funk
Prof. Dr. Kerstin Schepanski

Published online on the
Publication Server of the University of Potsdam:
https://doi.org/10.25932/publishup-57489
https://nbn-resolving.org/urn:nbn:de:kobv:517-opus4-574897

Abstract - English

Among the multitude of geomorphological processes, aeolian shaping processes are of special character, Pedogenic dust is one of the most important sources of atmospheric aerosols and therefore regarded as a key player for atmospheric processes. Soil dust emissions, being complex in composition and properties, influence atmospheric processes and air quality and has impacts on other ecosystems. In this because even though their immediate impact can be considered low (exceptions exist), their constant and large-scale force makes them a powerful player in the earth system. dissertation, we unravel a novel scientific understanding of this complex system based on a holistic dataset acquired during a series of field experiments on arable land in La Pampa, Argentina. The field experiments as well as the generated data provide information about topography, various soil parameters, the atmospheric dynamics in the very lower atmosphere (4m height) as well as measurements regarding aeolian particle movement across a wide range of particle size classes between 0.2 m up to the coarse sand.

The investigations focus on three topics: (a) the effects of low-scale landscape structures on aeolian transport processes of the coarse particle fraction, (b) the horizontal and vertical fluxes of the very fine particles and (c) the impact of wind gusts on particle emissions.

Among other considerations presented in this thesis, it could in particular be shown, that even though the small-scale topology does have a clear impact on erosion and deposition patterns, also physical soil parameters need to be taken into account for a robust statistical modelling of the latter. Furthermore, specifically the vertical fluxes of particulate matter have different characteristics for the particle size classes. Finally, a novel statistical measure was introduced to quantify the impact of wind gusts on the particle uptake and its application on the provided data set. The aforementioned measure shows significantly increased particle concentrations during points in time defined as gust event.

With its holistic approach, this thesis further contributes to the fundamental understanding of how atmosphere and pedosphere are intertwined and affect each other.

Abstract – Spanish

La erosión eólica es un factor geológico, morfogenético natural dentro de la evolución del paisaje, pero en determinadas regiones del planeta los procesos de denudación (perdida) superan los de formación y el suelo empieza a sufrir un deterioro progresivo. La magnitud de la erosión eólica puede incrementarse drásticamente debido a la acción antrópica, transformándose en un proceso de degradación irreversible del suelo. La erosión eólica de suelos de regiones áridas y semiáridas es una de las mayores fuentes de aerosoles atmosféricos y, por lo tanto, se considera un factor clave en los procesos de la atmósfera. Las emisiones de polvo del suelo, al ser complejas en composición y propiedades, influyen en los procesos atmosféricos, en la calidad del aire y, además, puede afectar la dinámica de nutrientes y ciclos biogeoquímicos de ecosistemas terrestres y marítimos. Con el fin de contribuir a la comprensión científica de este complejo proceso, esta tesis documenta publicaciones basadas en datos obtenidos durante una serie de experimentos de campo en suelos agrícolas de la provincia de La Pampa, Argentina.

Las mediciones a campo, así como los datos generados con modelos, brindan información sobre la topografía, varios parámetros del suelo, la dinámica atmosférica en la parte baja de la troposfera (4 m de altura), y, además, mediciones sobre el movimiento de partículas erosionadas en un amplio rango de tamaños (0,002mm hasta 2mm). Las investigaciones se centran en tres temas: los efectos de las estructuras paisajísticas de baja escala en los procesos de transporte eólico de la fracción de partículas gruesas, los flujos horizontales y verticales de las partículas muy finas y el impacto de las ráfagas de viento en las emisiones de partículas.

Otras consideraciones, en base a los datos de esta tesis, permiten demostrar que, si bien la topología a pequeña escala tiene un claro impacto en los patrones de erosión y deposición de material, también se debe tener en cuenta los parámetros físicos del suelo para un modelado estadístico robusto del proceso. Además, de que los flujos verticales de material particulado tienen diferentes características según el tamaño de partículas.

Finalmente, se obtuvo una medida estadística novedosa para cuantificar el impacto de las ráfagas de viento en la absorción de partículas y su aplicación en el conjunto de datos, proporcionando muestras de concentraciones de partículas significativamente mayores durante los puntos en el tiempo definidos como eventos de ráfagas. Con un enfoque integral, esta tesis

contribuye a la comprensión de cómo la atmósfera y la pedosfera se entrelazan y se afectan mutuamente.

Abstract – German

Unter der Vielzahl geomorphologischer Prozesse nehmen äolische Formgebungsprozesse eine besondere Stellung ein, denn obwohl ihre unmittelbaren Auswirkungen als gering einzuschätzen sind (Ausnahmen existieren), sind sie aufgrund ihrer konstanten und großen Kraft ein mächtiger Akteur im Erdsystem. Pedogener Staub ist eine der wichtigsten Quellen atmosphärischer Aerosole und kann daher als Schlüsselfaktor für atmosphärische Prozesse angesehen werden.

Bodenstaubemissionen, die in Zusammensetzung und Eigenschaften komplex sind, beeinflussen atmosphärische Prozesse und Luftqualität und haben Auswirkungen auf andere Ökosysteme. Um zum wissenschaftlichen Verständnis dieses komplexen Systems beizutragen, dokumentiert diese Arbeit eine Reihe von Veröffentlichungen, die alle auf einem ganzheitlichen Datensatz basieren, die während einer Reihe von Feldexperimenten auf Ackerland in La Pampa, Argentinien, gewonnen wurden. Die Feldexperimente sowie die generierten Daten liefern Informationen über Topographie, verschiedene Bodenparameter, die atmosphärische Dynamik in der unteren Atmosphäre (4 m Höhe) sowie Messungen zur äolischen Partikelbewegung über einen weiten Bereich von Partikelgrößenklassen zwischen 0,2µm und groben Sand.

Die Untersuchungen konzentrieren sich auf drei Themen: Die Auswirkungen kleinräumiger Landschaftsstrukturen auf äolische Transportprozesse der groben Partikelfraktion, die horizontalen und vertikalen Strömungen der sehr feinen Partikel und der Einfluss von Windböen auf die Partikelemissionen.

Neben anderen in dieser Arbeit vorgestellten Überlegungen konnte insbesondere gezeigt werden, dass, obwohl die kleinräumige Topologie einen deutlichen Einfluss auf Erosions- und Ablagerungsmuster hat, auch physikalische Bodenparameter für eine robuste statistische Modellierung berücksichtigt werden müssen. Darüber hinaus weisen speziell die vertikalen Feinstaubflüsse unterschiedliche Eigenschaften für die Partikelgrößenklassen auf. Schließlich wurde ein neuartiges statistisches Maß eingeführt, um den Einfluss von Windböen auf die Partikelkonzentration der Luft zu quantifizieren, und seine Anwendung auf den bereitgestellten Datensatz zeigt signifikant erhöhte Partikelkonzentrationen zu Zeitpunkten, die als Böen definiert wurden. Mit ihrem ganzheitlichen Ansatz trägt diese Arbeit weiter zum grundlegenden Verständnis bei, wie Atmosphäre und Pedosphäre miteinander verflochten sind und sich gegenseitig beeinflussen.

Acknowledgement

I would like to thank the following for their support during my work on this manuscript:
First, and foremost, my supervisor Dr. Roger Funk for the patient cooperation in all publications and for always having an open ear for all sorts of technical and methodological questions. I thank Prof. Dr. Michael Sommer for the scientific supervision of this thesis. I would also like to thank my Argentinean colleagues for the many stimulating discussions, pragmatic support in the field work and their exceptional hospitality with Mate and Asado.
Finally, I thank my husband Jonatan, my tireless source of motivation in all the ups and downs of scientific life.

Abbreviations

MWAC: Modified Wilson and Cooke Sampler

INTA: Instituto Nacional de Tecnología Agropecuaria

USDA: United States Department of Agriculture

GuE: Gust uptake Efficiency

Table of Content

Abstract - English iii
Abstract – Spanish iv
Abstract – German vi
Acknowledgement vii
Abbreviations viii
1. Introduction 1
1.1 Wind particle uptake 1
1.2 Study Area, Experimental Setup, Data Processing and Analytics 3
1.3 Research questions 4
1.4 Contributing publications 5
2. Publications 7
2.1 Effects of low-scale landscape structures on aeolian transport processes on arable land 7
2.2 Horizontal and vertical fluxes of particulate matter during wind erosion on arable land in the province La Pampa, Argentina 19
2.3 From Gustiness to Dustiness - The Impact of Wind Gusts on Particulate Matter Emissions in Field Experiments in La Pampa, Argentina 34
3. Discussion 49
4. Summary 54
5. Bibliography 55

1. Introduction

1.1 Wind particle uptake

Erosion built the surface of our earth - and is still doing so. A multitude of biological, geomorphological, and atmospheric processes continuously scratch, wipe, blow, wash, break, burst, freeze, and grind the upper layer of the earth's crust. As much as these shaping processes have implications on literally all other biogeological systems, also all human societies are fundamentally bound and based on a specific product, which is a result of a complex and dynamic combination of geo-ecological transformation processes: soil.

While water and ice both have a very high immediate shaping force, aeolian processes generally generate a lower immediate force, yet can still largely contribute to landscape transformation processes due to their enduring character. Areas with dominating aeolian processes are mostly in arid and semi-arid zones with a continuous or temporal absence of water and a lack of vegetation cover (Bubenzer 2007).

Next to the immediate local consequences of erosion and deposition processes, pedogenic dust has gained rising scientific interest during the last decade, being one of the most important sources of atmospheric aerosols and therefore regarded as a key player for atmospheric processes (Knippertz & Stuut 2014; Shao 2001). Soil dust emissions influence physical and chemical processes in the atmosphere, influence air quality and can have both positive and negative impacts on other ecosystems (Aimar et al. 2012). Main source areas of mineral dust are large deserts, but also agriculturally used land is of increasing importance with respect to quantities and qualities of emitted dust (Conen & Leifeld 2014; Steinke et al. 2020). Dust from agricultural land is complex in composition and properties because it can contain mineral and organic soil components, nutrients from fertilizers, agents of pesticides, as well as microbes and micro plastic from sludge or wastewater treatments (Acosta-Martínez et al. 2015; Mendez et al. 2017; Rezaei et al. 2019).

Next to this aeolian transport of the very fine particle section of soils (dust) also wind induced particle relocation of coarser particles is an important factor for shaping landscapes as well as influencing soils physical and chemical characteristics. These processes, largely associated with "creeping" and "saltation", are not separate from dust emissions, but rather closely entwined with the generation and uptake of the smaller particle fraction (Mirzamostafa et al. 1998; Shao 2000).

In addition to these already very complex interactions, moving air as the driver of wind erosion is characterized by a large degree of unsteadiness. Induced by the roughness of the land surface, wind in the lowest atmospheric layer is often gusty. There wind velocity fluctuations can be considered to result in temporal variations of the transport intensities as well.

Having in mind the multitude of factors influencing the wind soil erosion and deposition processes, this system can clearly be characterized as a multiscale or multidimension complex. In order to cope with such a system, scientific publications often follow the approach to fix as many of these factors as possible and only vary one of them systematically. In this way, it's possible to characterize the impact of the one scale on the others. Such an approach is, for example, used when conducting wind tunnel experiments, where a given soil sample is exposed to varying wind velocities (see e.g., Panebianco 2016 and may others). Furthermore, field experiments often focus on one specific process like saltation *or* emission, generating data sets and related analytics with a clear focus to describe this one process comprehensively (e.g., Li 2015 and many others).

In contrast to such a scale-selective approach, this thesis documents a sequence of publications all based on data acquired during a series of field experiments approaching the aeolian soil processes with a more holistic setting. The experiments and measurements specifically covered

(i) a high-resolution topographic model of the experimental area,

(ii) a wide range of physical and chemical soil characteristics,

(iii) measurements regarding aeolian particle movement across a large section of the particle size scale, ranging from 0.2µm up to the coarse sand particles,

(iv) a very high temporal resolution measurement of atmospheric parameters to cover also short-term fluctuations (gusts) in two different heights

(v) and in addition, all these measured over an entire campaign of experiments covering 7 different "wind events" during the year 2016.

The result is an exhaustive data set describing the atmospheric and pedologic conditions on the study site during the respective wind events.

The selection of analyses conducted on this data set so far - represented by the manuscripts contributing to this publication - only cover a small part of the possible investigations of such a big data set. Nevertheless, this thesis attempts to mirror the holistic approach of the data set by three manuscripts covering as much of the above-described scales: full local *special scale* in combination

with the coarser part of the *particle size scale* (Publication I), *wind speed and shear velocity scale* in combination with three different particle size classes (Publication II) and the *wind dynamics scale* in combination with the *particle size scale* of the aeolian section (Publication III). All these investigations have a clear focus on quantitative analytics, making maximum possible use of the generated data set.

In a nutshell, this thesis delivers the attempt to contribute to a better systematic understanding of how atmosphere and pedosphere interact and how this is shaping both - the landscape we live in and the soil we live from.

1.2 Study Area, Experimental Setup, Data Processing and Analytics

The sequence of the research papers contributing to this thesis is based on data collected and

processed from a series of field experiments, conducted in Argentina between August and September 2016. The study site is located in the north-eastern part of Argentina's province La Pampa, is part of the Anguil Experimental Station of the Instituto Nacional de Tecnología Agropecuarias (INTA) and has been under continuous agricultural management since the 1950s. The climate of this region is determined by an annual mean temperature of 16°C and a mean annual rainfall of 550mm, where most of the rain occurs during the southern hemispheric summertime (Aliaga et al. 2016; Casagrande and Vergara 1996).

The area is dominated by Typic Ustipsamment according to the USDA classification, the small-scale topography is hardly noticeable at field scale. A more detailed description of the research field as well as the surrounding area and the natural vegetation can be found in Publication I of this thesis (Siegmund et al. 2018).

The plot was investigated regarding physical and chemical soil parameters. For that, a dense net of soil samples, Pürckhauer augerings and other soil data collections were conducted. In addition, the topographic structure of the plot was measured in high special resolution using an optical level. This resulted in a comprehensive high-resolution data set about, e.g., topsoil thickness, soil texture parameter, carbon content, nitrogen content, pH value and others plus a digital terrain model.

The equipment for measuring wind erosion, namely:

a) Modified Wilson and Cooke (MWAC, Kuntze et al. 1990) samplers for saltation measurement,

b) Environmental Dust Monitors for measuring dust concentrations of PM_{10}, $PM_{2.5}$ and $PM_{1.0}$ (mg/m3) and
c) two meteorological stations which measure wind velocity, wind direction, temperature, and air humidity

was placed at 1- and 4-meter heights. The setup was installed on the plot once a wind event of erosive magnitude (v > 6 m/s) was expected to come. The traps, sensors and monitors were installed at the plot shortly before the wind events started and were collected immediately after the wind events or before announced or observed rainfall.
Illustrations as well as more detailed descriptions of the experimental setup can be found in Siegmund et al. 2018 and Siegmund et al. 2022a.

1.3 Research questions

The overarching research question unifying the three publications contributing to this thesis is:

How do the small-scale geomorphological characteristics of a location, as well as the highly dynamic parameters of a wind event, determine the wind erosion processes across various soil particle size classes, ranging from coarse sand to ultra-fine dust aerosols?

More specifically, this thesis shall investigate via:

Publication I:

- Can small-scale erosion and deposition patterns originating from saltation be explained by the land surface topology?
- Which specific topology parameters are crucial for the saltation processes?
- How are the small-scale erosion and deposition patterns linked to the physical and chemical soil parameters?

Publication II:

- In how far do the horizontal and vertical dust fluxes differ between the different partitions PM_{10}, $PM_{2.5}$ and $PM_{1.0}$?

Publication III:

- How should a new statistical measure be defined to quantify the “gust create dust” effect that is observable in situ with a data driven approach?
- Do gusts extraordinarily contribute to soil particle uptake?

1.4 Contributing publications

Siegmund, N., Funk, R., Koszinsky, S., Buschiazzo, D. E. and Sommer, M. (2018): Effects of low-scale landscape structures on aeolian transport processes on arable land. *Aeolean Research*, 32, 181-191.

Summary: This article presents the research findings regarding temporary wind uptake of larger soil particles - *saltation* - derived from the MWAC data collected. We follow the question in how far this wind erosion process is determined by the existing small scale land surface structure.

My contributions to the publication:

- Execution of the field experiments
- Data collection
- Data processing
- Article concept
- Data analytics and interpretation
- Illustrations
- Writing the article

Siegmund, N., Funk, R., Sommer, M., Avecilla, F., Panebiaco, J. E., Itturi, L. A., and Buschiazzo, D. E. (2022a): Horizontal and vertical fluxes of particulate matter during wind erosion on arable land in the province La Pampa, Argentina. *International Journal of Sediment Research*, 37, 539-552.

Summary: In this research paper we focus on the smaller soil particles, PM_{10} and smaller, and in how far the examined wind events induce horizontal and vertical fluxes of the latter. Especially wind speed is used as a predictor to model those fluxes and to explain the regarding wind erosion processes.

My contributions to the publication:

- Execution of the field experiments
- Data collection
- Data processing
- Data analytics and interpretation
- Writing the article

Siegmund, N., Panebiaco, J. E., Avecilla, F., Itturi, L. A., Sommer, M., Buschiazzo, D. E. and Funk, R. (2022b): From Gustiness to Dustiness - The Impact of Wind Gusts on Particulate Matter Emissions in Field Experiments in La Pampa, Argentina. *Atmoshpere*, 13, 1173.

Summary: This article focuses on a specific prevalent characteristic of strong wind events in general and of the investigated events in La Pampa specifically: gustiness. The hypothesis that wind gusts do over-proportionally contribute to the wind erosion was created from field observations. Gusts led to clearly visible dust plumes, a very small-scale event in the temporal as well as the special dimension. The article suggests a novel approach on how to statistically quantify this relationship – something that so far had only qualitatively been described.

My contributions to the publication:

- Execution of the field experiments
- Data collection
- Data processing
- Article concept
- Data analytics and interpretation
- Illustrations
- Writing the article

2. Publications

2.1 Effects of low-scale landscape structures on aeolian transport processes on arable land

Aeolian Research 32 (2018) 181–191

Contents lists available at ScienceDirect

Aeolian Research

journal homepage: www.elsevier.com/locate/aeolia

Effects of low-scale landscape structures on aeolian transport processes on arable land

Nicole Siegmund[a,b,*], Roger Funk[a], Sylvia Koszinsky[a], Daniel Eduardo Buschiazzo[c,d,e], Michael Sommer[a,b]

[a] Leibniz-Centre for Agricultural Landscape Research (ZALF), Research Area 1 "Landscape Functioning", Eberswalder Str. 84, D-15374 Müncheberg, Germany
[b] Institute of Earth and Environmental Science, University of Potsdam, Karl-Liebknecht-Straße 24-25, 14476 Potsdam-Golm, Germany
[c] Faculty of Agronomy, National University of La Pampa (UNLPam), cc 300, 6300 Santa Rosa, Argentina
[d] Institute for Earth and Environmental Sciences of La Pampa (INCITAP), National Council of Scientific and Technical Research (CONICET), cc 300, 6300 Santa Rosa, Argentina
[e] National Institute for Agricultural Technology (INTA), cc 11, 6326 Anguil, Argentina

ARTICLE INFO

Keywords:
Argentina
La Pampa
Wind erosion
Deposition
Topography
Mass transport
MWAC
Multiple regression

ABSTRACT

The landscape of the semiarid Pampa in central Argentina is characterized by late Pleistocene aeolian deposits, covering large plains with sporadic dune structures. Since the current land use changed from extensive livestock production within the Caldenal forest ecosystem to arable land, the wind erosion risk increased distinctly. We measured wind erosion and deposition patterns at the plot scale and investigated the spatial variability of the erosion processes. The wind-induced mass-transport was measured with 18 Modified Wilson and Cooke samplers (MWAC), installed on a 1.44 ha large field in a 20 × 40 m grid. Physical and chemical soil properties from the upper soil as well as a digital elevation model were recorded in a 20 × 20 m grid. In a 5-month measuring campaign data from seven storms with three different wind directions was obtained. Results show very heterogeneous patterns of erosion and deposition for each storm and indicate favoured erosion on windward and deposits on leeward terrain positions. Furthermore, a multiple regression model was build, explaining up to 70% of the spatial variance of erosion by just using four predictors: topsoil thickness, relative elevation, soil organic carbon content and slope direction. Our findings suggest a structure-process-structure complex where the landscape structure determines the effects of recent wind erosion processes which again slowly influence the structure, leading to a gradual increase of soil heterogeneity.

1. Introduction

The land surface of the western parts of La Pampa, Argentina has in large parts been formed by aeolian processes. Intensive winds led to a distribution of sandy and silty aeolian sediment deposits, building the parent material of the soil in the study area (Zarate and Tripaldi, 2012; Zarate, 2003). Today's landscape structure is characterized by large plains with sporadic dune structures. Because of the semiarid climatic conditions, La Pampa is in the transition zone between steppe pasture and rainfed agriculture. In the last decade the share of arable land has increased considerably, accelerated by the good prices for soy beans and corn at the world market. Under cultivation the soils of La Pampa are affected by wind erosion again. Soil losses of 0.9 t ha^{-1} were measured on soils of loess material by Buschiazzo et al. (2007) and 1.8 t ha^{-1} on a sandy soil, which is in the same order of magnitude like annual dust depositions in this region (0.4 to 0.8 t ha^{-1}, Buschiazzo et al., 1999; Ramsperger et al., 1998). Yet, areas of the Pampa with sandy soils show much higher erosion rates which can be seen by fresh dunes, buried fences or roads covered by sand. Extreme events are also documented by satellite images as in March 2009 and January 2010 (NASA Earth Observatory). Michelena and Irurtia (1995) estimated annual potential soil loss rates up to 178 t ha^{-1} t in the Province La Pampa caused by wind erosion, which are in better agreement to the observed soil relocations. Besides those singular strong events, wind erosion has been recognized as a gradual soil degradation process which predominantly removes the finest and most valuable particles of a soil like silt and clay particles as well as the soil organic matter (Funk et al., 2008; Iturri et al., 2017).

While landscape structures resulting from aeolian processes are already quite well understood, the recent wind-soil interactions at the

* Corresponding author at: Leibniz-Centre for Agricultural Landscape Research (ZALF), Research Area 1 "Landscape Functioning", Eberswalder Str. 84, D-15374 Müncheberg, Germany.
E-mail address: siegmund@zalf.de (N. Siegmund).

https://doi.org/10.1016/j.aeolia.2018.03.003
Received 15 October 2017; Received in revised form 6 March 2018; Accepted 6 March 2018
Available online 24 March 2018
1875-9637/

local scale have rarely been addressed in scientific investigations so far. Erosion and deposition processes take place at the same locations and are therefore difficult to separate, because diverse factors condition erosion/deposition patterns in landscapes. Local investigations have been limited by the availability of appropriate methods for measuring aeolian sediment transport dynamics (Thomas and Wiggs, 2008; Zobeck et al., 2003). The usage of sediment catchers in large number provides a profound method for quantifying horizontal sediment transport in a high spatial resolution as shown in some studies (Sterk et al., 2012; Sterk and Raats, 1996; Uzun et al., 2016; Zobeck et al., 2003). Many studies investigated wind erosion processes on sand dunes in desert or coastal environments including topographic characteristics (Bauer et al., 2009; Hesp, 2002; Tsoar et al., 2004; Walker and Nickling, 2002). Other studies analyzed wind erosion on plane agricultural plots or only with low elevation change (Buschiazzo et al., 2007; Colazo and Buschiazzo, 2015; Uzun et al., 2016; Zhao et al., 2006) but the number of these studies still remains small (Zobeck et al., 2003; Hoffmann et al., 2008a).

The aim of this study is to investigate the effect of small local landscape structures on the spatial variability of aeolian transport processes. Special emphasis is given to the variability of transport intensity, the dynamic patterns of erosion and deposition areas and theirs relation to the topographical variability on the plot. We will investigate upon the hypothesis that wind events parallel to the topographical structure result in low aeolian transport yet high material net loss and wind events orthogonal to the topographical structure result in high transport and low net loss.

2. Materials and methods

2.1. Study area and experimental Design

The study site is located at 63.9885° W and 36.577° S (165 m asl.) in the north-eastern part of Argentina's province La Pampa (Fig. 1, left).

The site is part of the Anguil Experimental Station of the Instituto Nacional de Tecnología Agropecuarias (INTA) and has been under continuous agricultural management since the 1950s. Aeolian sediments of Holocene origin cover the entire region (INTA, 1980). In the group of 'Chaqueño' vegetation classes the natural vegetation of the study area is classified as 'Pampeana'. This class is characterized by predominant grass steppes altering with semi-open Calden forests, *Prosopis caldenia* (Cabrera, 1976). In the study region the mean annual temperature is 16 °C and the mean annual rainfall is 550 mm, most of it during summer (between December to March) with about 80 mm per month (Aliaga et al., 2016; Casagrande and Vergara, 1996).

The experimental setup was aligned to the dominance of northern and southern winds in La Pampa. The plot was 240 m long, orientated to the main wind directions from N and S, and 60 m wide (Fig. S1). At the field site the small scale topography is hardly noticeable, but can be identified already at the larger scale by areas of lower plant cover on the aerial image of Fig. 1, taken few years ago before our measurements.

The area is dominated by Typic Ustipsamment according to the USDA classification, i.e. weakly developed A-C-profiles from sandy sediments. The mean thickness of Ah horizons is 20 cm; a petrocalcic horizon (Ck, Tosca) is partly present at around 100 cm. For the selected plot a detailed soil survey has been performed by Pürckhauer augerings in a 20 × 20 m raster (Fig. 1, right panel) to determine thicknesses and morphological properties of soil horizons and sediment layers. In this study "topsoil thickness" is defined as the sum of layers with dominating Ah characteristics. Further, 48 samples from the topsoil were taken for physical and chemical analysis. Soil texture was determined for a transect passing the plot and its topographical structure from north to south (Fig. 1, right panel). The location of the transect was chosen in the middle part of the plot, assuming that the variations in carbon content, nitrogen content and pH value are determined by topographical influences.

The equipment for measuring wind erosion was placed on the plot once a wind event of erosive magnitude ($v > 6$ m/s, de Oro and Buschiazzo, 2008) was expected to come. The setup of the erosion measurement was as follows: 24 MWAC samplers on a 20 × 40 m grid and two meteorological stations which measure wind velocity, wind direction, temperature and air humidity in 1 m height were installed at the northern and southern part.

The experimental setup is orientated on the predominance of northern and southern winds, shown in Fig. 2. Especially during the

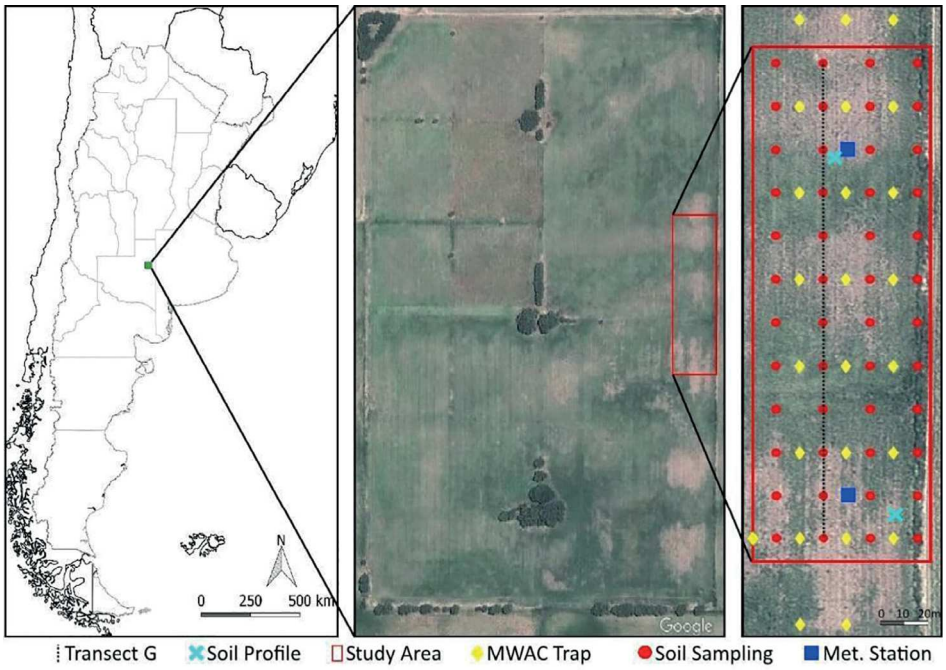

Fig. 1. Left: location of the study area in the central plateau of Argentina, South America. Center: Aerial photography of the study area. Right: experimental setup with the locations of the MWAC samplers, the soil profile pits, the transect G for texture analysis, and the meteorological stations. Source of the aerial photos: © Google Earth (2013).

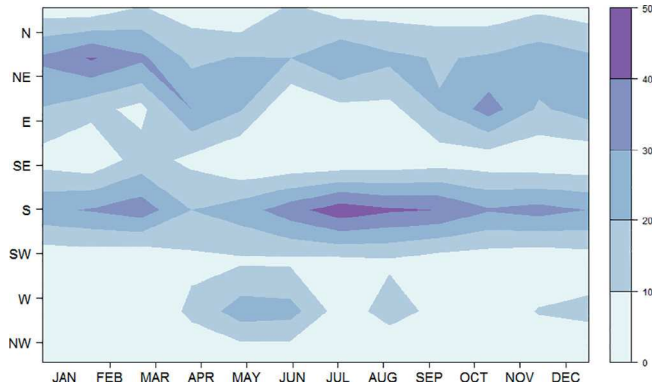

Fig. 2. Percentage of daily wind directions per month at the study site between 2012 and 2016. Included are only days with an average wind speed > 6 m/s. Data Source: http://siga2.inta.gov.ar/en/datoshistoricos/.

southern hemispheric winter to spring months these directions prevail. Against expectations, two westerly wind events have been measured during the campaign. Yet, the focus of this study is clearly on northern and southern wind events.

For this study, all shown wind measurements are averages between the two meteorological stations for the measurements 1 m above ground. Few days before the measurements the plot was prepared with a disc harrow for a bare surface. The field around the plot was under corn cultivation, but used as winter pasture for cattle. So, the plot was surrounded by an area of flat corn residues, which could be considered as non-erodible by a complete coverage of corn leaves and recumbent stems. Solely sparsely distributed annual weeds remained on the plot, covering less than 5% of the area. While the vegetation cover was insignificant for the first five erosion events, the events No. 6 and 7 had around 5% soil cover by weeds. Additionally, the plot has a fence on the eastern border, leading to a narrow vegetation covered strip.

At three spots of the middle transect, soil samples with 3 replicates have been taken for laboratory analyses to determine erodible fraction (EF_{sieved}) and the dry aggregate stability (DAS) of the soil previous to each event.

2.2. Meteorological conditions

In preparation for the measuring campaign meteorological data was analyzed to find the auspicious time of the year for wind erosion measurements and the predominant wind direction. The average annual wind-velocity is 15 km/h. The highest wind velocities arise between August and October with an average of 20–25 km/h and gusts reaching more than 60 km/h (Casagrande and Vergara, 1996). The most dominant wind direction during this period is southern and northern/northeastern, together contributing up to 80% of the windy days (Fig. 2). Based on this analysis we decided to orientate the measuring in N-S direction.

Especially during this time of the year (southern hemispheric winter and spring) agriculturally used areas are often not covered with plants and therefore susceptible to wind erosion.

2.3. Topography

The topographic structure of the plot was measured with an optical level (Pentax AP-022) with a vertical resolution of 1 cm in a grid of 20 m. In addition, 36 points were measured outside the plot (200 m south and north, 100 m east and west) to estimate the plot's landscape position on a larger scale. The data are used to generate a digital terrain model. The measured elevation was interpolated using the ordinary point kriging interpolation algorithm provided by the ArcGIS spatial analyst toolbox. Furthermore, we used ArcGIS to calculate the topographic position index (Jenness, TPI), slope percent (Sperc) and slope direction (SD) for each of the interpolated grid points.

2.4. Chemical and physical soil analysis

Topsoil samples were air-dried and sieved through a 2 mm mesh. The pH was determined using a 0.01 M $CaCl_2$ solution with a soil-solution ratio of 1:2.5 using the Altronix/TPXIII (Schlichting et al., 1995). The total carbon (Ct) and total nitrogen content (Nt) was determined by elemental analysis (dry combustion at 1250 °C, TruSpec, LECO, Mönchengladbach) in duplicate (Din ISO 10694, 1996). Total carbon equals soil organic carbon (SOC) as all topsoils showed no carbonates. All analyses were carried out at the Central Laboratory of the ZALF in Müncheberg, Germany.

12 topsoil samples of the middle transect shown in Fig. 1 were analyzed concerning soil texture using the wet sieving and pipette method (DIN ISO 11277, 2002; Gee and Bauder, 1986). Based on these analyses the erodible fraction (EF_c) was calculated according Fryrear et al. (1998):

$$EF_c = \frac{29.09 + 0.31 \cdot Sa + 0.17 \cdot Si + 0.33\frac{Sa}{Cl} - 2.59 \cdot OM - 0.95 \cdot CaCo_3}{100},$$

where Sa = sand content [wt.%], Si = silt content [wt.%], Sa/Cl = sand to clay ratio, OM = organic matter [wt.%] and $CaCO_3$ = calcium carbonate [wt.%].

For determining dry aggregate stability (DAS), three samples from a N-S transect at the middle of the plot were taken before each event. The three samples were sieved in a rotary sieve with 0.42 mm, 0.84 mm, 2 mm, 6.4 mm and 19.2 mm meshes (Chepil 1962). The percentage of the aggregates < 0.84 mm in diameter representing the erodible fraction (EF_{sieved}) was calculated following Colazo and Buschiazzo (2010):

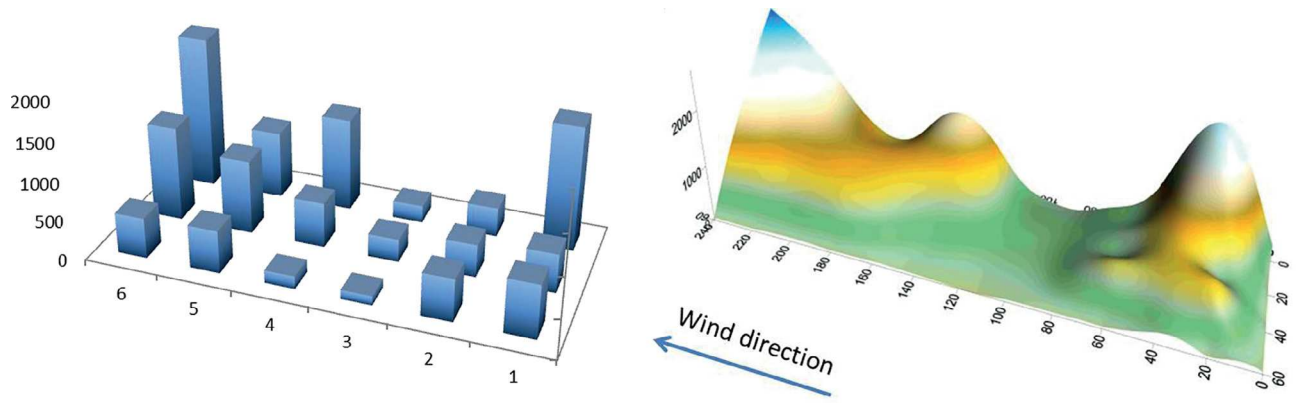

Fig. 3. Left: calculated Q of each MWAC, right: interpolated 1 m – grid of the entire plot, example is the event at the 26.08.2016.

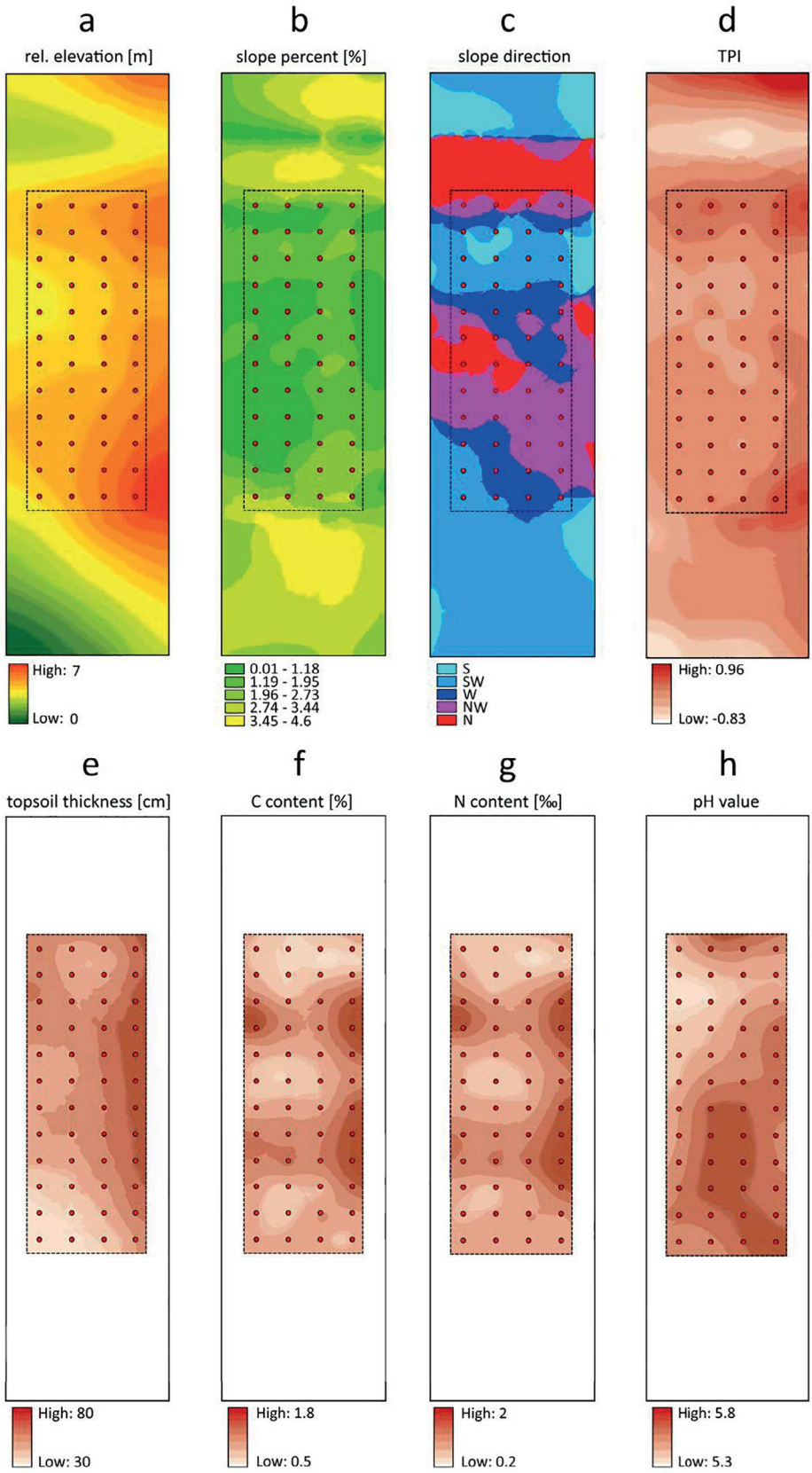

Fig. 4. Relative elevation, the slope percent, the slope direction and the topographic position index as derived from the digital elevation model (upper panels) and topsoil thickness, C and N content and the pH value as interpolated from the analysis of the topsoil samples.

Table 1
Summarized data of the seven erosion events during August 2016 to December 2016.

Date	Event	Time	Duration	measuring Interval	WFI_6	WFI_6 h^{-1}	Wind direction				Wind speed				EF_{sieved}	DAS
								mean	SD	max_{dev}	mean ms^{-1}	min ms^{-1}	max ms^{-1}	SD ms^{-1}		
		hh:mm:ss	hh:mm:ss	s											%	%
26. Aug.	1	09:52:05–15:09:35	05:17:30	5	23,049	4356	SSW	198	35	142	8	0	13	2	–	–
13. Sept.	2	09:25:00–15:39:00	06:14:00	60	119,559	19,816	SSW	199	7	17	9	6	12	1	52	74
18. Nov.	3	09:20:01–14:40:01	05:20:00	60	39,821	7471	N	8	7	18	8	3	11	1	60	71
20. Nov.	4	10:19:00–17:40:00	07:21:00	60	34,154	4647	SSE	155	14	42	7	3	10	1	54	81
04. Dec.	5	10:50:00–17:40:00	06:50:00	60	75,295	11,024	NNE	22	14	96	8	0	12	1	61	67
10. Dec.	6	10:16:00–19:10:00	08:54:00	60	99,391	11,168	WNW	303	42	84	8	1	12	1	60	68
12. Dec.	7	14:52:00–19:10:00	04:18:00	60	56,631	13,170	WSW	234	28	3	9	2	12	1	60	69

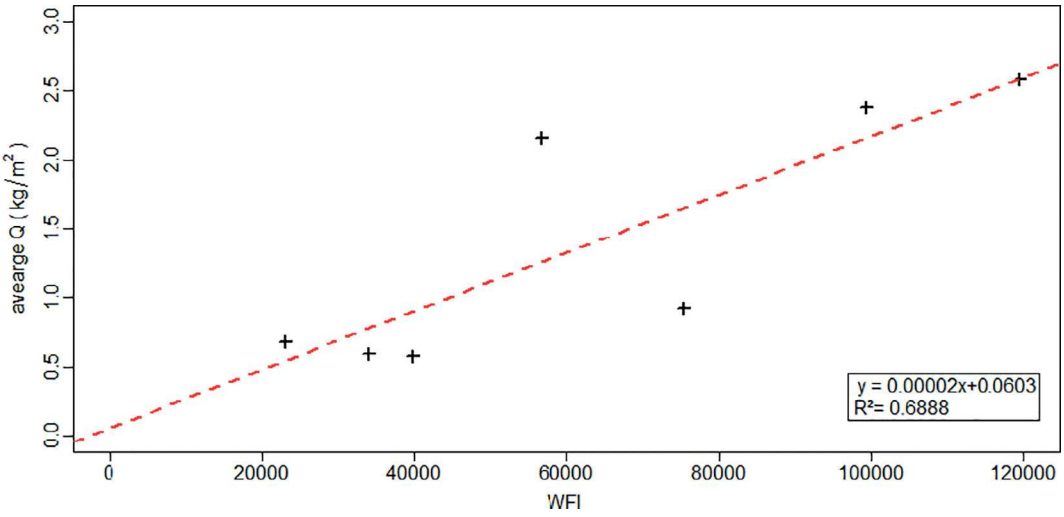

Fig. 5. Average transport rate Q on the plot in dependence on the Wind Force Integrals of each erosion event.

$$EF_{sieved} = \frac{W < 0.84}{TW} \cdot 100,$$

where EF_{sieved} = erodible fraction [%], W < 0.84 = weight of < 0.84 mm aggregates [g] and TW = initial weight of total sample [g].

After a second dry sieving of each aggregate size the dry aggregate stability (DAS) was calculated following Skidmore et al. (1994):

$$DAS = \left[1 - \frac{W < 0.84_2}{W > 0.84_1}\right] \cdot 100,$$

where $W < 0.84_2$ = weight of < 0.84 mm aggregates after a second sieving [g] and $W > 0.84_1$ = weight of > 0.84 mm aggregates after first sieving [g].

2.5. Measurement and calculation of soil erosion

18 Modified Wilson and Cooke (MWAC, Kuntze et al., 1990) samplers were installed on a regular 20 × 40 m grid covering the study area and additionally 6 MWAC surrounding the plot (Fig. 1, right panel). Each sampler was equipped with four bottle traps at heights of 7.5 cm, 22.5 cm, 55 cm and 110 cm. The central poles of the MWAC have wind sails in order to make sure that the devices are always aligned with wind direction. The reference height (z = 0) was set by spanning a 10 m line across the installation point of each MWAC in an acute angle to the tillage direction. Similar experimental setups have previously been used for studies like Funk et al. (2004), Mendez et al. (2011), Sterk et al. (2012) or Sterk and Raats (1996).

The traps were installed at the plot shortly before the wind events started and were collected immediately after the wind events or before announced rainfall. The trapped material of each bottle (q_z) was weighed (accuracy = 0.001 g) and used to calculate vertical profiles of q_z by regression analysis. Two regression models were used, $q_z = f(\ln z)$ and $\ln q_z = f(\ln z)$, and the one with the better R^2 was chosen to calculate the vertical integrated sediment transport rate (Q in g m^{-1}) for the heights from 0.005 m to 1.10 m (Zobeck et al. 2003) with integration steps of 0.007 m (MWAC inlet diameter), converted to 1 m width:

$$Q = \sum_{z=0.005}^{1.1} q_z \times f_{MWAC}$$

where $f_{MWAC} = \frac{7000}{38.48}$ with 7000 mm^2 resulting from the conversion to 1 m width and 38.48 mm^2 from the inlet area of the sampler ($\pi * r^2$).

To create maps of transport rates, first triangulation with linear interpolation was used to create a simple map in 1 × 1 m grid. Data was smoothed by Modified Shepard's method, which uses a quadratic polynomial fit in the neighborhood of each data point. The result is an inverse distance weighting (IDW) interpolator, but not showing the bull's-eye effect as produced by IDW. The map in the 1-m resolution was used to calculate the balance of the sediment transport at the plot by summing up the grid cells at the incoming and outgoing boundaries in relation to the wind direction of each event. As one example illustration, Fig. 3 shows the calculated Q of each MWAC at its location on the plot and the spatial interpolated Q in a 1 m – grid for the entire plot. The southern boundary was set to zero, because of the good plant residue cover at that time.

In August–September the plot was surrounded by a non-erodible pasture and soil material input from that area could be excluded. For spatial interpolation purposes the windward boundaries of the plot were set to zero. In November–December the measuring plot was influenced by possible additional inputs because of seedbed preparations on the surrounding field and additional traps were also installed outside in north, south and west.

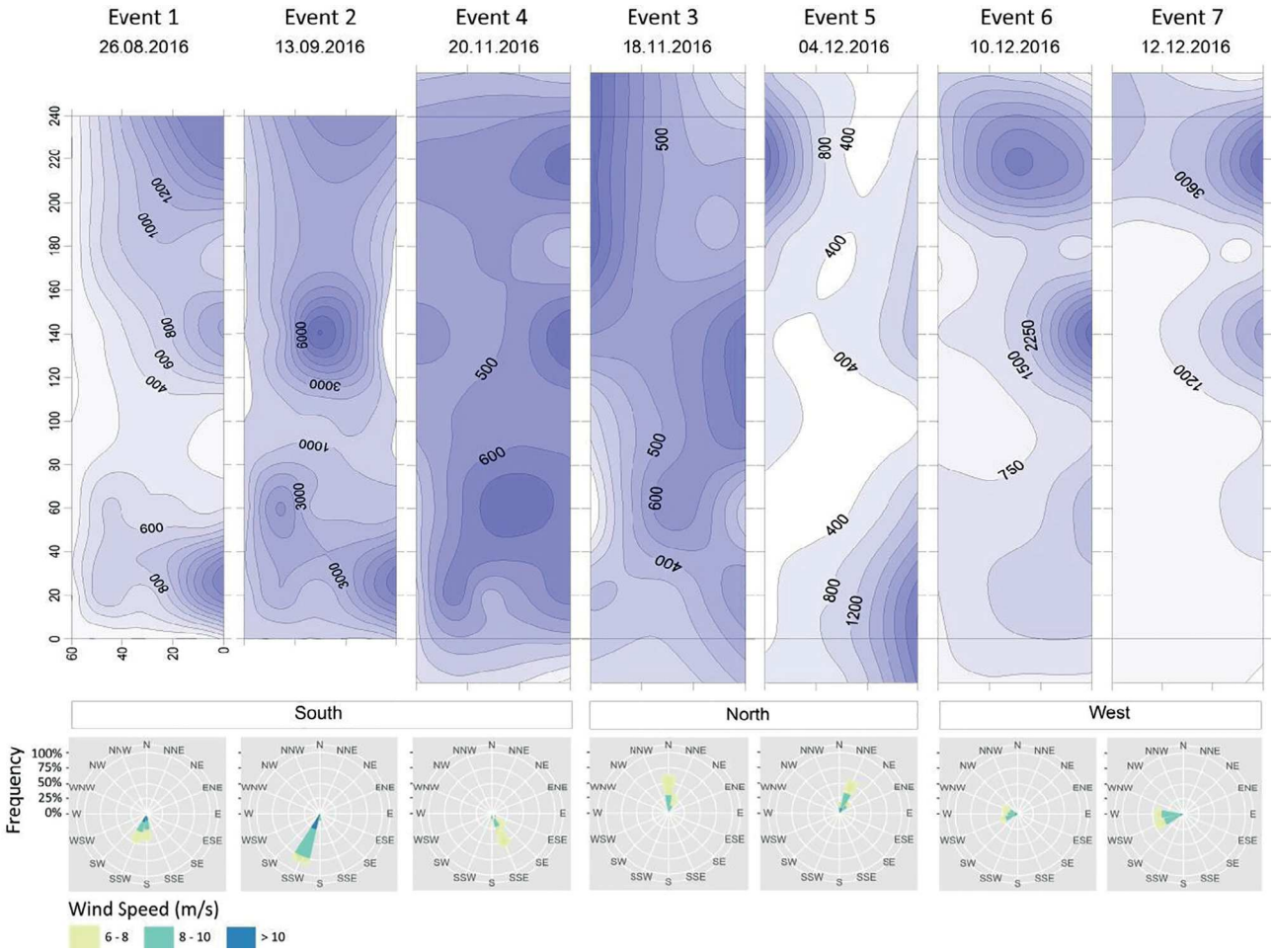

Fig. 6. Spatial distribution of the transport rates [g m^{-1}] on the plot for all measured events and frequencies of associated wind speeds and its directions.

Table 2
Accounting of net mass transport on the plot during the seven wind events. "netto" in this case is "out–in".

	Event 1 26.08.2016 SSW	Event 2 13.09.2016 SSW	Event 3 18.11.2016 N	Event 4 20.11.2016 SSE	Event 5 04.12.2016 NNE	Event 6 10.12.2016 WNW	Event 7 12.12.2016 WSW
Q_{in} [kg]	0	0	45	33	79	190	258
Q_{out} [kg]	351	588	29	38	113	730	895
average Q [g/m^2]	680	2570	580	600	920	2370	2150
loss netto [kg]	351	588	−16	5	34	540	637
loss netto [kg/ha]	244	408	−11	3	24	375	443

As transport rates are not necessarily correlated to local soil losses, the spatial distribution of soil loss was calculated using

$$SL_{x,y} = Q_{x,y} - Q_{x+1,y+1}$$

where $Q_{x,y}$ denotes the transport rate at position x,y of the plot and $Q_{x+1,\ y+1}$ the transport rate at next leeward raster cell. Thus, negative SL indicate erosion, positive indicate deposition in the direction of transport.

Since the events also differ by wind intensity, we calculate the wind force integral (WFI) for wind speeds at the height of 1 m according to Fryberger and Dean (1979):

$$WFI = \Sigma_t((v_t - 6)v_t^2)\cdot\Theta(v_t - 6),$$

where v_t is the wind velocity at time t and Θ describes the Heaviside function giving 0 if $v_t - 6 < 0$ and 1 if $v_t - 6 > 0$. Finally, we normalize the WFIs according to the individual duration of each event, resulting in WFI per hour. A similar procedure has already been suggested by Hoffmann et al. (2008b).

2.6. Spatial modelling of the input parameter

For showing the spatial structure of the data and to model semivariograms we used the geostatistical software GS+ (Gamma Design, St. Plainwell, Ml). Spherical and exponential models were fitted to the experimental semivariograms and used for ordinary kriging interpolation of relative elevation, topographic position index (TPI), topsoil thickness (TT), Ct content and Nt content (Fig. S2 and Table S1). All the data was computed untransformed since data was normally distributed. The models with the highest efficiency (R^2) and the smallest residuals were determined in order to provide the input parameters for interpolation.

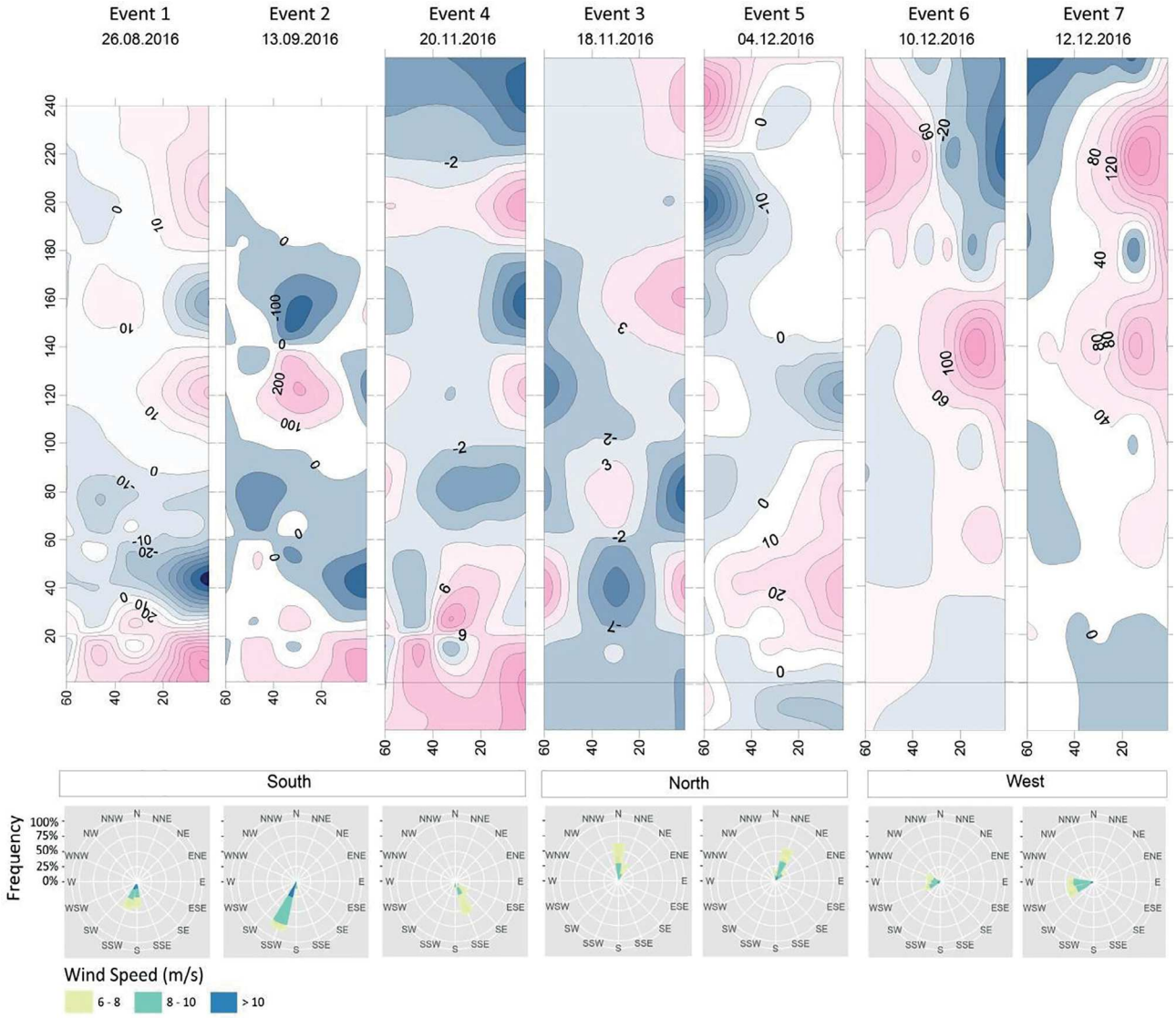

Fig. 7. Spatial distribution of erosion (red colors) and deposition (blue colors) in g m^{-1} for the seven wind events measured with MWAC sediment traps. (For interpretation of the references to colour in this figure legend, the reader is referred to the web version of this article.)

2.7. Modelling erosion by site parameter

In order to investigate the statistical relationships between pairs of soil properties as well as between pairs of erosion data and soil properties we calculate linear Pearson correlation coefficient and a standard student *t*-test was applied in order to proof for significance ($\alpha = 0.05$). Subsequently, a multiple linear regression model using four selected soil parameters as predictors was set up for the explanation of the measured erosion following the general equation:

$$y = a + b_1 \cdot x_1 + b_2 \cdot x_2 + \ldots + b_n \cdot x_n$$

In order to avoid multi-collinearity between the predictors (i.e. to assure statistical independency and to avoid overfitting), we only chose those parameters for the regression model, which show a correlation between each other lower than r = 0.5. The statistical evaluations were performed using R (R Core Team, 2014).

3. Results and discussion

3.1. Spatial patterns of terrain attributes and soil properties

Our plot shows gentle ups and downs resulting in a relative elevation difference of two meters between the highest and lowest part. The relief is very gentle with slopes less than 5 per cent (Fig. 4, b) with mainly north and south orientated slope directions (Fig. 4, c and d). The topsoil thickness is generally higher on the topographically higher parts of the plot reaching up to 63 cm (Fig. 4, e). This can also be observed for Ct and Nt contents on these elevated positions, indicating insignificance of water erosion processes (Fig. 4, f and g). The pH values show a very low variation. When comparing the soil parameters (Fig. 4, f and g) to the topographical features as rel. elevation and TPI (Fig. 4, a–d) no common patterns can be seen obviously. Contrarily, the comparatively low pH values in the northwestern part of the samples area (Fig. 4, h): exactly in this area the terrain properties also show variation in terms of low elevation (Fig. 4, a) and southern slope direction (Fig. 4, c). Nevertheless, the patterns of the soil properties exhibit high similarity amongst each other: Ct and Nt show very similar patterns.

3.2. Spatial variation of aeolian soil transport

During the southern hemispheric winter and spring season 2016 (August to December) seven erosive wind events have been measured. They differed in intensity, direction and duration but all caused measurable soil transports at the plot. Information about the dates,

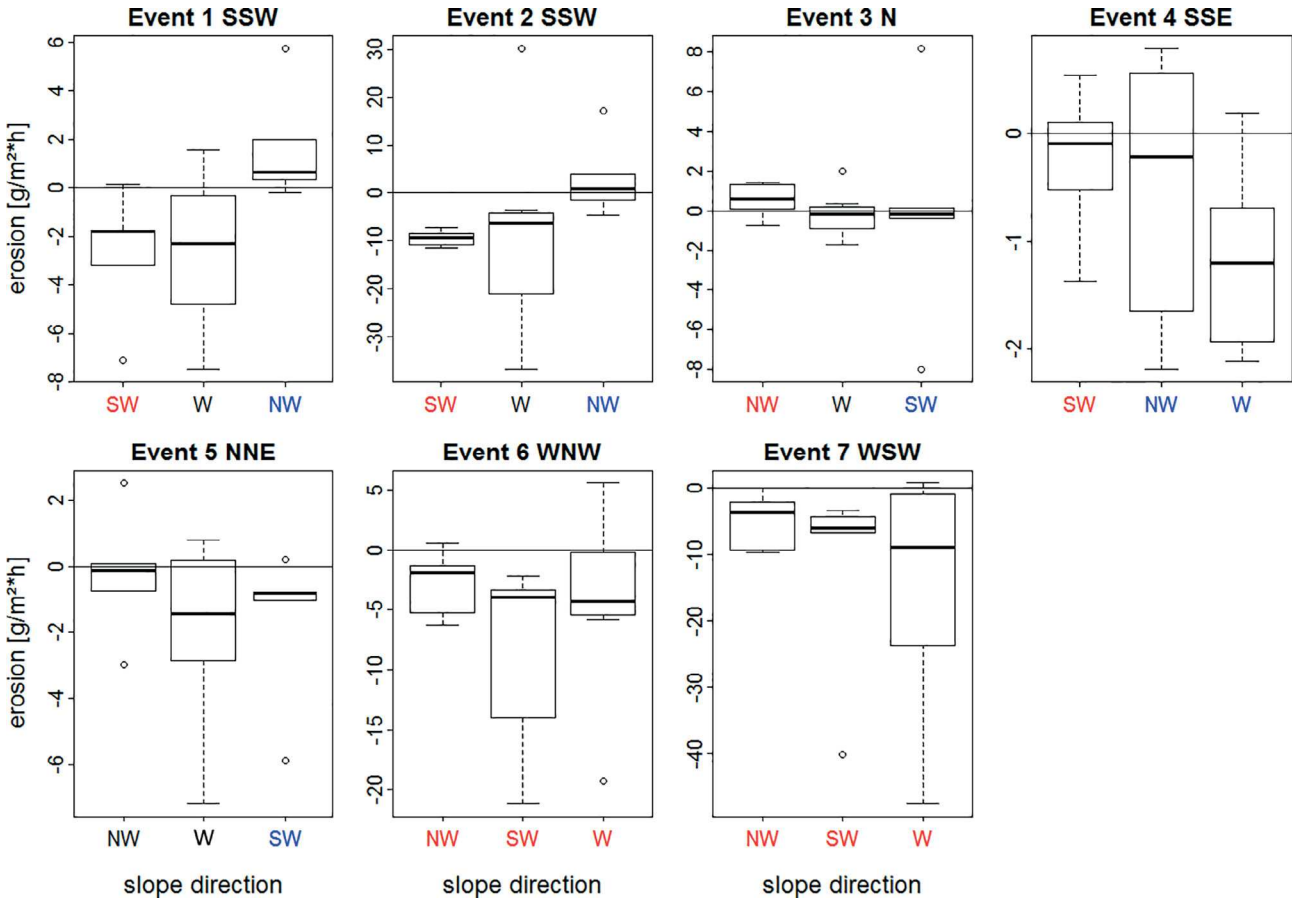

Fig. 8. Boxplots of measured erosion values of the seven wind events, classified by three slope directions: NW, SW and W. Negative values denote erosion, positive deposition. With respect to the main wind direction of the wind event, red highlighted wind directions marks windward sides, blue marks leeward sides and black text marks slopes that are parallel to the event's wind direction. (For interpretation of the references to colour in this figure legend, the reader is referred to the web version of this article.)

durations and intensities of the wind events are summarized in Table 1.

Two pedological parameters that are often discussed when investigating wind erosion are the erodible fraction and the soil aggregate stability (Kohake et al., 2010; Skidmore and Layton, 1992). Both are assumed to systematically influence the potential soil erosion during a given wind event (Colazo and Buschiazzo, 2010; Skidmore and Layton, 1992; Zobeck and Popham, 1990). In this study, we determined both parameters before every event in order to get their temporal variability.

DAS and EF_{sieved} change only slightly between the events. While DAS has a decreasing tendency on the plot, the EF_{sieved} and the erodibility on the plot increases. The percentage of erodible fractions was always smaller than 60%. Consequently, the transport rates were supply-limited. The trapped amounts and calculated transport rates were relatively low and deposits at the plot were not caused by limitations of the transport capacity of the wind.

There is a close relationship between the wind forces (WFI) and the transport rates, shown in Fig. 5 giving average transport intensity of each erosion event at the plot Despite this clear dependence between wind speed and transport rate, all events have a high spatial variability of transport rates (Fig. 6). The patterns of the spatial distribution show that the transport rates are influenced by the topographic structure, especially by windward and leeward orientated slopes. In cases where the wind direction is orthogonal to the topographic structure, increase and decrease of the transport rate follow the relief (Fig. 6, events with north–south or south-north wind directions). Wind erosion events parallel to the topographic structure are characterized by a steady increase of the transport rate with plot length, caused by the windward facing of the slopes (events 6 and 7). The very low transport rates in the south of the plot during these two west-wind events may also be a result of coverage by weeds of around 5–10% in this area.

The calculated soil losses of this study (Table 2) agree very well with previous measurements of wind erosion in the province La Pampa. Buschiazzo et al. (2007) found losses between 4 and 900 kg ha^{-1} and accumulations between 3 and 580 kg ha^{-1} on typical soil types of this region. Ramsperger et al. (1998) reported deposits between 114 and 365 kg ha^{-1} month^{-1}, mainly of the dust fractions. The erosion values found in this study ranged between 5 and 500 kg ha^{-1} per event which fit well to the previously measured erosion rates for this region of Argentina. As already stated by Sterk and Stein (1997) and Visser et al. (2004), the simple comparison of incoming and outgoing fluxes can result in incorrect estimates of soil transport at a field, it is more useful to distinguish erosion and deposition areas in the plot. An important consequence results, if horizontal fluxes are related to vertical fluxes (dust emissions).

3.3. Spatial patterns of erosion and deposition

Converting the transport rates into spatial patterns of erosion and deposition results in the maps shown in Fig. 7. Areas of erosion and deposition alternate in small patterns and are located in immediate vicinity, especially for the North and South events. Events from the same direction show similar patterns.

To indicate the influence of the slope direction on spatial patterns, the calculated values of erosion or deposition from the maps in Fig. 7 are illustrated with boxplots, where all MWAC positioned within the same category of slope direction contribute to one boxplot (Fig. 8). Windward and leeward positions show clearly differing distribution parameters, where especially strong events show distinct differences

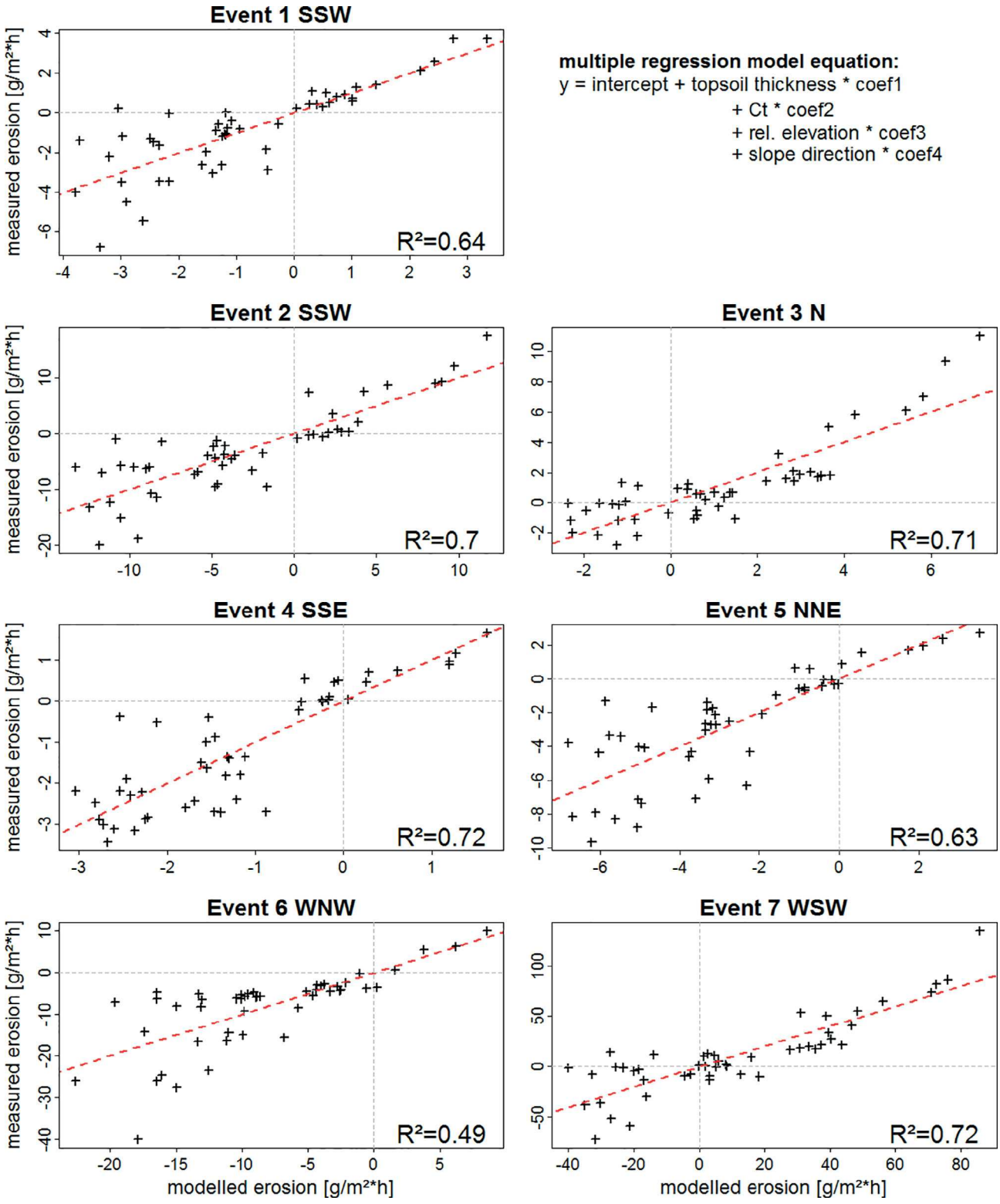

Fig. 9. Measured versus modelled erosion for all seven wind events and the related explained variance (R^2) using a multiple linear regression model with topsoil thickness, Ct, relative elevation and slope direction as predictors. The red lines mark x = y. (For interpretation of the references to colour in this figure legend, the reader is referred to the web version of this article.)

between erosion and deposition areas. For opposite wind directions (N–S, S–N) windward and leeward positions change, i.e. these positions alter between deposition and erosion areas.

A similar analysis was performed for the impact of different TPI positions on erosion (Fig. S3), but erosion and deposition were not linked with this topographical characteristics. The TPI information therefore is excluded from the following analyses.

The strong spatial variability of wind erosion at the plot clearly underlines the intensive affection of erosion processes by even only small topographic changes. Uzun et al. (2016), Visser et al. (2004) and Sterk et al. (2004) also presented maps of spatial erosion distributions for study areas with even lower topographical variability, but also

Table 3
Intercept and the coefficients of the seven multiple regression models for the erosion resulting from the seven wind events.

event	intercept	coef1 TT	coef2 Ct	coef3 Ele	coef4 SD
1	−221.47	−0.05	1.18	2.23	0.06
2	−810.34	−0.16	5.54	8.15	0.15
3	−340.83	−0.04	1.78	3.45	0.10
4	−158.90	−0.03	1.26	1.59	−0.03
5	−338.82	−0.06	1.82	3.40	−0.18
6	−868.02	−0.21	1.51	8.74	−0.23
7	−4111.69	−0.79	29.30	41.60	0.37

indicated such heterogenic patterns. Similar to our findings, Uzun et al. (2016) also revealed that the heterogeneity of erosion and deposition is increasing with stronger wind events.

A critical issue on studies like this, dealing with sediment catchers for soil erosion measurements, is the question of uncertainty. Uncertainty can come into effect on both, the measurement and the data processing side: even small errors/uncertainties in the measurements can, as a result of the integrating data processing, propagate and finally accumulate – bearing a high potential for uncertainty in the results. Tidjani et al. (2011) comprehensively investigated on the uncertainties for soil erosion measurements and calculations like in our analysis. Following Tidjani et al. (2011), the largest part of uncertainty comes due to weighing uncertainty, because this effect accumulates through the calculations. We used a Precisa 125A with a precision of 0.001 g where the weighing was conducted under laboratory conditions. The uncertainty of measuring with MWAC samplers strongly depends on the trapping efficiency. The MWAC traps used in this study have inlet diameters of 7 mm, which prove to come with very high trapping efficiency (~90%) in comparison to other models.

3.4. Statistical modelling of erosion and deposition

Before constructing a multiple regression model using topographic and soil parameters as predictors for wind erosion/deposition in the spatial domain, we conducted a comprehensive correlation analyses for all possible pairs of topographic soil parameters (see Table S3, where only significant correlation coefficients are given. Significance was tested using a standard Student T-test with alpha = 0.05). This allows for the construction of a multiple linear regression model, on the one hand including all parameters that are well correlated with erosion ("forward-selection" approach) and on the other hand excluding multicollinearity and therefore over-fitting as far as possible. Based on this correlation matrix, the following parameters were chosen for the construction of the regression models (Fig. 9): topsoil thickness (TT [cm]), Ct [‰], relative elevation (Ele [m]) and slope direction (SD [no unit]), resulting in the general regression equation:

$$y = intercept + top\ soil\ thickness{\cdot}coef_1 + Ct{\cdot}coef_2 + rel.\ elevation{\cdot}coef_3 + slope\ direction{\cdot}coef_4$$

Although the slope direction (SD) does not show significant correlations with erosion in Table S3 (a), this parameter was included into the model because in Fig. 8 the clear influence of classified slope directions at least for some of the events could already be shown. In order to transform slope direction (SD) into a variable giving information about wind- and leewards directed slopes, we apply:

$$SD^n = cos(SD - \overline{wdir_n})$$

,where $\overline{wdir_n}$ is the mean wind direction of the specific event n. The new variable SD^n is 1 when the slope direction is fully windward to the average wind direction of event n and −1 when the slope direction is fully leeward to the average wind direction of event n. For simplicity, yet, SD^n is consistently abbreviated by SD in the remaining.

The coefficients of the predictors (Table 3) vary for each individual event.

The explained variance (R^2) of the modelled erosion/deposition ranges from 50% to 75% where most of the models exhibit an $R^2 > 0.7$. Except of the events 3 and 7, the model almost never mismatches positive and negative erosion. A skewness of the distribution of residuals cannot be seen which makes the linear modelling approach seem reasonable for the given data set.

Except for slope direction, the coefficients are consistently either positive or negative for all events which means, that greater topsoil thickness is linked to higher erosion (negative coefficient) and a higher Ct content is always linked to higher deposits (positive coefficient) in every wind event.

Investigations of Hong et al. (2014) or Zobeck et al. (2013) presented similar studies, showing models with explained variances of around 0.61 and 0.94 using the topsoil water content, soil fractions, wind erodible fraction (EF) and organic matter as predictors. The fact that the models perform well for all seven wind events underlines the importance of topographical changes on wind erosion/deposition processes and shall sensitize for designs of field experiments.

The analysis of the soil texture along the transect shown in Fig. 1 revealed only marginal variations of soil texture within the plot. Therefore no further statistical evaluations with texture have been conducted.

4. Conclusions

This study shows that the topographical structures in the study area influence the variability of recent aeolian processes, whereas pedology has lower importance caused by the homogeneous soil parameter in the investigation area. Based on investigations of the spatial distribution of the sediment fluxes, maps of erosion/deposition patterns were derived. Depending on the wind direction of each erosion event, distinct patterns of erosion/deposition could be identified. Soil material is preferentially eroded from the windward slopes and deposited on the leeward flanks in the immediate. This is a direct impact on the structure itself and slowly changes the terrain and soil properties of the plot. Over long periods these changes can evolve, because of the predominance of only two wind directions in La Pampa in the periods with bare soils, and the removal of SOM and nutrients with the dust fractions. Our study verifies the strong spatial variability of wind erosion processes caused by even small changes of the controlling factors. These spatial variabilities lead to a gradual change of the soil heterogeneity and should be considered in experimental setups for field measurements.

Acknowledgements

This study is funded by the Deutsche Forschungsgemeinschaft (DFG-GZ: Fu 247/10-1). We thank Dr. Esteban J. Panebianco and Dr. Antonela L. Iturri from the Faculty of Agronomy, National University of La Pampa (Argentina), who provided support for our field experiments.

Appendix A. Supplementary data

Supplementary data associated with this article can be found, in the online version, at http://dx.doi.org/10.1016/j.aeolia.2018.03.003.

References

Aliaga, V.S., Ferrelli, F., Alberdi-Algañaraz, E.D., Bohn, V.Y., Piccolo, M.C., 2016. Distribución y variabilidad de la precipitación en la región Pampeana, Argentina. Cuader. Investig. Geogr. 42 (1), 261–280.

Bauer, B., Davidson-Arnott, R., Hesp, P., Namikas, L., Ollerhead, J., Walker, I., 2009. Aeolian sediment transport on a beach: surface moisture, wind fetch and mean transport. Geomorphology 105, 106–116.

Buschiazzo, D.E., Zobeck, T.M., Abascal, S.A., 2007. Wind erosion quantity and quality of an Entic Haplustoll of the semi-arid pampas of Argentina. J. Arid Environ. 69, 29–39.

Buschiazzo, D.E., Zobeck, T.M., Aimar, S., 1999. Wind erosion in loess soils of the semiarid Argentinian pampas. Soil Sci. 164 (2), 133–138.
Cabrera, A.L., 1976. Regiones fitogeográficas argentinas. In: Kugler, W.F. (Ed.), Enciclopedia Argentina de Agricultura y Jardineria II. ACME, Buenos Aires, pp. 1–85.
Casagrande, G., Vergara, G., 1996. Características climática de la region. In: Buschiazzo, D.E., Panigatti, J.L., Babinec, F.J. (Eds.), Labranzas en la región semiárida Argentina. INTA, pp. 11–19.
Chepil, W.S., 1962. A compact rotary sieve and the importance of dry sieving in physical soil analysis. Soil Sci. Soc. Am. Proc. 26, 4–6.
Colazo, J.C., Buschiazzo, D.E., 2010. Soil dry aggregate stability and wind erodible fraction in a semiarid environment of Argentina. Geoderma 159, 228–236.
Colazo, J.C., Buschiazzo, D.E., 2015. The impact of agriculture on soil texture due to wind erosion. Land Degrad. Dev. 26, 62–70.
De Oro, L., Buschiazzo, D.E., 2008. Threshold wind velocity as an index of soil susceptibility to wind erosion under variable climatic conditions. Land Degrad. Dev. 20, 14–21.
DIN ISO 10694, 1996. Soil Quality – Determination of Organic and Total Carbon After Dry Combustion (Elementary Analysis) (ISO 10694:1995). Beuth Verlag, Berlin.
DIN ISO 11277, 2002. Soil Quality – Determination of Particle Size Distribution in Mineral Soil Material – Method by Sieving and Sedimentation (ISO 11277:2009). Beuth Verlag, Berlin.
Fryberger, S.G., Dean, G., 1979. Dune Forms and Wind Regime. in: McKee, E.D. (Ed.), A Study of Global Sand.
Fryrear, D.W., Saleh, A., Bilbro, H.M., Schomberg, J.E., Zobeck, T.M., 1998. Revised Wind Erosion Equation (RWEQ). Technical Bulletin 1. Southern Plains Area Cropping Systems Research Laboratory, Wind Erosion & Water Conservation Research Unit, USDA-ARS.
Funk, R., Reuter, H.I., Hoffmann, C., Engel, W., Otti, D., 2008. Effect of moisture on fine dust emission from tillage operations on agricultural soils. Earth Surf. Proc. Land. 33 (12), 1851–1863.
Funk, R., Skidmore, E.L., Hagen, L.J., 2004. Comparison of wind erosion measurements in Germany with simulated soil losses by WEPS. Environ. Modell. Software 19, 177–183.
Gee, G.W., Bauder, J.W., 1986. Particle size analysis. In: Klute, A. (Ed.), Methods of Soil Analysis, Part 1: Physical and Mineralogical Methods. American Society of Agronomy, Soil Science Society of America, pp. 383–411.
Hesp, P., 2002. Foredunes and blowouts: initiation, geomorphology and dynamics. Geomorphology 48, 245–268.
Hoffmann, C., Funk, R., Wieland, R., Li, Y., Sommer, M., 2008a. Effects of grazing and topography on dust flux and deposition in the Xilingele grassland, Inner Mongolia. J. Arid Environ. 72, 792–807.
Hoffmann, C., Funk, R., Li, Y., Sommer, M., 2008b. Effect of grazing on wind driven carbon and nitrogen ratios in the grasslands of Inner Mongolia. Catena 75 (2), 182–190.
Hong, S.-W., Lee, I.-B., Seo, I.-H., Kwon, K.-S., Kim, T.-W., Son, Y.-H., Kim, M., 2014. Measurement and prediction of soil erosion in dry field using portable wind erosion tunnel. Biosyst. Eng. 118, 68–82.
INTA, 1980. Caracterización general de la provincia, in: Inventario integrado de los recursos naturales de la provincia de La Pampa, Buenos Aires, pp. 36–38.
Iturri, L.A., Funk, R., Leue, M., Sommer, M., Buschiazzo, D.E., 2017. Wind sorting affects differently the organo-mineral composition of saltating an particulate materials in contrasting texture agricultural soils. Aeolian Res. 28, 39–49.
Kohake, D.J., Hagen, L.J., Skidmore, E.L., 2010. Wind erodibility of Organic Soils. Soil Sci. Soc. Am. J. 74 (1), 250–257.
Kuntze, H., Beinhauer, R., Tetzlaff, G., 1990. Quantification of Soil Erosion by Wind: I. Final Report of the BMFT Project. Project No. 0339058 A, B, C. Institute of Meteorology and Climatology, University of Hannover, Germany.
Mendez, M.J., Funk, R., Buschiazzo, D.E., 2011. Field wind erosion measurements with big spring number eight (BSNE) and modified Wilson and Cook (MWAC) samplers. Geomorphology 129 (1–2), 43–48.
Michelena, R.O., Irurtia, C.B., 1995. Suspectibility of soil to wind erosion in La Pampa province, Argentina. Arid Soil Res. Rehabil. 9, 227–234.
R Core Team, 2014. R: A Language and Environment for Statistical Computation. R Foundation for Statistical Computing, Vienna, Austria URL: www.R-project.org.
Ramsperger, B., Peinemann, N., Stahr, K., 1998. Deposition rates and characteristics of aeolian dust in the semi-arid and sub-humid regions of the Argentinean Pampa. J. Arid Environ. 39, 467–476.
Schlichting, E., Blume, H.P., Stahr, K., 1995. Bodenkundliches Praktikum. Hamburg-Berlin. Seas, US Government Printing Office, Washington D.C., pp. 137–169.
Skidmore, E.L., Hagen, L.J., Armburst, D.V., Durar, A.A., Fryrear, D.W., Potter, K.N., Wagner, L.E., Zobeck, T.M., 1994. Methods for investigating basic processes and conditions affecting wind erosion. In: Lal, R. (Ed.), Soil Erosion Research Methods. Soil & W. Cons. Soc, Ankeny, USA, pp. 259–330.
Skidmore, E.L., Layton, J.B., 1992. Dry soil aggregate stability as influenced by selected soil properties. Soil Sci. Soc. Am. J. 56 (2), 557–561.
Sterk, G., Raats, P.A.C., 1996. Comparison of models describing the vertical distribution of wind-eroded sediment. Soil Sci. Soc. Am. J. 60 (6), 1914–1919.
Sterk, G., Parigiani, J., Cittadini, E., Peters, P., Scholberg, J., Peri, P., 2012. Aeolian sediment mass fluxes on a sandy soil in Central Patagonia. Catena 95, 112–123.
Sterk, G., Stein, A., 1997. Mapping wind-blown mass transport by modeling variability in space and time. Soil Sci. Soc. Am. J. 61 (1), 232–239.
Sterk, G., Stein, A., Stroosnijder, L., 2004. Wind effects on spatial variability in pearl millet yields in the Sahel. Soil Tillage Res. 76, 25–37.
Thomas, D.S.G., Wiggs, G.F.S., 2008. Aeolian system responses to global change: challenges of scale, process and temporal integration. Earth Surf. Proc. Land. 33 (9), 1396–1418.
Tidjani, A.D., Bielders, C.L., Rosillon, D., Ambouda, K.J.M., 2011. Uncertainties in plot-scale mass balance measurements using aeolian sediment traps. Soil Water Manage. Conserv. 75 (2), 708–718.
Tsoar, H., Blumberg, D., Stoler, Y., 2004. Elongation and migration of sand dunes. Geomorphology 57, 293–302.
Uzun, O., Kaplan, S., Basaran, M., Saygin, S., Youssef, F., Nouri, A., Ozcan, A., Erpul, G., 2016. Spatial distribution of wind-driven sediment transport rate in a fallow plot in Central Anatolia, Turkey. Arid Land Res. Manage. 31 (2), 1–15.
Visser, S., Sterk, G., Snepvangers, J., 2004. Spatial variation in wind-blown sediment transport in geomorphic units in northern Burkina Faso using geostatistical mapping. Geoderma 120, 95–107.
Walker, I., Nickling, W., 2002. Dynamics of secondary airflow and sediment transport over and in the lee of traverse dunes. Prog. Phys. Geogr. 26 (1), 47–75.
Zarate, M.A., 2003. Loess of southern South America. Quat. Sci. Rev. 22 (18–19), 1987–2006.
Zarate, M.A., Tripaldi, A., 2012. The aeolian system of central Argentina. Aeolian Res. 3, 401–417.
Zhao, H.L., Yi, X.Y., Zhou, R.L., Zhao, X.Y., Zhang, T.H., Drake, S., 2006. Wind erosion and sand accumulation effects on soil properties in Horqin Sandy Farmland, Inner Mongolia. Catena 65 (1), 71–79.
Zobeck, T.M., Popham, T.W., 1990. Dry aggregate size distribution of sandy soils as influenced by tillage and precipitation. Soil Sci. Soc. Am. J. 54 (1), 198–204.
Zobeck, T.M., Sterk, G., Funk, R., Rajot, J.L., Stout, J., van Pelt, R.S., 2003. Measurement and data analysis methods for field-scale wind erosion studies and model validation. Earth Surf. Proc. Land. 28, 1163–1188.
Zobeck, T.M., Baddock, M., Van Pelt, R.S., Tatarko, J., Acosta-Martinez, V., 2013. Soil property effects on wind erosion of organic soils. Aeolian Res. 10, 43–51.

2.2 Horizontal and vertical fluxes of particulate matter during wind erosion on arable land in the province La Pampa, Argentina

International Journal of Sediment Research 37 (2022) 539–552

Contents lists available at ScienceDirect

International Journal of Sediment Research

journal homepage: www.elsevier.com/locate/ijsrc

Original Research

Horizontal and vertical fluxes of particulate matter during wind erosion on arable land in the province La Pampa, Argentina

Nicole Siegmund [a, d, *], Roger Funk [a, *], Michael Sommer [a, d], Fernando Avecilla [b], Juan Esteban Panebianco [b], Laura Antonela Iturri [b, c], Daniel Eduardo Buschiazzo [b, c]

[a] Leibniz Centre for Agricultural Landscape Research (ZALF), Working Group Landscape Pedology, Müncheberg, Germany
[b] Institute of Earth and Environmental Sciences of La Pampa (INCITAP), Santa Rosa, Argentina
[c] National University of La Pampa, Faculty of Agronomy (UNLPam), Santa Rosa, Argentina
[d] Institute of Environmental Science and Geography, University of Potsdam, Potsdam, Germany

ARTICLE INFO

Article history:
Received 30 September 2020
Received in revised form
27 January 2022
Accepted 29 January 2022
Available online 31 March 2022

Keywords:
PM_{10}, $PM_{2.5}$, and $PM_{1.0}$ concentrations
Field measurements
Horizontal flux
Vertical flux
PM balances

ABSTRACT

A detailed analysis of horizontal and vertical particulate matter (PM) fluxes during wind erosion has been done, based on measurements of PM smaller than 10, 2.5, and 1.0 μm, at windward and leeward positions on a measuring field. The three fractions of PM measurement are differently influenced by the increasing wind and shear velocities of the wind. The measured concentrations of the coarser fractions of the fine dust, PM_{10}, and $PM_{2.5}$, increase with wind and shear velocity, whereas the $PM_{1.0}$ concentrations show no clear correlation to the shear velocity. The share of $PM_{2.5}$ on PM_{10} depends on the measurement height and wind speed and varies between 4 and 12 m/s at the 1 m height ranging from 25% to 7% (average 10%), and at the 4 m height from 39% to 23% (average 30%). Although general relationships between wind speed, PM concentration, and horizontal and vertical fluxes could be found, the contribution of the measuring field was very low, as balances of incoming and outgoing fluxes show. Consequently, the measured PM concentrations are determined from a variety of sources, such as traffic on unpaved roads, cattle drives, tillage operations, and wind erosion, and thus, represent all components of land use and landscape structure in the near and far surroundings of the measuring field. The current results may reflect factors from the landscape scale rather than the influence of field-related variables. The measuring devices used to monitor PM concentrations showed differences of up to 20%, which led to considerable deviations when determining total balances. Differences up to 67% between the calculated fluxes prove the necessity of a previous calibration of the devices used.

1. Introduction

Mineral dust emitted by wind erosion is one of the most important sources of atmospheric aerosols and is regarded as an omnipresent key player for atmospheric processes (Knippertz & Stuut, 2014; Shao, 2001). Main source areas of mineral dust are large deserts, but also agriculturally used land in the semiarid and arid climates is of increasing importance with respect to quantities and qualities of emitted dust (Conen & Leifeld, 2014; Steinke et al., 2020). Dust from agricultural land is complex in composition and properties, because it can contain soil and plant derived components, nutrients from fertilizers, agents of pesticides, as well as microbes and micro plastic from sludge or wastewater treatments (Acosta-Martínez et al., 2015; Mendez et al., 2017; Rezaei et al., 2019). Different release processes, such as wind erosion, tillage operations, or crop harvesting contribute to the great variability of agricultural dust (Baker et al., 2005; Funk et al., 2008; Gao et al., 2014; Katra, 2020; Sharratt et al., 2010). As a wide variety of soils is used as arable land to produce food and renewable resources, they represent a huge diversity of sources for dust and the specific particulate matter (PM) fractions with diameters smaller than 10, 2.5, and 1.0 μm in diameter (PM_{10}, $PM_{2.5}$, and $PM_{1.0}$, respectively) (Aimar et al., 2012; Alfaro, 2008; Carvacho et al., 2004). Especially these fine PM fractions have attracted increasing scientific interest in recent years due to their harmful effects on human health and their involvement in pollution and global climate change problems (Imboden et al., 2009; Webb et al., 2020). The direction of the future changes in dust emissions is, thereby, not fully clear (Intergovernmental Panel on Climate Change (IPCC), 2018),

* Corresponding authors.
E-mail addresses: nicole.siegmund@gmx.de (N. Siegmund), rfunk@zalf.de (R. Funk).

https://doi.org/10.1016/j.ijsrc.2022.01.004

although a continuing global trend of conversion from forest or pasture to arable land can be observed (Fehlenberg et al., 2017; Frühauf et al., 2020; NASA, 2020; Viglizzo & Frank, 2006).

Generally, wind erosion initiates three major modes of particle motion: creeping, saltation, and suspension. Because every mode is related to specific grain sizes and transport distances, wind erosion also is a very effective sorting process (Shao, 2000). Generally, there are two quantities to measure within one erosion event: the horizontal saltation flux and the vertical dust flux (Alfaro et al., 2004; Gillette et al., 1997). Reliable measurements of both fluxes are regarded as the most problematic procedures in aeolian research (Goossens & Offer, 2000). The dust or suspension fraction can be released by three processes: (i) direct entrainment of loose particles of this size by wind forces, (ii) abrasion of surface crusts or aggregates by saltating particles, and (iii) breakage of saltating particles or aggregates by collisions (Mirzamostafa et al., 1998). In addition to these mechanical release processes, the soil water content also has a major influence, especially the interstitial water as the last binding agent between coarse and fine particles. The PM_{10} emission potential of sandy soils increased by 10 times after heating to 60 and 105 °C, compared to air-dried conditions (Funk et al., 2008). Silty soils experience doubled PM_{10} emissions, whereas clay and organic soils were not affected by the drying treatments. Since bare soils can be heated up by solar radiation directly at the surface up to 40–60 °C, this aspect deserves consideration when assessing PM emissions of soils.

Direct measurements of PM in the field during wind erosion events are rare (Avecilla et al., 2017; Claiborn et al., 1998; Park et al., 2011), most measurements are made by means of wind tunnels (Edri et al., 2016; Etyemezian et al., 2007; Houser & Nickling, 2001; Li et al., 2015; Panebianco et al., 2016; Singh et al., 2012; Van Pelt et al., 2013, 2017). The available measuring techniques have a number of limitations, so the choice of suitable PM measuring equipment for field campaigns is quite difficult (Amaral et al., 2015; Sharratt & Pi, 2018). Most devices were developed to monitor air quality, the characteristics of which differ considerably from the operational conditions at a field site during wind erosion. The ranges of concentrations and particle sizes to measure are the main parameters to be considered, but also measurement principles, energy consumption, robustness against weather conditions, maintenance requirements, as well as limits in collecting or identifying greater amounts or higher concentrations play important roles in the choice of the appropriate device. Good agreement of the measurement results should also exist between several instruments of the same type in order to calculate reliable values even with small concentration differences. Short measurement intervals are important if a relation to meteorological data is to be established, so that functional dependencies can be derived, especially to the most fluctuating variable wind speed.

Apart from real measurements, computer simulations are another way of researching the complex interdependencies of dust, landscape, and wind. One example is the work of Feng and Ning (2010), simulating sand fluxes over complex microtopography.

Wind erosion processes have been an essential part of soil formation in the Argentinean region of La Pampa (Zarate & Tripaldi, 2012). Today wind erosion is a cause for soil degradation, promoted by frequent strong winds, susceptible soils, and changing land use from former pastures into arable land (Berhongaray et al., 2013; Cabrini et al., 2019). Argentinean soils affected by wind erosion are aeolian deposits of sandy to loamy sand texture. Sandy soils have a tendency toward higher erodibility under cultivation, because of low variation in aggregate formation, while soils with higher clay content have a wider range of aggregation (Leys et al., 1996; Webb & Strong, 2011). Soil losses of 0.9 t/ha were measured on soils of loess material (Buschiazzo et al., 2007) and 1.8 t/ha on a sandy soil, which is on the same order of magnitude as annual dust deposition 0.4–0.8 t/ha (Buschiazzo et al., 1999; Ramsperger et al., 1998). Areas of the Pampa composed of sandy soils have much higher erosion rates, which can be seen as fresh dunes with heights up to 1 m, and fences and roads covered by sandy deposits. Extreme events in the La Pampa region also were monitored repeatedly by satellites (NASA, 2019), showing huge dust plumes over the Atlantic Ocean.

The aim of the current study is a detailed analysis of horizontal and vertical PM fluxes during wind erosion events. The analyses are based on measurements of PM_{10}, $PM_{2.5}$, and $PM_{1.0}$ concentrations at windward and leeward positions on a measuring field on arable land in the Province La Pampa, Argentina. One focus is the subdivision of the PM_{10} fraction by additionally regarding the classes $PM_{2.5}$ and $PM_{1.0}$. Measurements of PM concentrations were taken at two places on a measuring field at two heights and are used to derive horizontal and vertical fluxes and to calculate the balance of incoming and outgoing fluxes of PM on the field. A better description of the functional relations between wind or shear velocity, PM concentration, and horizontal and vertical fluxes will contribute to the improved understanding of the dust emission processes from arable land.

2. Materials and methods

2.1. Site description

The PM measurements were made between November and December 2016 at the Agricultural Experimental Station of Instituto Nacional de TecnologiaAgropecuaria (INTA) in the north-eastern part of Argentina's province La Pampa (63.9885°W and 36.577°S) (Fig. 1). The dimensions of the plot are 240 m in the North–South direction and 60 m in the East–West direction. As part of a former dune field the plot has a gentle topography, with a difference of about 2 m between the deepest and highest positions.

The climate is continental with mean annual values of temperature of 15.8 °C, precipitation of 585 mm, potential evapotranspiration of 1390 mm, and wind velocity of 4.17 m/s. Most of the rain occurs between December and March with about 80 mm per month. The highest wind velocities occur between October and December with wind speeds of 5.5–7 m/s and gusts of about 17 m/s (Aliaga et al., 2016; Casagrande & Vergara, 1996; FAO, 2005).

The predominant grass steppe types (vegetation class: Pampeana, vegetation group: Chaqueño) are altered with semi-open Calden forests, *Prosopiscaldenia* (Cabrera, 1976). The semi-arid region is covered by aeolian sediment of Holocene origin (INTA, 1980, pp. 36–38) and the soil type at the experimental site is a Typic Ustipsamment (U.S. Department of Agriculture (USDA), 1999, p. 436). Texture analysis resulted in a sand content of 76%, a silt content of 16.8%, and a clay content of 6.5%, see Table 1. The texture class is loamy sand (FAO, 2006), having medium to high erodibility following the German classification standard (DIN 19706).

A few days before the planned measurement campaign, the field was tilled with a disc harrow to remove and bury germinated weeds. The tillage direction was from north to south, along the prevailing wind directions. No soil tillage was done between the events from November 18, 2016 to December 12, 2016 (Table 2).

2.2. Dust measurements

2.2.1. Dust monitor calibration

Wind erosion measurements in terms of saltation on the experimental plot have been described in Siegmund et al. (2018), who focused on dust measurements during wind events. Dust concentrations of PM_{10}, $PM_{2.5}$, and $PM_{1.0}$ ($\mu g/m^3$) were measured simultaneously with four Environmental Dust Monitors (EDM)

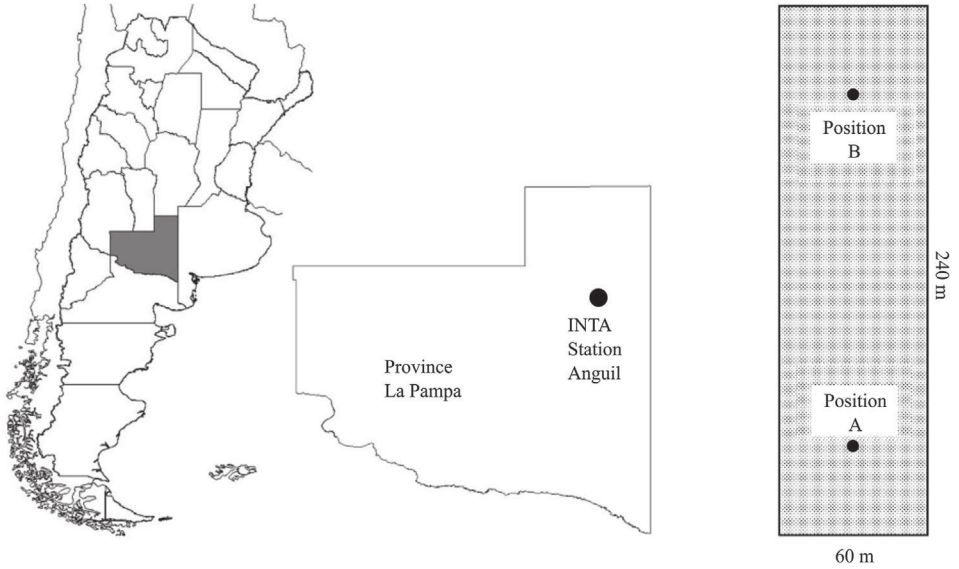

Fig. 1. Location of the experimental plot in the province La Pampa and positions of the PM measurements on the measuring field.

(two EDM107 and two EDM164, GRIMM Aerosol Technique). Both types of EDM count and classify dust particles within a size range from 0.25 to 32 μm in 31 size classes as number per liter (nL^{-1}). The fractions of PM_{10}, $PM_{2.5}$, and $PM_{1.0}$ are determined as mass in μg/m^3. The difference between the two types of EDMs is that the EDM107 represents just the basic device, which aspirates the air just via a 10 cm long omnidirectional probe to the measuring chamber, whereas the EDM164 is installed in a weather housing getting the air via a 50 cm long sampling inlet probe, which can be heated in cases with air humidity >60%. For field use, the EDM107 was placed into a weatherproof box and the inlet of the omnidirectional probe was protected with a spherical sieve against the entry of coarser particles.

All EDMs used have recently passed the company's calibration procedure, but due to the different EDM setups it was decided to do a comparison measurement immediately before the installation at the field site. All inlets of the 4 EDMs were placed directly side by side and a parallel run was started for several hours with the same measuring interval of 1 min that is also used for the planned field measurements. Based on this measurement, adjustment factors (f_{EDM_n}) were calculated using the EDM with the highest accumulated amount of PM_{10}, $PM_{2.5}$, or $PM_{1.0}$ as the reference:

$$f_{EDM_n} = \frac{\sum EDM_{max}}{\sum EDM_n} \quad (1)$$

where $\sum EDM_{max}$ is the maximum value of the summarized PM concentrations during the 2 h among all the EDMs and n is the counter for all other EDMs.

The comparison between the 4 EDMs resulted in deviations of the accumulated values of 15%–20.5% for PM_{10}, 1.2%–13.3% for $PM_{2.5}$, and 1.9%–26.2% for $PM_{1.0}$ in the measured period of time, compared to the EDM which measured the highest amount (= 100%). The differences are highest for PM_{10} as a whole, but they also vary in the smaller fractions of $PM_{2.5}$ and $PM_{1.0}$. A device-dependent trend for the deviations could not be identified. Nevertheless, the deviations are within the accepted tolerance of 25% for PM_{10} measurements of air quality (EC, 2010; SenUVK, 2019), but for flux calculations of expected low to medium concentrations, more correct values are necessary. Using the

Table 1
Soil particle size distribution.

	Degree south	Degree west	Soil depth (cm)	Sand (0.063–2 mm) (%)	Silt (0.006–0.063 mm) (%)	Clay (<0.002 mm) (%)
Position A	36.5783687	63.9879023	0–15	78.7	16.8	4.6
Position B	36.5768567	63.9882065	0–15	74.8	16.8	8.6

Table 2
Parameters of the measured wind erosion events.

Date	Begin–end of event	Duration total event u > 6 m/s (hh:mm)	Wind direction	Mean wind velocity 1 m height (m/s)	Mean friction velocity (m/s)	Wind force integral WFI
November 18, 2016	09:26–14:40	05:14	N	IN: 7.8	0.73	25.130
		04:51		OUT: 8.3	0.66	53.890
November 20, 2016	10:19–17:40	07:21	SSE	IN: 7.0	0.82	33.558
		06:03		OUT: 7.1	0.52	34.749
December 04, 2016	10:50–17:40	06:50	NNE	IN: 8.2	0.70	71.843
		06:41		OUT: 8.3	0.70	78.396
December 10, 2016	10:16–17:53	07:37	WSW	North: 8.1	0.59	77.622
		07:09		South: 8.7	0.76	109.189
December 12, 2016	14:53–19:10	04:17	WSW	North: 8.7	0.59	58.378
		04:14		South: 8.5	0.66	54.881

Table 3
Comparison among the 4 EDMs and derived correction factors.

	Correction factor		
	PM_{10}	$PM_{2.5}$	$PM_{1.0}$
EDM164 Station A	1.205	1.012	1.000
EDM164 Station B	1.150	1.000	1.019
EDM107 No. 1	1.000	1.131	1.262
EDM107 No. 2	1.168	1.133	1.191

correction factors, identical sums of PM were considered for all four EDMs. In the different PM classes different EDMs were determined as the reference (Table 3). There were no clear differences between the two setups for PM_{10}, more similar values were obtained for $PM_{2.5}$ and $PM_{1.0}$ if the two configurations are considered separately.

2.2.2. Field measurements

In the field the EDMs were placed at positions in the north and south of the plot. At each position one EDM164 and one EDM107 were installed, measuring at 1 m and 4 m heights and recording the data in 1-min intervals. The EDM164s are equipped with a two dimensional (2D) ultrasonic anemometer for wind velocity and wind direction and sensors for temperature and air humidity, the EDM107s are equipped with sensors for temperature and air humidity (Fig. 2).

The installation took place in the morning of a day with announced wind speeds above 6 m/s, following the regional threshold indication of De Oro and Buschiazzo (2009). Wind profiles were measured at both positions of the EDM setups with 3 cup anemometers placed at 0.33, 0.85, and 1.67 m heights to estimate shear velocity, u^*, and aerodynamic roughness length, z_0, and to calculate the wind velocity at a height of 4 m from the measurement at 1 m using the logarithmic wind profile equation for neutral stability conditions:

$$u_z = \frac{u^*}{\kappa} \ln\left(\frac{z}{z_0}\right) \tag{2}$$

where u_z is the wind velocity at height z, and κ is the von Karman constant of 0.4. The transport capacity of the wind (W_{tc}, kg/ms) was calculated for every measuring interval using the regional indicated threshold wind velocity (following the approach of De Oro and Buschiazzo (2009)) as follows:

$$W_{tc} = (u - u_t)u^2 \tag{3}$$

where u is the wind velocity and u_t the threshold wind velocity of 6 m/s. W_{tc} is set to zero in the case of $u < u_t$. A comparison between the events is based on the W_{tc} which were summed for the entire duration of each event to comprise the wind force integrals (WFI).

Concentrations of PM_{10}, $PM_{2.5}$, and $PM_{1.0}$ ($\mu g/m^3$) were measured at 1 and 4 m heights and horizontal fluxes, $q(z)$, of PM_{10}, $PM_{2.5}$, and $PM_{1.0}$ ($\mu g/(m^2 \cdot s)$) were calculated from concentration and horizontal velocity with

$$q(z) = c(z)u(z) \tag{4}$$

where $c(z)$ is the concentration at height z. The fluxes at the windward and leeward positions were calculated for simultaneous time and summed for the measuring intervals with $u > u_t$ for each

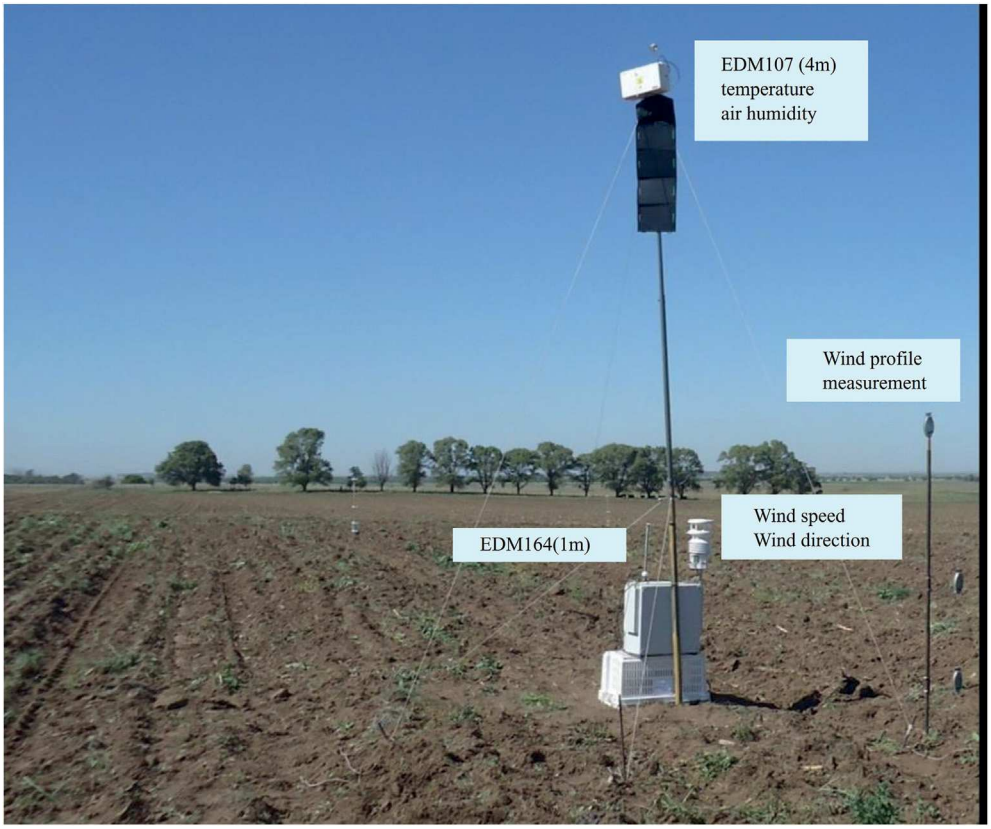

Fig. 2. Installation of the EDMs in the field.

event. As only two measuring heights were available the calculation of the vertical integrated horizontal mass flux, Q, followed the assumption of a log-normal-dependency as follows:

$$q(z) = m\ln z + b \tag{5}$$

where $q(z)$ is the mass flux at height z, and m and b are the empirically determined constants which are determined to be in agreement with the calculation of the vertical fluxes. Integration steps were 1 m following the units of $\mu g/(m^2 \cdot s)$.

$$Q = \int_1^4 q(z)\mathrm{d}z \tag{6}$$

Multiplied with the duration of the event, the discharge or sum of horizontal fluxes of each event was obtained.

The vertical dust fluxes (F_v) were calculated at both positions using

$$F_v = \frac{-\kappa u^*(C_2 - C_1)}{\ln(z_2/z_1)} \tag{7}$$

where C_1 and C_2 are the PM concentrations at the measurement heights z_1 and z_2, respectively. The fluxes were calculated for every measuring interval and summed for the periods when $u > u_t$ for both positions.

Correlation and regression analyses were done with Frontline Systems' Excel Add-In "XLMiner Analysis ToolPak". If not mentioned separately, all analyses meet the 95% confidence level.

In total five erosion events were measured in November–December campaign (Table 2). Three events had wind directions along the longitudinal side of the plot and the dust loaded air passed over both measuring points, designated as IN and OUT. Two events occurred for wind across the main orientation of the plot and hence both measuring points have to be regarded as independent (North and South).

3. Results and discussion

3.1. PM concentrations and horizontal and vertical fluxes

The correlation between the PM concentrations and the shear velocity on the measuring field is shown in Figs. 3–5. The data set was reduced by summarizing mean values for wind speed ranges in steps of 1 m/s (4.1–5 m/s, 5.1–6.0 m/s, …).

The concentrations were at relatively low levels, but in the same range as found by other authors working in the same area (Avecilla et al., 2017) or from areas with similar soils and pasture dominated land use (Hoffmann et al., 2008b). According to a dust storm classification which considers PM_{10} concentrations and wind velocities, the measured events were all in the lowest category of "dusty air" (Hoffmann et al., 2008a; Zeydabadi et al., 2019). These results correspond also to the measured saltation transport, which is characterized by a high spatial variability of closely adjacent erosion/deposition pattern on the plot and soil losses of maximal 0.44 Mg/ha (Siegmund et al., 2018).

The different fractions of PM are influenced by the increasing wind and shear velocities of the wind differently. With increasing with wind and shear velocity, the measured concentrations of the coarser (i.e., PM_{10} and $PM_{2.5}$) fractions of the fine dust also increase, whereas $PM_{1.0}$ concentrations show no clear correlation to the shear velocity, or rather decrease if the events are regarded separately. The coarser fractions also vary with height. The PM_{10} concentrations close to the surface increase strongly with the shear velocity, which occurs in a weakened form at the height of 4 m (see Fig. 3). Thus, the ratio of PM_{10} concentrations at 1 m height to 4 m height also changes with the shear velocity. While Avecilla et al. (2017) show seasonal ratios of PM_{10} concentrations measured in 1.8 and 3.5 m heights of 5.13 in autumn/winter and 1.92 in spring/summer, the current mean ratio for the spring season is 2.56, with a range from about 1 at lower wind velocities of 4 m/s ($u^* = 0.35$ m/s) to 3.5 at higher wind velocities of 12 m/s ($u^* > 1$ m/s).

The $PM_{2.5}$ concentrations also increase with shear velocity, but without distinct differences between 1 and 4 m heights (Fig. 4). $PM_{1.0}$ concentrations are not influenced by wind velocity (Fig. 5). Differences are more affected by the intensities of the individual

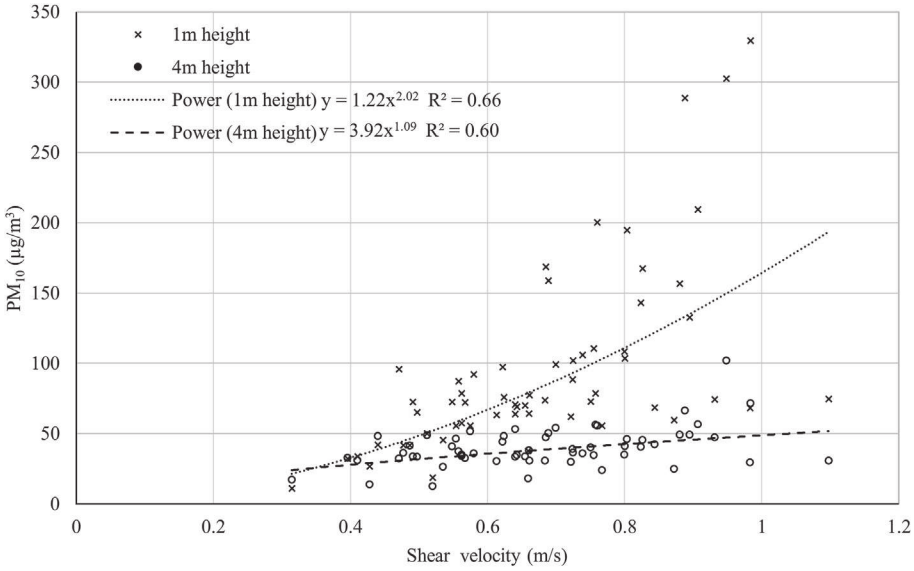

Fig. 3. Measured PM_{10} concentrations at 1 and 4 m heights in relation to shear velocity on the measuring field (note: R^2 is the coefficient of determination).

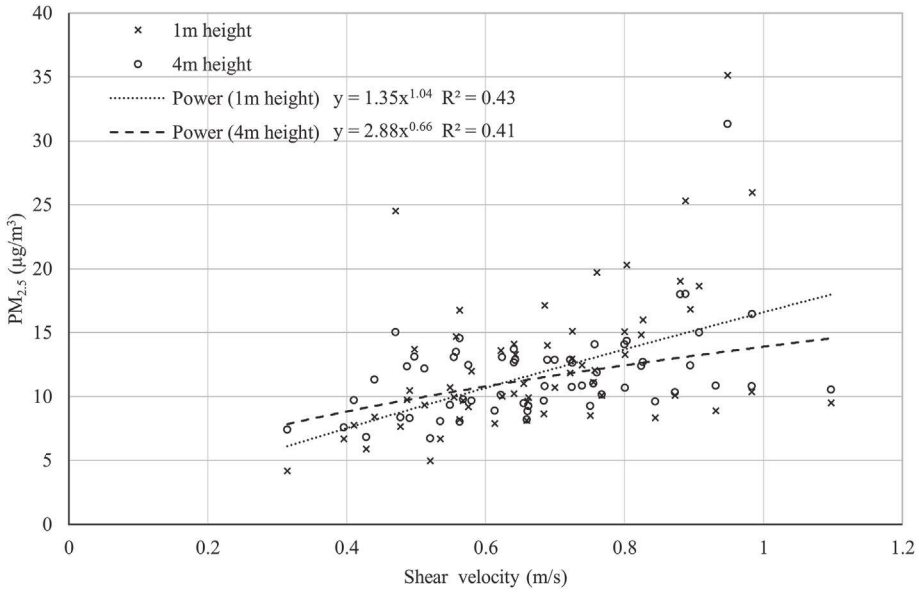

Fig. 4. Measured $PM_{2.5}$ concentrations at 1 and 4 m heights in relation to the shear velocity on the measuring field.

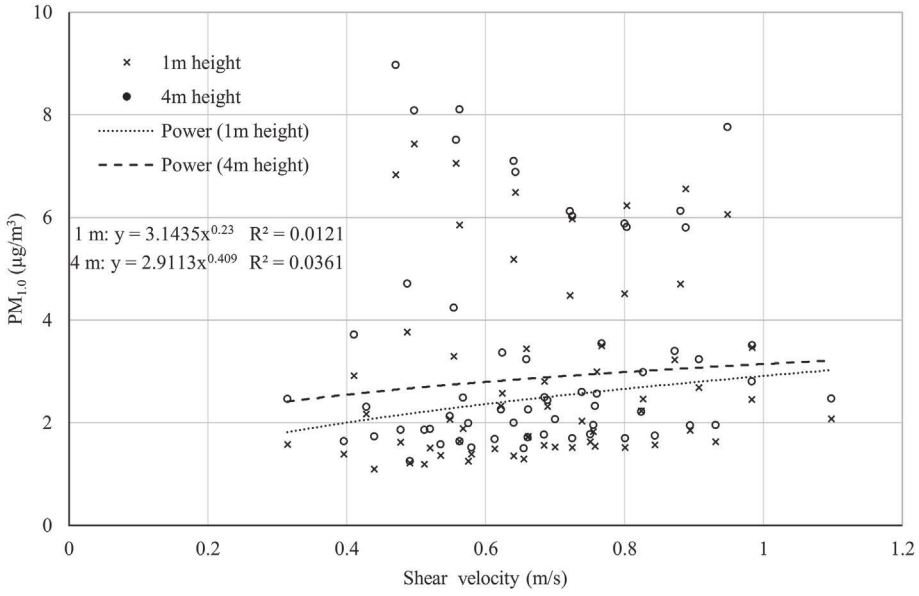

Fig. 5. Measured $PM_{1.0}$ concentrations at 1 and 4 m heights in relation to the shear velocity on the measuring field.

events, which to a lesser extent was the case for the PM_{10} and $PM_{2.5}$ concentrations.

The horizontal fluxes of PM_{10}, $PM_{2.5}$, and $PM_{1.0}$ at both measurement heights, calculated using Eq. (4), are shown in Figs. 6–8. Using wind velocity as a factor results in larger increases for PM_{10} with increasing wind velocity, the exponents for the fitting curves at 1 and 4 m heights increase both by 1. The horizontal flux of PM_{10} is still higher at the ground at the 1m height, but $PM_{2.5}$ and $PM_{1.0}$ have higher horizontal fluxes at the 4 m height due to the higher wind velocity and only small concentration differences between the heights.

Fig. 9 shows these total horizontal fluxes of PM_{10}, $PM_{2.5}$, and $PM_{1.0}$ as functions of the wind force integrals (WFI). Since the exponential increase of the transport capacity is already included in the WFI calculation, a linear relation can be derived for the discharge of PM.

One important parameter to describe the composition of PM emissions is the $PM_{2.5}/PM_{10}$ ratio. At 1 m height $PM_{2.5}$ is 10.7% of the PM_{10} load, at 4 m height the share increases to 27.9% (Fig. 10). The $PM_{2.5}/PM_{10}$ ratio is, thus, variable over the height, which means that it is also necessary to indicate the height of the measurements when showing this relation. The $PM_{2.5}/PM_{10}$ ratio close to the surface at 1 m height corresponds to ratios estimated in suspension chambers or wind tunnels to describe emission potentials of soils, and thus, represents a maximum of all involved fractions, while at a height of 4 m the ratio shifts towards the finer $PM_{2.5}$ fraction as a result of advanced sorting processes, mainly decreasing shares of the PM_{10} fraction (Carvacho et al., 2004; Funk et al., 2008). The average $PM_{2.5}/PM_{10}$ ratio of the total fluxes is 19.9%. There also is a dependency of the $PM_{2.5}/PM_{10}$ ratio on the wind speed. The ratio decreases at 1 m height linearly from 25% at 4 m/s to 7% at 12 m/s ($y = -2.157x + 32.8$; $R^2 = 0.58$), and

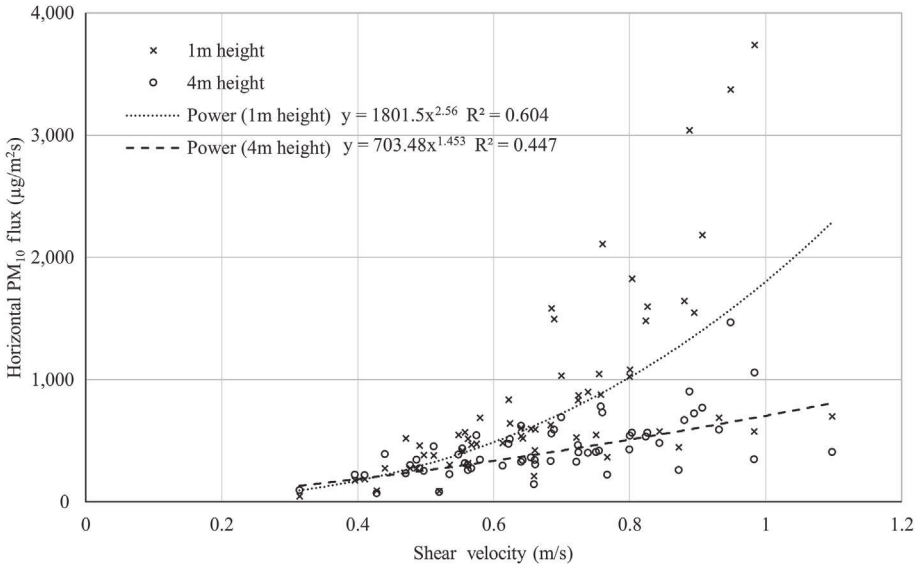

Fig. 6. Horizontal flux of PM_{10} at 1 and 4 m heights in relation to the shear velocity on the measuring field.

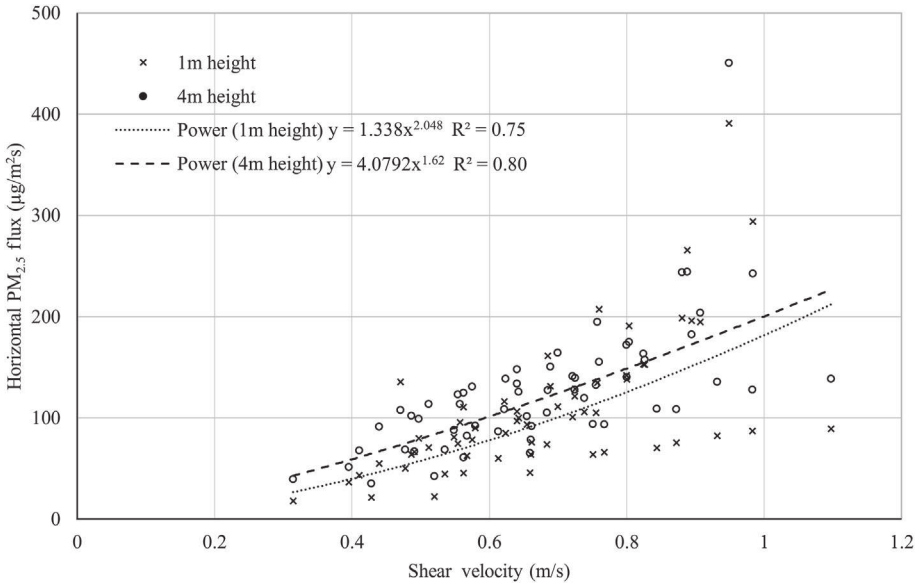

Fig. 7. Horizontal flux of $PM_{2.5}$ at 1 and 4 m heights in relation to the shear velocity on the measuring field.

decreases at 4 m height from 39% at 4 m/s to 23% at 12 m/s ($y = -1.951x + 46.5$; $R^2 = 0.22$).

The vertical fluxes of PM were calculated from the concentration differences at both heights (Eq. (7)). Here, positive values indicate an upward and, negative values indicate a downward direction of the flux (Figs. 11–13). The vertical flux of PM_{10} shows the typical exponential increase with higher shear velocities, with a clear upward directed flux (Fig. 11). This continues, to a lesser extent for $PM_{2.5}$ (Fig. 12), with already increasing shares of downward fluxes. The vertical fluxes of $PM_{1.0}$ have a decreasing correlation to the shear velocity and are dominated by downward directed fluxes (Fig. 13).

The relation between horizontal and vertical PM fluxes is shown in Figs. 14–16. There is a close correlation between both for PM_{10} with the vertical flux equaling a constant share of about 2% of the horizontal flux (Fig. 14). The vertical fluxes of $PM_{2.5}$ are less than 1% of the horizontal fluxes (Fig. 15), and the vertical fluxes of $PM_{1.0}$ are not correlated to the horizontal and show rather a decreasing trend (Fig. 16).

The PM_{10} discharges (sum of the fluxes) of each event had no significant correlation ($p > 0.05$) to the saltation, measured at heights below 1 m with the Modified Wilson and Cooke samplers (MWAC) in Siegmund et al. (2018), although a tendency becomes clear, because both processes are influenced by the wind or shear velocity (Fig. 17).

There was no correlation to the MWAC placed next, nor to the MWAC placed in front of the PM measurement with regard to the corresponding wind direction. This can be explained by the very low intensity of the saltation fluxes; their great spatial heterogeneity on the measuring field, characterized by intermittent

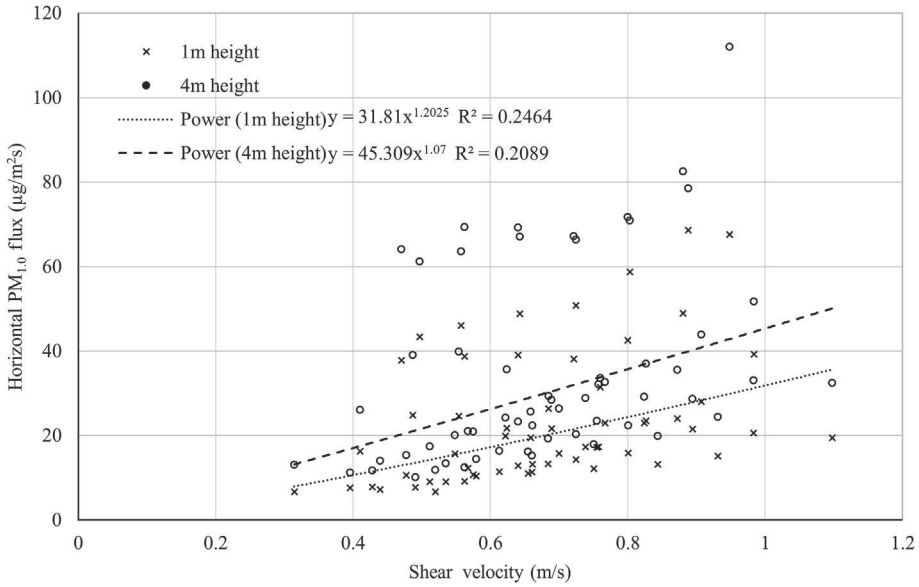

Fig. 8. Horizontal flux of $PM_{1.0}$ at 1 and 4 m heights in relation to the shear velocity on the measuring field.

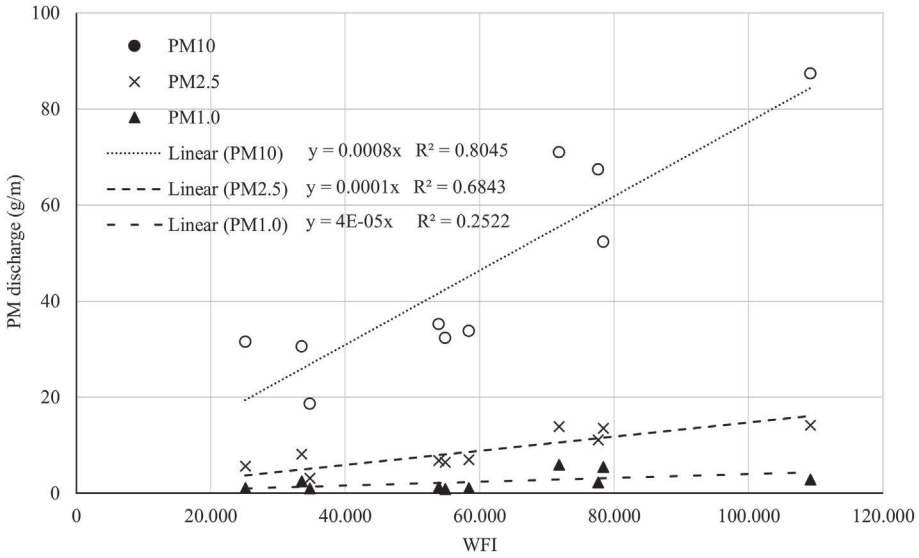

Fig. 9. PM discharge (1–4 m height) at both positions in relation to the transport capacity of the wind for each event expressed by the wind force integrals (WFI).

erosion and deposition during an event; and the already high base load of PM in the incoming air. The measured saltation fluxes were highest at the windward borders of the measuring field because both North and South sides have slope directions into the wind. Further, saltation could not develop continuously because of relatively good roughness and stable aggregation of the soil surface after preparing the field with a disc harrow under good soil moisture conditions.

3.2. Balances of incoming and outgoing PM

The calculated discharges of PM were used to make balances between the windward (IN) and leeward (OUT) positions on the plot. The points are 160 m apart. Only the first three events could be considered, where the wind crossed the measuring field in the longitudinal direction (Table 4). The events of December 10th and 12th are listed here only for the purpose of completeness.

Generally, the additional contribution of the measuring field on the total PM load can be characterized as a sink rather than a source for PM. The vertical profiles of the IN and OUT positions for the 3 events show three completely different relations, which can only be explained by including the spatial variability of the saltation transport and the chronological sequence of the events (Fig. 18).

Only the first event after the tillage at November 18, 2016 showed an increase of the PM fluxes over the measuring field close to the surface, resulting in 10% of the total discharge. In Siegmund et al. (2018) this event had the lowest average transport rate of saltation (580 g/m^2) and a negative soil loss was calculated. The saltation transport rate was constant within the first two thirds of the measuring field, resulting in a balanced deposition of material in the transport direction, which increased shortly before the point of the PM measurement and decreased strongly after this point, resulting in a negative balance of saltation for the entire field. The PM load, or suspension fraction, will not be affected in such a direct

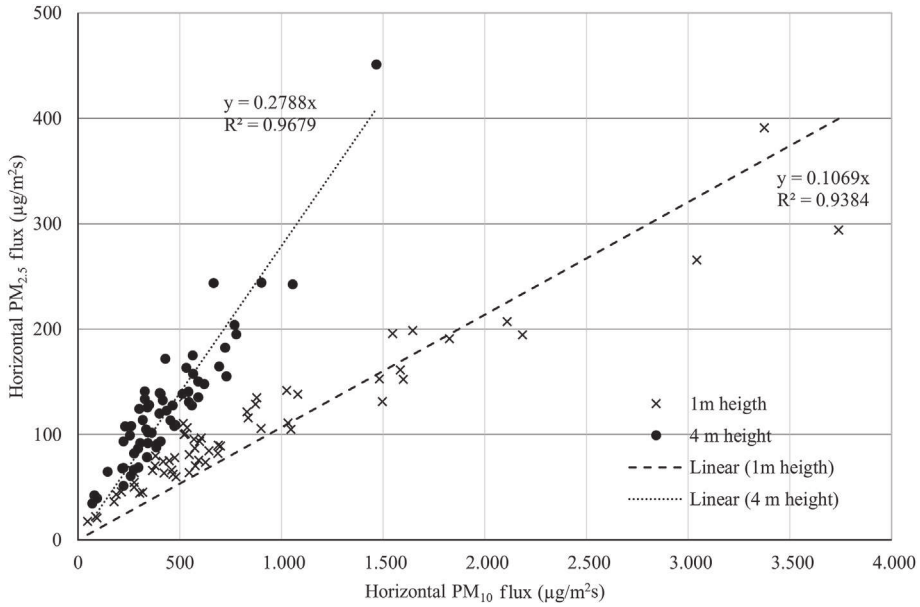

Fig. 10. Relation of horizontal fluxes of PM_{10} and $PM_{2.5}$ at 1 and 4 m heights (regression lines are forced through zero).

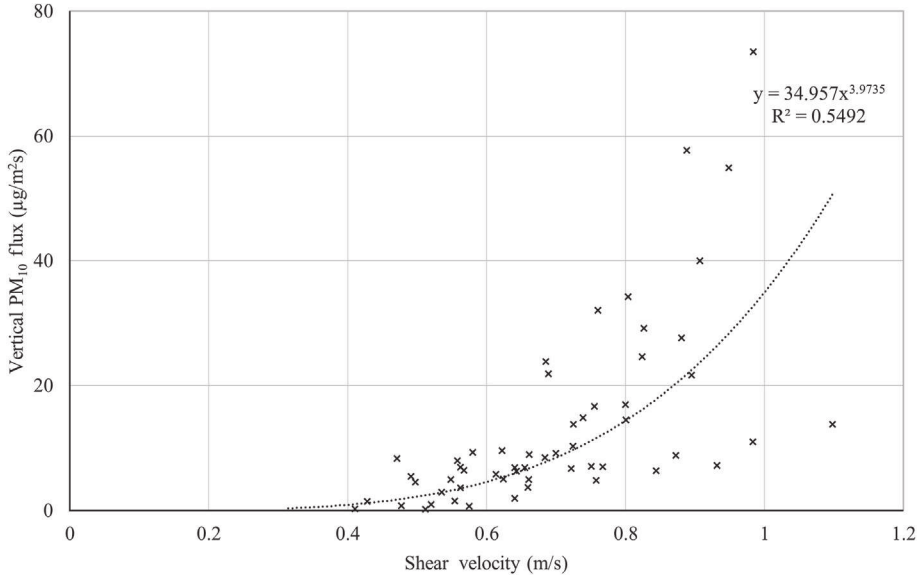

Fig. 11. Vertical flux of PM_{10} in relation to the shear velocity (two values below zero have been removed).

way, and, once emitted, particles remain in the air stream for a certain time. That can be seen in the vertical profiles at the IN and OUT positions. The horizontal flux of PM_{10} remains relatively constant at the height of 4 m, whereas at 1 m height the flux increases as a result of the increasing saltation shortly before the measurement point. Theoretically, a minimum distance of about 50 m is needed ($u = 8$ m/s, $u^* = 0.7$ m/s) to mix particles from the surface to the height of 4 m, so that this repeated rise of the saltation transport is not reflected in the PM_{10} values at 4 m height. Thus, drawing conclusions about a direct area relation between the saltation and PM fluxes on the measuring field is difficult.

The wind of the next event at November 20, 2016 came from the opposite direction, which resulted in a different erosion and deposition pattern, caused by the opposite windward and leeward positions of the relief. The average transport rate of saltation was 600 g/m^2, and, therefore, was similar to that in the previous event. This event was characterized by a fast increase of the saltation transport intensity within the first 50 m of the measuring field remaining constant for the rest of the distance. The vertical profile of the PM_{10} fluxes shows equal values at 1 m height and a distinct decrease at 4 m height (Fig. 18). Probably most PM_{10} was already emitted during the first event, and the saltation flux was not intense enough to release new dust particles. Also the highest air humidity was measured, which is a parameter that lowers PM emissions. So, in total a negative emission rate was calculated, indicating deposition rather than emission of PM on the measuring field.

The event at December 04, 2016 was characterized by the highest wind velocities with the WFI twice as much as the previous events (see Table 2) resulting in an average saltation transport rate

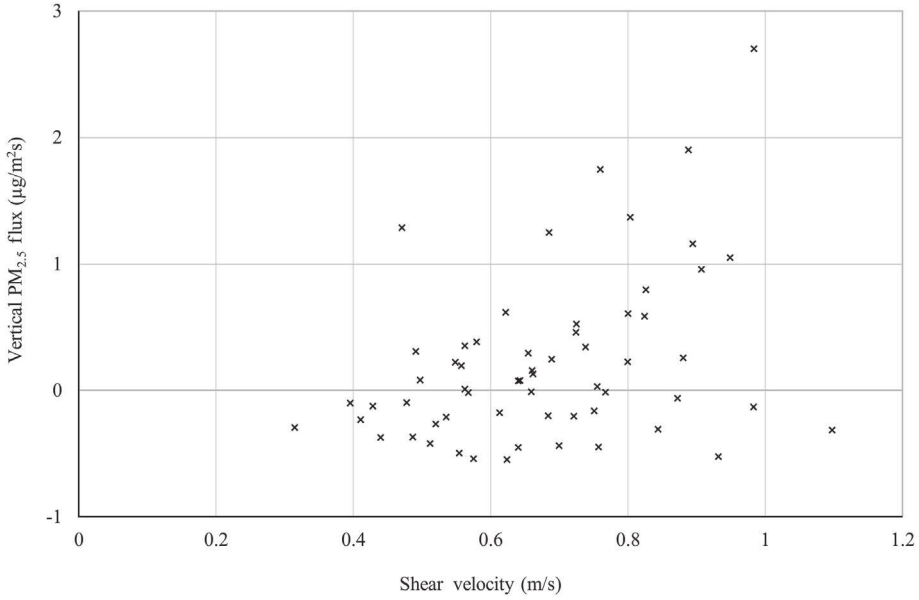

Fig. 12. Vertical flux of $PM_{2.5}$ in relation to the shear velocity.

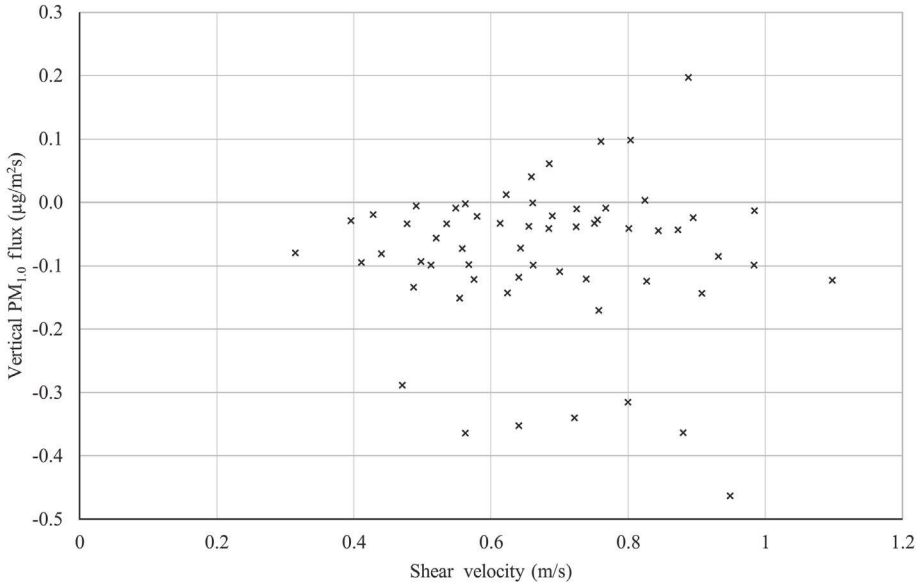

Fig. 13. Vertical flux of $PM_{1.0}$ in relation to the shear velocity.

of 920 g/m^2. Nevertheless, the saltation transport rates at the center line were not very different from the previous events. A strong increase of saltation was recorded in the last quarter, but without any influence on the horizontal PM fluxes. The PM profiles (Fig. 18) show distinctly higher horizontal flux over the entire height of the incoming air at the measuring point. The outgoing PM fluxes are constantly lower, so the highest negative horizontal fluxes of PM were calculated, indicating deposition processes. The measuring field, therefore, contributes to no further PM emissions. The reason for this is the limited availability of erodible material, which had been exhausted after two previous erosion events. So, only very limited material for the main driving process of PM release, saltation, was available. The turbulent dispersion of the PM load of the incoming air also continues above the measuring field and without additional PM emissions from the measuring field the concentrations decrease just by dispersion and deposition.

3.3. Additional considerations

The soil of the plot belongs to the soil type loamy sand, which has been identified as less affected by drying effects on PM release (Funk et al., 2008; Hoffmann & Funk, 2015). The binding forces caused by the interstitial water are stable enough to maintain established connections between the particles in the air-dry status, as found during the field measurements. Only after further artificially forced drying in the oven at 60 and 105 °C increased PM emissions from this soil type could be initiated. This condition would correspond to intensive solar radiation over several hours at the field site and this condition was not reached during the measurement campaign in spring, 2016.

Although generally low PM concentrations were measured, they are in accordance with measurements in the same region (Avecilla et al., 2017) or on similar soils and land uses, as in the steppe

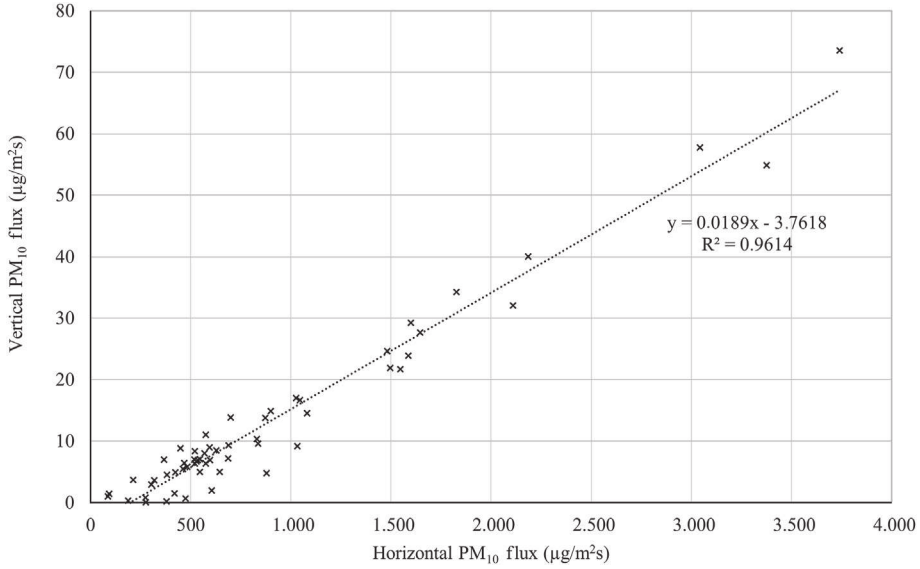

Fig. 14. Correlation between the horizontal and vertical fluxes of PM_{10}.

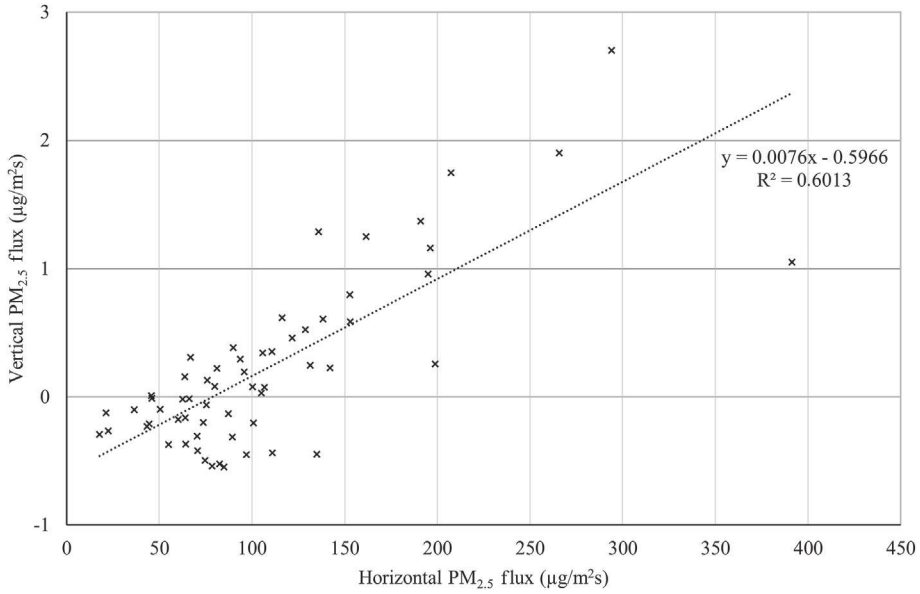

Fig. 15. Correlation between the horizontal and vertical fluxes of $PM_{2.5}$.

regions of Inner Mongolia dominated by pastureland (Hoffmann et al., 2008b).

Air humidity has been identified as a further influencing factor on PM emissions of soils (Ravi et al., 2004) with a threshold of 20% in this region determined by Avecilla et al. (2017). In the current measurement campaign air humidity fell below this value only during the last erosion event (December 12, 2016), without any detectable effect. Most likely, the previous events led to the depletion of the transportable surface material and the effects of air humidity are only relevant if all other factors stay constant.

The measuring devices used to monitor PM concentrations showed differences of up to 20%, which have to be considered, especially if the PM concentrations are low, as was the case in the current study which was below 50 $\mu g/m^3$. Also different setups of the PM measuring devices (EDM 164 and EDM 107) influence the results and should be compared prior to field measurements are made. The tolerances, acceptable under other operating conditions, can lead to considerable deviations when determining total balances, i.e., the direct comparison of the calculated fluxes at two or more measuring points. Differences up to 67% between the calculated fluxes prove the necessity of a previous calibration of the measuring devices.

The share of $PM_{2.5}$ on PM_{10} depends on the measurement height and wind speed and varies between 4 and 12 m/s at 1 m height from 25% to 7% (average 10%), and at 4 m height from 39% to 23% (average 30%). Thus, the external conditions represent a substantial influence and should always be mentioned when determining this ratio.

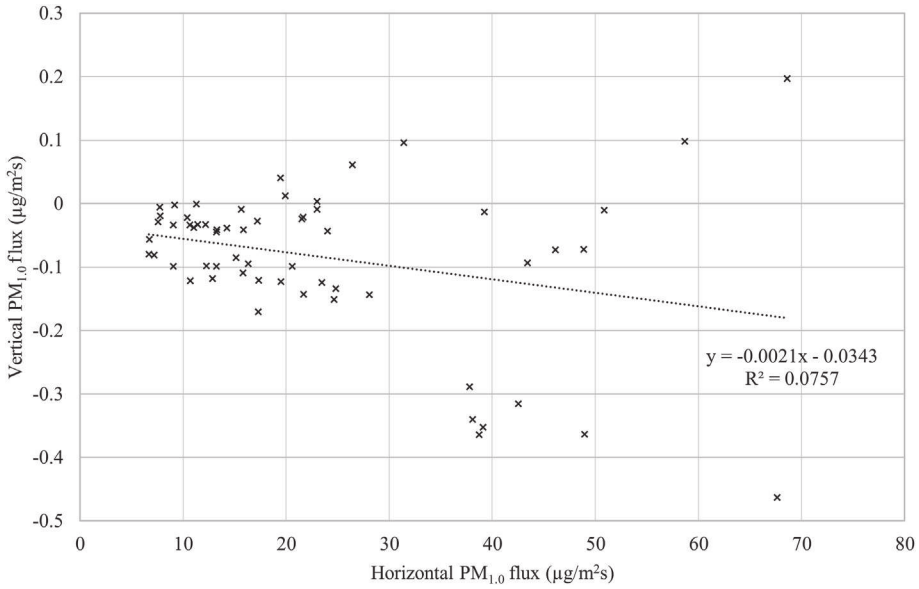

Fig. 16. Correlation between the horizontal and vertical fluxes of $PM_{1.0}$.

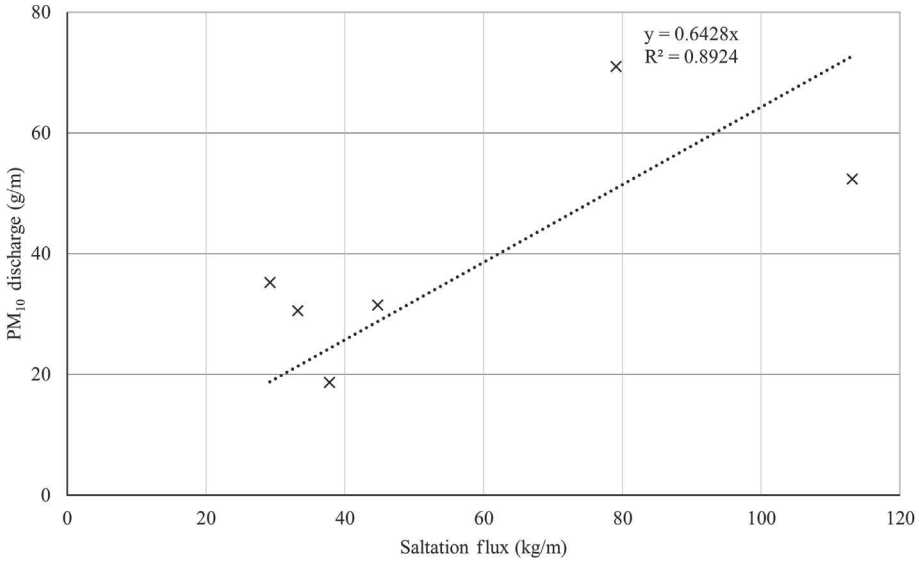

Fig. 17. Correlation between the saltation and the PM_{10} discharge at the IN and OUT positions forthe events on November 18 and 20 and December 04, 2016.

The high spatial variability of the wind induced transport processes on the measuring field has been discussed already in Siegmund et al. (2018). The generally low saltation transport can be regarded as the cause for the low PM emissions. Without saltation a fast depletion of the surface material occurs (Houser & Nickling, 2001), and now material can only be made available by a repeated disturbance of the surface by tillage. Thus, tillage is the decisive factor for the susceptibility of these soils to wind erosion. Soil forms sufficiently stable aggregates if tilled under moist conditions. By choosing the right time and tillage tool a good aggregate size distribution can be guaranteed, which is stable enough to resist devastating wind erosion on these soil types. At low soil moisture levels, repeated mechanical stress (driving, trampling by cattle, tillage) causes pulverization of the soil, which strongly promotes wind erosion and PM emissions. Consequently, natural factors have less effect than the anthropogenic factors which are determining the wind erosion processes. In summary it can be concluded that to

Table 4
PM_{10}, $PM_{2.5}$, $PM_{1.0}$ discharge (sum of horizontal flux) between 1 and 4 m height for each event at the corresponding "IN" and "OUT" stations.

Date	Position	Horizontal flux (g/m)		
		PM_{10}	$PM_{2.5}$	$PM_{1.0}$
November 18, 2016	IN (B)	31.54	5.68	1.07
	OUT (A)	35.27	6.84	1.24
	OUT–IN	3.73	1.16	0.17
November 20, 2016	IN (A)	30.55	8.20	2.51
	OUT (B)	18.69	3.12	0.97
	OUT–IN	−11.86	−5.08	−1.54
December 04, 2016	IN (B)	71.03	13.87	5.90
	OUT (A)	52.38	13.52	5.44
	OUT–IN	−18.65	−0.35	−0.46
December 10, 2016	South (A)	87.39	14.21	2.87
	North (B)	67.43	11.09	2.24
December 12, 2016	South (A)	32.36	6.48	0.91
	North (B)	33.81	6.97	1.05

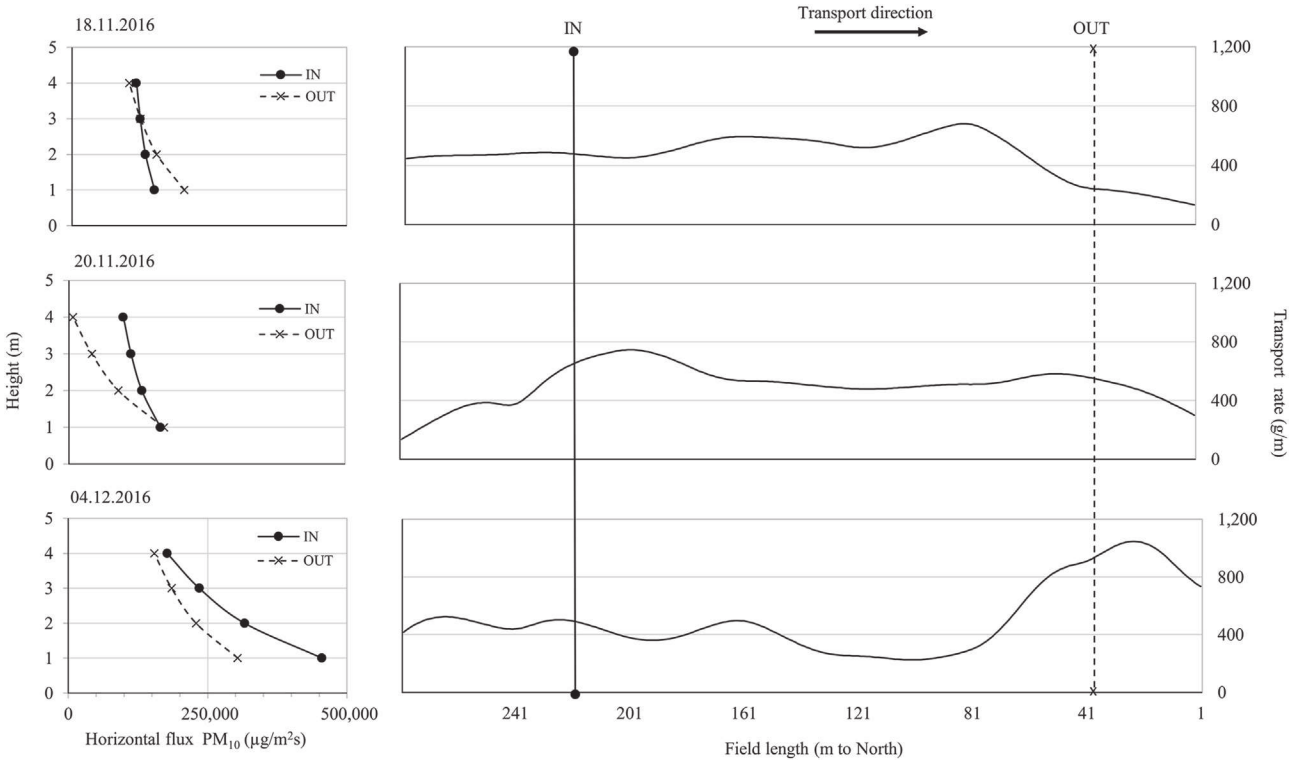

Fig. 18. Vertical profiles of the horizontal fluxes at the IN and OUT position of the measuring field (left), and corresponding saltation transport rate at the center line of the field from Siegmund et al. (2018) (right), curve forthe event at November 20, 2016 has been turned to have the same direction.

a certain extent, the wind erosion risk can be managed with a careful, soil property-adapted tillage strategy.

4. Conclusions

A detailed analysis of horizontal and vertical PM fluxes during wind erosion has been done, based on measurements of PM_{10}, $PM_{2.5}$, and $PM_{1.0}$ concentrations at windward and leeward positions on a measuring field. Although generally low PM concentrations were measured, they are in accordance with measurements in the same region (Avecilla et al., 2017) or on similar soils and land uses, as in the steppe regions of Inner Mongolia dominated by pasture land (Hoffmann et al., 2008b). While concentrations and fluxes of PM_{10} showed a clear dependency on shear velocity or wind speed (WFI) and measurement height, this dependency gradually decreased for $PM_{2.5}$ and $PM_{1.0}$. Although general relations between wind speed, PM concentration, and horizontal and vertical fluxes could be found, the PM contribution of the measuring field was very low, documented by the balances of incoming and outgoing fluxes. Consequently, the measured PM concentrations are determined by a variety of sources, such as traffic on unpaved roads, cattle drives, tillage operations, and wind erosion, and thus, represent all components of land use and landscape structure in the near and far surroundings of the measuring field. Unlike wind erosion measurements, external influences are difficult to eliminate in PM measurements. The currentresults may, therefore, be more likely reflecting factors from the landscape scale rather than being influenced by field-related variables.

Declaration of competing interest

The authors declare that they have no known competing financial interests or personal relationships that could have appeared to influence the work reported in this paper.

Acknowledgements

This study was supported by the joint project “Multiscale analysis of quantitative and qualitative fine particulate matter emissions from agricultural soils of La Pampa, Argentina” funded by the Deutsche Forschungsgemeinschaft (DFG) of Germany (Grant No. DFG-GZ: Fu 247/10-1) and the National Council for Research and Technology of Argentina (CONICET).

Disclaimer

Trade names or commercial products are only mentioned for the purpose of exact description and transparency of the methods used. They are neither recommendations nor endorsements.

References

Acosta-Martínez, V., Van Pelt, S., Moore-Kucera, J., Baddock, M. C., & Zobeck, T. M. (2015). Microbiology of wind-eroded sediments: Current knowledge and future research directions. *Aeolian Research, 18*, 99–113.

Aimar, S. B., Mendez, M. J., Funk, R., & Buschiazzo, D. E. (2012). Soil properties related to potential particulate matter emissions (PM_{10}) of sandy soils. *Aeolian Research, 3*, 437–443.

Alfaro, S. C. (2008). Influence of soil texture on the binding energies of fine mineral dust particles potentially released by wind erosion. *Geomorphology, 93*, 157–167.

Alfaro, S. C., Rajot, J. L., & Nickling, W. (2004). Estimation of PM_{20} emissions by wind erosion: Main sources of uncertainties. *Geomorphology, 59*, 63–74.

Aliaga, V. S., Ferrelli, F., Alberdi-Algañaraz, E. D., Bohn, V. Y., & Piccolo, M. C. (2016). Distribución y variabilidad de la precipitaciónen la regiónPampeana, Argentina. *Cuadernos de InvestigaciónGeográfica, 42*(1), 261–280. *(In Spanish)*

Amaral, S., de Carvalho, J., Jr., Costa, M., & Pinheiro, C. (2015). An overview of particulate matter measurement instruments. *Atmosphere, 6*, 1327–1345.

Avecilla, F., Panebianco, J. E., & Buschiazzo, D. E. (2017). Meteorological conditions during dust (PM_{10}) emission from a tilled loam soil: Identifying variables and thresholds. *Agricultural and Forest Meteorology, 244–245*, 21–32.

Baker, J. B., Southard, R. J., & Mitchell, J. P. (2005). Agricultural dust production in standard and conservation tillage systems in the San Joaquin Valley. *Journal of Environmental Quality, 34*, 1260–1269.

Berhongaray, G., Alvarez, R., De Paepe, J., Caride, C., & Cantet, R. (2013). Land use effects on soil carbon in the Argentine Pampas. *Geoderma, 192*, 97–110.

Buschiazzo, D. E., Zobeck, T. M., & Abascal, S. (2007). Wind erosion quantity and quality of an Entic Haplustoll of the semi-arid pampas of Argentina. *Journal of Arid Environments, 69*, 29–39.

Buschiazzo, D. E., Zobeck, T. M., & Aimar, S. B. (1999). Wind erosion in loess soils of the Argentinian Pampas. *Soil Science, 164*(2), 133–138.

Cabrera, A. L. (1976). Regiones fitogeográficas argentinas. In W. F. Kugler (Ed.), *Enciclopedia Argentina de Agricultura y jardineria II* (pp. 1–85). Buenos Aires: Acme. *(In Spanish)*

Cabrini, S. M., Portela, S. I., Cano, P. B., & López, D. A. (2019). Heterogeneity in agricultural land use decisions in Argentine Rolling Pampas: The effects on environmental and economic indicators. *Cogent Environmental Science, 5*, 1667709.

Carvacho, O. F., Ashbaugh, L. L., Brown, M. S., & Flocchini, R. G. (2004). Measurement of $PM_{2.5}$ emission potential from soil using the UC Davis resuspension test chamber. *Geomorphology, 59*, 75–80.

Casagrande, G., & Vergara, G. (1996). Característicasclimática de la region. In D. E. Buschiazzo, J. L. Panigatti, & F. J. Babinec (Eds.), *Labranzas en la region semiárida Argentina* (pp. 11–19). Instituto Nacional de Tecnologia Agropecuaria (INTA). *(In Spanish)*

Claiborn, C., Lamb, B., Miller, A., Beseda, J., Clode, B., Vaughan, J., Kang, L., & Newvine, C. (1998). Regional measurements and modeling of windblown agricultural dust: The Columbia Plateau PM_{10} Program. *Journal of Geophysical Research, 103*(D16), 19753–19767.

Conen, F., & Leifeld, J. (2014). A new facet of soil organic matter. *Agriculture, Ecosystems & Environment, 185*, 186–187.

De Oro, L., & Buschiazzo, D. E. (2009). Threshold wind velocity as an index of soil susceptibility to wind erosion under variable climatic conditions. *Land Degradation & Development, 20*, 14–21.

DIN 19706:2013-02. Soil quality - determination of the soil exposure risk from wind erosion. Deutsches Institut für Normung e.V. (German National Standard), 2013-02, Beuth Verlag. doi: 10.31030/1934215.

Edri, A., Dody, A., Tanner, S., Swet, N., & Katra, I. (2016). Variations in dust-related PM_{10} emission from an arid land due to surface composition and topsoil disturbance. *Arabian Journal of Geosciences, 9*, 607.

Etyemezian, V., Nikolich, G., Ahonen, S., Pitchford, M., Sweeney, M., Purcell, R., … Kuhns, H. (2007). The portable in situ wind erosion laboratory (PI-SWERL): A new method to measure PM_{10} windblown dust properties and potential for emissions. *Atmospheric Environment, 41*, 3789–3796.

European Commission (EC). (2010). *European commission working group on guidance for the demonstration of equivalence of ambient air monitoring methods*.. Retrieved from https://ec.europa.eu/environment/air/quality/legislation/pdf/equivalence.pdf. (Accessed 15 April 2020).

Fehlenberg, V., Baumann, M., Gasparri, N. I., Piquer-Rodriguez, M., Gavier-Pizarro, G., & Kuemmerle, T. (2017). The role of soybean production as an underlying driver of deforestation in the South American Chaco. *Global Environmental Change, 45*, 24–34.

Feng, S., & Ning, H. (2010). Computational simulations of blown sand fluxes over the surfaces of complex microtopography. *Environmental Modelling & Software, 25*(3), 362–367.

Food and Agricultural Organization (FAO). (2005). *New_LocClim. Local climate estimator*. Rome: FAO and DeutscherWetterdienst (DWD)., 2005.

Food and Agricultural Organization (FAO). (2006). *Guidelines for soil description* (4th ed.). U.N. Food and Agricultural Organization Rome.

Frühauf, M., Guggenberger, G., Meinel, T., Theesfeld, I., & Lentz, S. (2020). *KULUNDA: Climate smart agriculture. South siberian agrosteppe pioneering region for sustainable landuse*. Cham, Switzlerland: Springer.

Funk, R., Reuter, H. I., Hoffmann, C., Engel, W., & Öttl, D. (2008). Effect of moisture on fine dust emission from tillage operations on agricultural soils. *Earth Surface Processes and Landforms, 33*, 1851–1863.

Gao, F., Feng, G., Sharratt, B., & Zhang, M. (2014). Tillage and straw management affect PM_{10} emission potential in subarctic Alaska. *Soil and Tillage Research, 144*, 1–7.

Gillette, D. A., Fryrear, D. W., Gill, T. E., Ley, T., Cahill, T. A., & Gearhart, E. A. (1997). Relation of vertical flux of particles smaller than 10 μm to total aeolian horizontal mass flux at Owens Lake. *Journal of Geophysical Research, 102*, 26009–26015.

Goossens, D., & Offer, Z. Y. (2000). Wind tunnel and field calibration of six aeolian dust samplers. *Atmospheric Environment, 34*, 1043–1057.

Hoffmann, C., & Funk, R. (2015). Diurnal changes of PM_{10}-emission from arable soils in NE-Germany. *Aeolian Research, 17*, 117–127.

Hoffmann, C., Funk, R., Sommer, M., & Li, Y. (2008a). Temporal variations in PM_{10} and particle size distribution during Asian dust storms in Inner Mongolia. *Atmospheric Environment, 42*, 8422–8431.

Hoffmann, C., Funk, R., Wieland, R., Li, Y., & Sommer, M. (2008b). Effects of grazing and topography on dust flux and deposition in the Xilingele grassland, Inner Mongolia. *Journal of Arid Environments, 72*, 792–807.

Houser, C., & Nickling, W. G. (2001). The emission and vertical flux of particulate matter <10 μm from a disturbed clay-crusted surface. *Sedimentology, 48*, 255–267.

Imboden, M., Schwartz, J., Schindler, C., Curjuric, I., Berger, W., Liu, S. L. J., Russi, E., Ackermann-Liebrich, U., Rochat, T., & Probst-Hensch, N. (2009). Decreased PM_{10} exposure attenuates age-related lung function decline: Genetic variants in p53, p21, and CCND1 modify this effect. *Environmental Health Perspectives, 117*, 1420–1427.

Instituto Nacional de TecnologiaAgropecuaria (INTA). (1980). *Caracterización general de la provincia* (pp. 36–38). Buenos Aires: Inventariointegrado de losrecursosnaturales de la provincia de La Pampa. *(In Spanish)*

Intergovernmental Panel on Climate Change (IPCC). (2018). *AR 6, chapter 2: Land-climate interactions*. Cambridge University Press. Available at: https://www.ipcc.ch/site/assets/uploads/2019/08/2c.-Chapter-2_FINAL.pdf. (Accessed 17 April 2020).

Katra, I. (2020). Soil erosion by wind and dust emission in semi-arid soils due to agricultural activities. *Agronomy, 10*(1), 89.

Knippertz, P., & Stuut, J.-B. (2014). *Mineral dust. A key player in the earth system*. Dordrocht, The Netherlands: Springer Science+Business.

Leys, J. F., Koen, T., & McTainsh, G. H. (1996). The effect of dry aggregation and percentage clay on sediment flux as measured by a portable field wind tunnel. *Australian Journal of Soil Research, 34*, 849–861.

Li, H., Tatarko, J., Kucharski, M., & Dong, Z. (2015). $PM_{2.5}$ and PM_{10} emissions from agricultural soils by wind erosion. *Aeolian Research, 19*, 171–182.

Mendez, M. J., Aimar, S. B., Aparicio, V. C., Ramirez Haberkon, N. B., Buschiazzo, D. E., De Gerónimo, E., & Costa, J. L. (2017). Glyphosate and aminomethylphosphonic acid (AMPA) contents in the respirable dust emitted by an agricultural soil of the central semiarid region of Argentina. *Aeolian Research, 29*, 23–29.

Mirzamostafa, N., Hagen, L. J., Stone, L. R., & Skidmore, E. L. (1998). Soil aggregate and texture effects on suspension components from wind erosion. *Soil Science Society of America Journal, 62*, 1351–1361.

National Aeronautics and Space Administration (NASA). (2019). *Earth obversatory*. Available at: https://earthobservatory.nasa.gov/search?q=Argentina+dust. (Accessed 11 June 2020).

National aeronautics and space administration (NASA). (2020). Available at: https://earthobservatory.nasa.gov/images/146731/deforestation-in-argentinas-gran-chaco. (Accessed 11 June 2020).

Panebianco, J. E., Mendez, M. J., & Buschiazzo, D. E. (2016). PM_{10} emission, sandblasting efficiency and vertical entrainment during successive wind-erosion events: A wind tunnel approach. *Boundary-Layer Meteorology, 161*, 335–353.

Park, M.-S., Park, S.-U., & Chun, Y. (2011). Improved parametrization of dust emission (PM_{10}) fluxes by the gradient method using the Naiman tower data at the Horqin Desert in China. *The Science of the Total Environment, 412/413*, 265–277.

Ramsperger, B., Peinemann, N., & Stahr, K. (1998). Deposition rates and characteristics of aeolian dust in the semi-arid and sub-humid regions ofthe Argentinean Pampa. *Journal of Arid Environments, 39*(3), 467–476.

Ravi, S., D'Odorico, P., Over, T. M., & Zobeck, T. M. (2004). On the effect of air humidity on soil susceptibility to wind erosion: The case of air-dry soils. *Geophysical Research Letters, 31*, L09501.

Rezaei, M., Riksen, M. J. P. M., Sirjani, E., Sameni, A., & Geissen, V. (2019). Wind erosion as a driver for transport of light density microplastics. *Science ofthe Total Environment, 669*, 273–281.

SenUVK. (2019). *PM_{10} Äquivalenznachweis für die automatischen Geräte des Typs Grimm-EDM180 für das Jahr 2018. Senatsverwaltung für Umwelt, Verkehr und Klimaschutz Berlin*. Available at: https://www.berlin.de/senuvk/umwelt/luftqualitaet/de/messnetz/download/pm10-aequinachweis_berlin_2018.pdf. (Accessed 31 March 2020). (*In German*).

Shao, Y. (2000). *Physics and modelling of wind erosion*. Dordrecht, The Netherlands: Atmospheric and Oceanographic Sciences Library.

Shao, Y. (2001). A model for mineral dust emission. *Journal of Geophysical Research, 106*(D17), 20239–20254.

Sharratt, B., & Pi, H. (2018). Field and laboratory comparison of PM_{10} instruments in high winds. *Aeolian Research, 32*, 42–52.

Sharratt, B., Wendling, L., & Feng, G. (2010). Windblown dust affected by tillage intensity during summer fallow. *Aeolian Research, 2*, 129–134.

Siegmund, N., Funk, R., Koszinsky, S., Buschiazzo, D. E., & Sommer, M. (2018). Effects of low-scale landscape structures on aeolian transport processes on arable land. *Aeolian Research, 32*, 181–191.

Singh, P., Sharratt, B., & Schillinger, W. F. (2012). Wind erosion and PM_{10} emission affected by tillage systems in the world's driest rainfed wheat region. *Soil and Tillage Research, 124*, 219–225.

Steinke, I., Hiranuma, N., Funk, R., Höhler, K., Tüllmann, N., Umo, N. S., … Leisner, T. (2020). Complex plant-derived organic aerosol as ice-nucleating particles - more than a sum of their parts? *Atmospheric Chemistry and Physics, 20*(14), 11387–11397.

U.S. Department of Agriculture (USDA). (1999). *Soil taxonomy: Abasic system of soil classification for making and interpreting soil surveys* (2nd ed.). Natural Resources Conservation Service Handbook.

Van Pelt, R. S., Baddock, M. C., Zobeck, T. M., D'Odorico, P., Ravi, S., & Bhattachan, A. (2017). Total vertical sediment flux and PM_{10} emissions from disturbed Chihuahuan Desert surfaces. *Geoderma, 293*, 19–25.

Van Pelt, R. S., Baddock, M. C., Zobeck, T. M., Schlegel, A. J., Vigil, M. F., & Acosta-Martinez, V. (2013). Field wind tunnel testing of two silt loam soils on the North American Central High Plains. *Aeolian Research, 10*, 53–59.

Viglizzo, E. F., & Frank, F. C. (2006). Ecological interactions, feedbacks, thresholds and collapses in the Argentine Pampas in response to climate and farming during the last century. *Quaternary International, 158*, 122–126.

Webb, N. P., Kachergis, E., Miller, S. W., McCord, S. E., Bestelmeyer, B. T., Brown, J. R., … Zwicke, G. (2020). Indicators and benchmarks for wind erosion monitoring, assessment and management. *Ecological Indicators, 110*, 105881.

Webb, N. P., & Strong, C. L. (2011). Soil erodibility dynamics and its representation for wind erosion and dust emission models. *Aeolian Research, 3*, 165–179.

Zarate, M. A., & Tripaldi, A. (2012). The aeolian system of central Argentina. *Aeolian Research, 3*, 401–417.

Zeydabadi, A., Naddafi, K., Nabizadeh, R., Hassanvand, M. S., & Golpaygani, A. G. (2019). Determination of dust storms by Hoffman index in Tehran, Iran and compare with remote sensing, and responsible organizations from March 2014 through March 2015. *Journal of Air Pollution and Health, 4*, 261–268.

2.3 From Gustiness to Dustiness - The Impact of Wind Gusts on Particulate Matter Emissions in Field Experiments in La Pampa, Argentina

atmosphere

MDPI

Article

From Gustiness to Dustiness—The Impact of Wind Gusts on Particulate Matter Emissions in Field Experiments in La Pampa, Argentina

Nicole Siegmund [1,2,*], Juan E. Panebianco [3], Fernando Avecilla [3], Laura A. Iturri [3,4], Michael Sommer [1,2], Daniel E. Buschiazzo [3,4] and Roger Funk [1,*]

1 WG Landscape Pedology, Leibniz Institute for Agricultural Landscape Research (ZALF e.V.), 15374 Müncheberg, Germany; sommer@zalf.de
2 Institute of Environmental Science and Geography, University of Potsdam, 14469 Potsdam, Germany
3 Institute of Earth and Environmental Sciences of La Pampa (INCITAP), Santa Rosa L6302, Argentina; juanpanebianco@yahoo.com (J.E.P.); ferave85@hotmail.com (F.A.); antonelaiturri@hotmail.com (L.A.I.); debuschiazzo@yahoo.com (D.E.B.)
4 Facultad de Ciencias Exactas y Naturales, National University of La Pampa (UNLPam), Santa Rosa L6302, Argentina
* Correspondence: nicole_siegmund@gmx.de (N.S.); rfunk@zalf.de (R.F.)

Abstract: This study delivers the first empirical data-driven analysis of the impact of turbulence induced gustiness on the fine dust emissions from a measuring field. For quantification of the gust impact, a new measure, the Gust uptake Efficiency (GuE) is introduced. GuE provides a percentage of over- or under-proportional dust uptake due to gust activity during a wind event. For the three analyzed wind events, GuE values of up to 150% could be found, yet they significantly differed per particle size class with a tendency for lower values for smaller particles. In addition, a high-resolution correlation analysis among 31 particle size classes and wind speed was conducted; it revealed strong negative correlation coefficients for very small particles and positive correlations for bigger particles, where 5 µm appears to be an empirical threshold dividing both directions. We conclude with a number of suggestions for further investigations: an optimized field experiment setup, a new particle size ratio ($PM_1/PM_{0.5}$ in addition to $PM_{10}/PM_{2.5}$), as well as a comprehensive data-driven search for an optimal wind gust definition in terms of soil erosivity.

Keywords: wind gusts; wind erosion; particle uptake; dust plumes

Citation: Siegmund, N.; Panebianco, J.E.; Avecilla, F.; Iturri, L.A.; Sommer, M.; Buschiazzo, D.E.; Funk, R. From Gustiness to Dustiness—The Impact of Wind Gusts on Particulate Matter Emissions in Field Experiments in La Pampa, Argentina. *Atmosphere* **2022**, *13*, 1173. https://doi.org/10.3390/atmos13081173

Academic Editors: Venkataraman Sivakumar, Hassan Benchérif and Eduardo Landulfo

Received: 23 June 2022
Accepted: 14 July 2022
Published: 25 July 2022

1. Introduction

Wind erosion is a widespread problem on agricultural land around the globe. To varying degrees, all climatic zones and all farming systems are affected [1]. Associated dust emissions influence physical and chemical processes in the atmosphere, impair air quality and disturb other ecosystems far away from the source areas [2]. Dust emitted from agricultural land has a ten times higher ice nucleation efficiency compared with desert dust and can be connected to local extreme thunderstorms in north-central Argentina [3,4]. The onsite effects are losses of organic matter (OM), silt, and clay particles, resulting generally in a deterioration of the physical and chemical properties of soil [5]. Since soils susceptible to wind erosion have only small shares of OM, silt, and clay, these losses contribute over-proportionally to soil degradation and are of high relevance for sustainable agriculture [6,7].

The province of La Pampa in Argentina is particularly affected due to its semi-arid climate, soils susceptible to wind erosion, and a gradual but steady land use change from pasture to arable land, with the consequence that soil surfaces are longer and more frequently exposed to wind without protection by vegetation [8,9]. Despite quite homogeneous soil conditions in large areas, wind erosion processes have a strong spatial variability

caused by little variations in other controlling parameters such as field length, landscape structure, or topography [10,11].

Wind, or moving air as the driver of wind erosion, is characterized by unsteadiness directly at the surface. This turbulent characteristic of the atmospheric boundary layer causes rapid fluctuations of the wind velocity. Historically, the consideration of wind gusts was closely connected to the development of the measuring techniques and various definitions exist. Most of them are based on a certain, absolute, or relative exceedance of an average. Wind gusts can be expressed by a gust factor G, describing the ratio of the wind speed within the gust to the average wind speed ($G = u_{max}/u$) [12]. The World Meteorological Organization (WMO) recommends defining a gust as the 3 s average of a 10 min sampling period, but gust factors have been derived for various measurement and averaging times [13,14]. Wind velocity fluctuations result in temporal variations in the transport intensities during wind erosion events. Most research is related to the saltation load or sand transport, which provides an immediate and distinct response to wind velocity or wind friction velocity fluctuations [15–19]. Wind fluctuations and saltation transport have been measured in temporal high resolution in many studies with devices for wind speed such as ultrasonic or hot wire anemometers, and for saltating grains with the Saltiphon (Eijkelkamp Soil and Water, [20]), the Sensit (Sensit Inc, [21]), or the Safire (Sabatech, [22]). The underlying measuring principle is the detection of impacts of colliding grains on a membrane. This is not applicable for dust particles, as their impacts are not strong enough, their particle number concentrations are too high, or they follow the air stream around the sensors because of their low inertia. Dust measurements are mainly based on technologies collecting or counting particles over a certain time. Thus, there are discrepancies in the possible measurement intervals of wind (5–20 Hz), saltation (~1 Hz), and dust (0.1–0.016 Hz).

Wind gusts over erodible surfaces lead to sudden occurrence of saltation streamers, which again initiate discontinuous, locally limited emissions of dust particles. The challenge for the measurement methodology here is that saltation and suspension cannot be measured together at the point of origin for technical reasons. This is only possible after separation of the two transport forms, i.e., after traveling a certain distance. As the settling velocity of dust particles is very low, they are mixed into much higher heights, and thus are not as directly affected by turbulent fluctuations of the flow as saltating particles [23]. The particles of the PM_{10} fraction remain in suspension for long times once airborne [24]. Their transport is often equated to that of momentum, as used for approximated flux calculations in turbulence-dominated boundary layers [25–27]. The long residence time of these particles in the atmosphere and the resulting long transport distances, make it clear that the dust concentrations measured at a particular location cannot be directly attributed to the surface properties below the measuring point or of the immediate surroundings. The measured quantity is rather the result of all windward located sources, called 'footprint' and representing the relative influence of all effective source areas upwind [28–32]. This is extremely difficult in a landscape such as that in La Pampa, due to the mobility of strong point sources of dust (tillage and harvest operations, traffic on unpaved roads), their distribution over large areas (cattle drives), and their discontinuity in time and space. Therefore, one strategy in measuring dust emissions on arable land is to place at least one measuring point relatively close above the surface to have a clear signal of the windward surroundings.

In field trials, all these aspects must be taken into account and brought together [33]. In this study, this micro-meteorological phenomenon is regarded from a data analytics-based perspective by quantifying the impact of peak values of dust concentrations on the overall dust uptake during wind erosion events.

The approach of this study therefore follows a hypothesis that was already brought forth by [34]: Gusts extraordinarily contribute to the gust uptake during a wind event. The statistical analyses presented here underline this hypothesis and deliver statistically robust proof.

This approach is new, because the fundamental mechanic of gusts contributing to the material uptake in wind erosion processes has historically been mentioned and suggested but never statistically quantified using field measurements.

2. Materials and Methods

2.1. Site Description

Wind, wind erosion, and dust concentrations were measured in the northeastern part of Argentina's province La Pampa at the experimental Station of the National Institute for Agricultural Technology (INTA) in Anguil (63.9885° W and 36.577° S). The topography of the site is characterized by soft hills with max elevation changes of 10 m. A measuring field was installed with a size of 1.44 ha (240 × 60 m) located within other agricultural land but surrounded by pastureland in its immediate vicinity. A direct input of saltating soil particles from the neighborhood were excluded, which was valid for the dust fraction in a limited way, whose origin may be also much more remote (Figure 1).

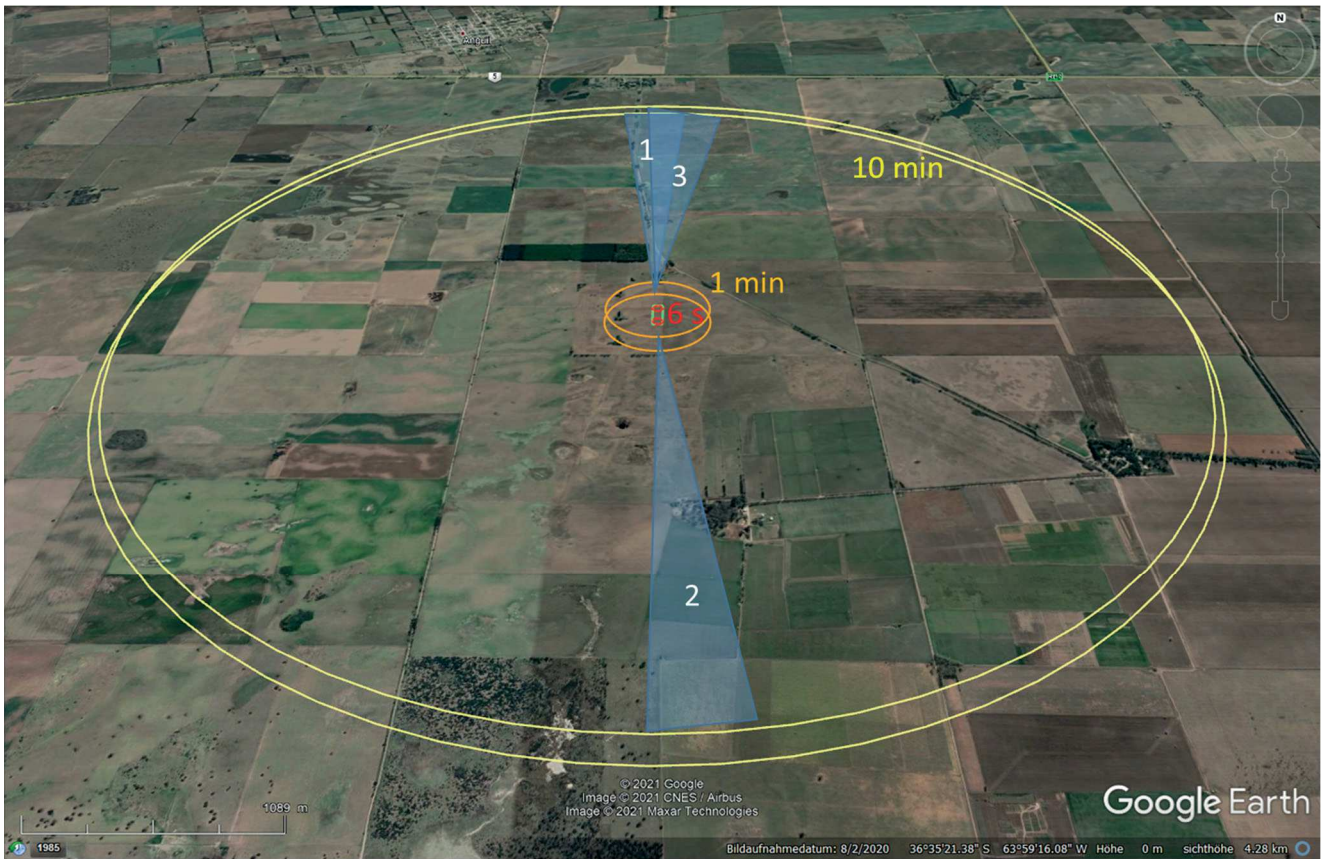

Figure 1. Location of the measuring field and travelled distance of air and particulate matter for both measuring points at the test field (green rectangle) for a wind velocity of 6 m s^{-1} and different measuring intervals (red circles: 6 s—highest temporal resolution of the EDM164; orange circles: 1 min—regular interval of the EDM164; yellow circles: 10 min—common interval of long-term meteorological measurements); blue sectors mark the wind directions of the three considered events.

The soil at the measuring field is a Typic Ustipsamment developed from aeolian deposits of Holocene origin with a sand content of 76%, a silt content of 17%, and a clay content of 7%. The texture class is loamy sand resulting in a medium to high susceptibility to wind erosion. The carbon content of the field varies between 0.5 and 1.8%, with the higher values at the higher relief positions [11].

2.2. Wind and Dust Measurements

The measurements took place between March and December 2016, of which 6 days with continuous measurements are in the focus of this study. The selection was made according to the prevailing wind direction of the day; only days were selected on which the wind came in the direction of the longitudinal orientation of the measurement field, in this case from north or south. Due to the opposite wind directions, we do not address the station "north" and "south" in the ongoing manuscript, but rather name "IN" and "OUT" instead. The measurement equipment was setup as shown in Figure 2. A comprehensive description of the study site can be found in [11].

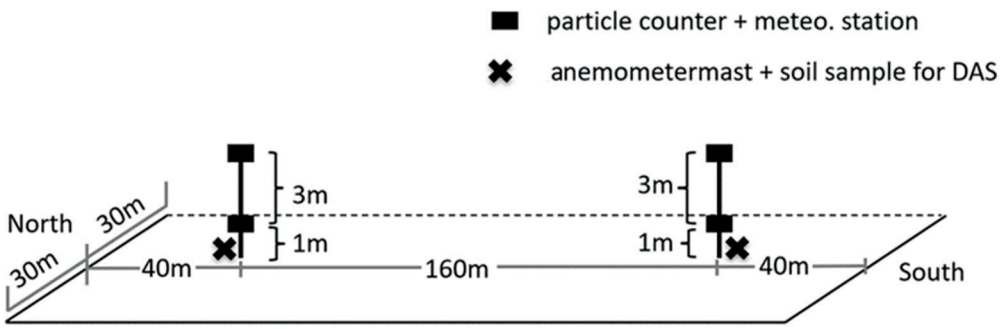

Figure 2. Experimental setup of the dust monitor, the meteorological.

Two compact all-in-one-weather stations (WS500-UMB, Lufft Mess- und Regeltechnik GmbH, Fellbach, Germany) measured temperature, air humidity, air pressure, wind velocity, and wind direction at a height of 1 m. Wind velocity and direction were measured with 2 D ultrasonic sensors. They have no moving parts and can therefore be used without concern even in dusty environmental conditions without affecting their measuring accuracy over time. Furthermore, they are not influenced by inertia and thus have a short reaction time to changes in wind velocity. The weather stations are connected to Environmental Dust Monitors of the type EDM164 (GRIMM Aerosol Technique GmbH, Ainring, Germany), where all data are stored together in one data logger. Dust concentrations were measured with four dust monitors in total, two EDM164 and two EDM107 at heights of 1 and 4 m, respectively. The relatively low height of 1 m for a dust measurement was chosen to achieve a large proportion of the measured quantities from the area of the measurement field, with 40 m to the field boundary at the "IN" position and 200 m at the "OUT" position. Both types of EDM measure mass concentrations of PM_{10}, $PM_{2.5}$, and PM_1 (in µg m^{-3}) and particle concentrations (in n dm^{-3}) for particle sizes between 0.25 and 32 µm in 31 classes.

The wind velocity (u) was used to calculate the transport capacity of the wind (W_{tc}) [35] for all wind velocities above a certain threshold (u_t) with:

$$W_{tc} = (u - u_t)\, u^2 \quad (1)$$

Additionally, wind measurements with three anemometers in the heights of 0.4, 0.8, and 1.6 m were used to derive the friction velocity u_* at the "IN" and "OUT" position from the logarithmic wind profiles as 1 h average several times per day.

$$u_* = \kappa \frac{(u_{z_2} - u_{z_1})}{(\ln z_2 - \ln z_1)} \quad (2)$$

where z_1 and z_2 are height 1 and 2; and u_{z1} and u_{z2} are the respective wind velocities at these locations.

The common measuring interval of the EDM is one minute, the shortest possible interval six seconds. The shortest interval of the connected weather station has five seconds. The smallest joint interval of both is 1 min. Therefore, the statistical measures are related to 10 values per minute for particulate matter and particles, and to 12 values per minute for

wind velocity. Compared with micrometeorological measurements the measuring intervals are quite large; however, for a landscape-related approach they are sufficient [13,36].

2.3. Derivation of Gusts

Wind gusts over bare land lead to sudden occurrences of saltation streamers, which initiate dust emissions running over a certain distance and can often be observed around noon or early afternoon. For identification and quantification of the impact of such gusts, we need a clear definition of such comparatively short-term events. Historically, a wide range of definitions of wind gusts exist. Most of them (e.g., the WMO's definition) are based on a certain exceedance of a threshold. For example, a 5 m s^{-1} higher wind speed than the average of the previous 10 min. Such definitions are only applicable for events/situations with relatively stationary wind speeds without mid-term trends which is the case at all three events of this study. Moreover, they are not appropriate for the comparison between events with different levels of average wind speed.

Thus, in this study, we define a gust as a wind speed which is at least 10% higher than the average of the previous 10 measurements. In the literature, higher threshold values can sometimes be found, ranging from 30% to 50%. This is because they normally refer to higher resolution measurement data. In this study, we used 1 min averages and thus, the threshold must be comparatively low to catch the important events. The final gust definition regarding the 10 min average interval also was derived by explorative analyses, where other gust definitions were also tested (e.g., a maximum change between two points in time or visibility graphs). In the results section it is shown that the chosen threshold definition captures all the relevant wind gusts. We can write the evidence of a gust (g) at a point in time (t):

$$g_t = \theta\left[\frac{v_t}{avg(v_{t-1} : v_{t-10}) * GIC}\right] \quad (3)$$

where v_t is the wind speed at time t and θ denotes the Heaviside step function here defined as θ (x) = 0 for ($v_t - 6$) <= 0 and θ (x) = 1 for ($v_t - 6$) > 0. We define GIC as the gust intensity coefficient, where the latter was set to 1.1 (i.e., 10% higher) for the purpose of our study. GIC defines the relative exceedance of the wind velocity of a gust in comparison to the average within the regarded time interval.

It should be noted that this approach is related to, but not identical with anomaly calculation of time series. Here one would rather relate a point in time to the surrounding (i.e., previous and following) points in time. Such an approach would not be suitable for this study, because we are specifically interested in events that occur suddenly, whereas the wind speed values following the gust are not of interest.

Because the EDM collect data in one-minute averages, the actual wind speed maximums during that one-minute gust can be weighted higher than the average. For the wind transport capacity, this is a bit lower. Hence, the 10% gust definition should catch most of the gusts. To quantify the impact of the wind gusts on the aerosol uptake, we defined the Gust uptake Efficiency (GuE):

$$GuE = \frac{PM_{gust1.1}}{PM_{total}} * 100 \quad (4)$$

where $PM_{gust1.1}$ is the average particulate matter concentration during gusts (using the gust definition described above with a GIC of 1.1) and PM_{total} is the average particulate matter concentration during all other times. If the wind gusts have an over-proportional impact on particle uptake, the GuE should be above 100%.

3. Results

3.1. Influence of Measuring Intervals on Mean Wind Velocity and Transport Capacity

The standard for estimating the mean wind, set by the WMO, is the 10 min average [13]. At the beginning of our campaign, we measured three events with the highest temporal

resolution of 5 s (03.03., 09.03. and 26.08. 2016). We average (upscale) these values from 5 s measuring to 1 min intervals in order to compare the results between the two setups: 5 s and 1 min averages. This analysis is used to analyze the influence of the measuring intervals on mean wind velocity. These three events cover a wide range of wind velocities and can be considered as weak, medium, and strong events. The frequency distribution of the measured wind velocities is shown in Figure 3; the frequency of each velocity class is on the left side, the summarized curves are at the right side. The wind velocity is 4 m s^{-1} (measured in a height of 1 m); the threshold shows that during the event at 03.03.2016 just 20% of all winds were above the threshold, about 70% at the 09.03.2016 and almost all wind velocities were above the threshold at the 26.08.2016 (Figure 3, right panel). It must be noted that the 4 m s^{-1} threshold is only used for illustration purposes here, the value is not used for any further statistical analyses. Taking into account earlier work from [34], the threshold is a rather variable value depending on meteorological conditions. Hence, the threshold can range between low values in winter and high values in autumn.

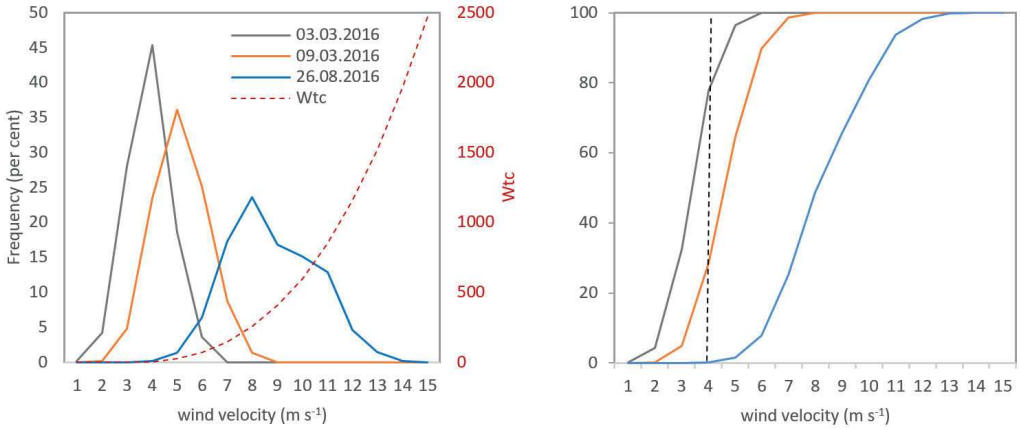

Figure 3. Frequencies of wind velocities of the three measuring campaigns; left: absolute values, W_{tc} for a threshold of 4 m s^{-1}; right: summarized values.

The relationship between the maximum wind velocity of the 5 s intervals and the 1 min averages is shown in Figure 4. In general, all events are on the same line, with a slight increasing tendency of the 5 s maxima at higher values of the 1 min averages, which is reflected in the increasing values of the slopes (m) of the regression lines. The maximum wind peaks are 18 to 24% higher than the averages, with a decreasing tendency at increasing average wind velocity. If these slopes are regarded as the gust factor, they are closer to the recommended conversion factors for open sea than for land surfaces [37].

The comparison of the transport capacity of the wind (Wtc) calculated from the 1 min averages and the mean of the 5 s intervals shows similar decreasing differences at increasing wind velocity (Figure 5). The weak event at the 03.03.2016 has a 52.2% higher transport capacity if the 5 s intervals are used for calculation, the medium event has 27.1% higher values, and the strong event comes even closer to the values of the 1 min averages, with only 8.4% higher values. This shows again that longer average time intervals cut the peaks of wind speed and therefore to a greater extent the transport capacity, which is derived from wind speed by an exponential relationship [38,39]. Lower wind speeds are more affected because individual wind peaks tend to be eliminated completely due to averaging.

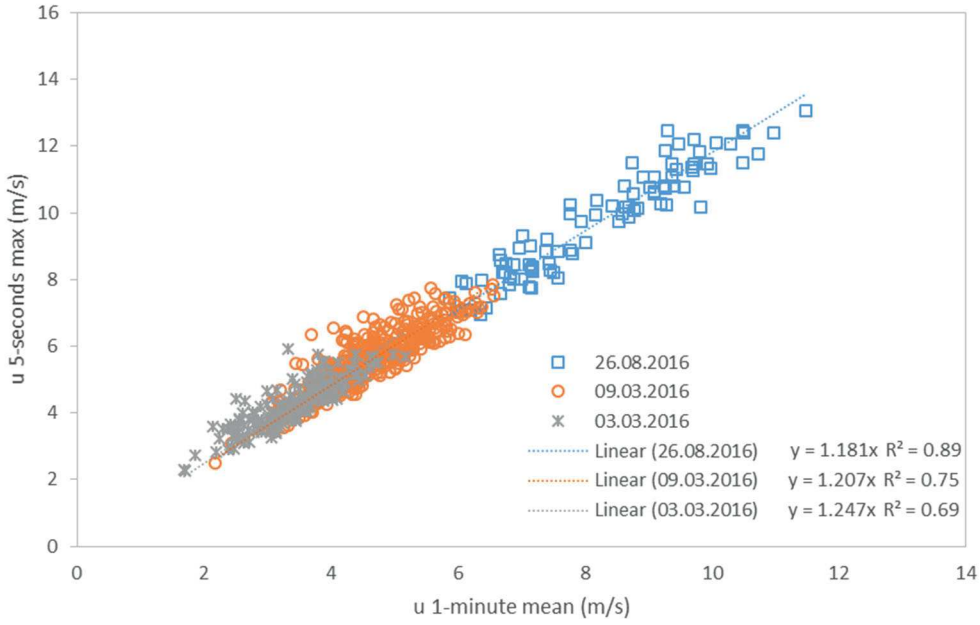

Figure 4. Comparison of the maximum wind velocity of a 5 s interval measured within a one-minute mean.

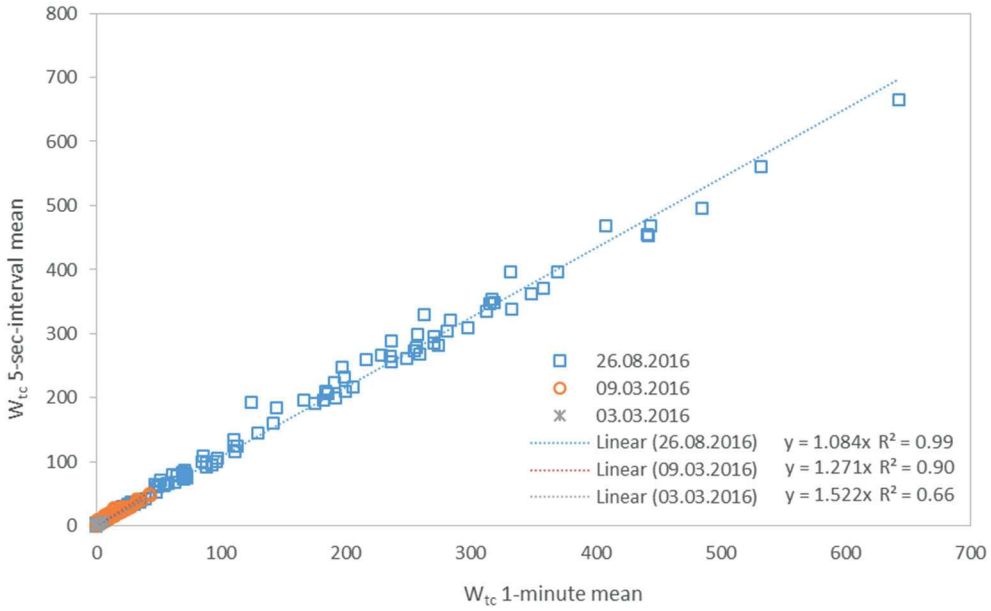

Figure 5. Comparison of the transport capacities of the wind derived from 1 min averages of wind velocity and from the 5 s intervals.

Following the analyses shown here, we conclude that a 1 min averaged measurement of wind speed and particulate matter values is an appropriate approach to quantify wind gust impacts, even though wind gusts itself can partly happen on lower temporal scales. Hence, in the following sections we use 1 min averaged data from three other wind events captured on 18 November 2016, 20 November 2016, and 4 December 2016, subsequently called Event I, Event II, and Event III, respectively (see Siegmund et al. 2022 [33]).

3.2. Impact of Gust Activity on Particle Uptake

Figure 6 illustrates the temporal wind speed variation and marks the gusts by the grey bars following the above definition for all three events. All events have in common that the gusts are relatively homogenously distributed over the event period and that the definition

matches visible peaks. However, a shortcoming of this approach can be identified: if a strong decrease in wind speed is immediately followed by a strong increase, it is not reflected by the averaging interval. Although one would obviously define those periods as gusts/gusty, for the study of wind erosion this is not a problem; we are predominantly interested in the acceleration of wind in comparison to the previous point in time ($t - 1$), not so much in comparison to the following point in time ($t + 1$).

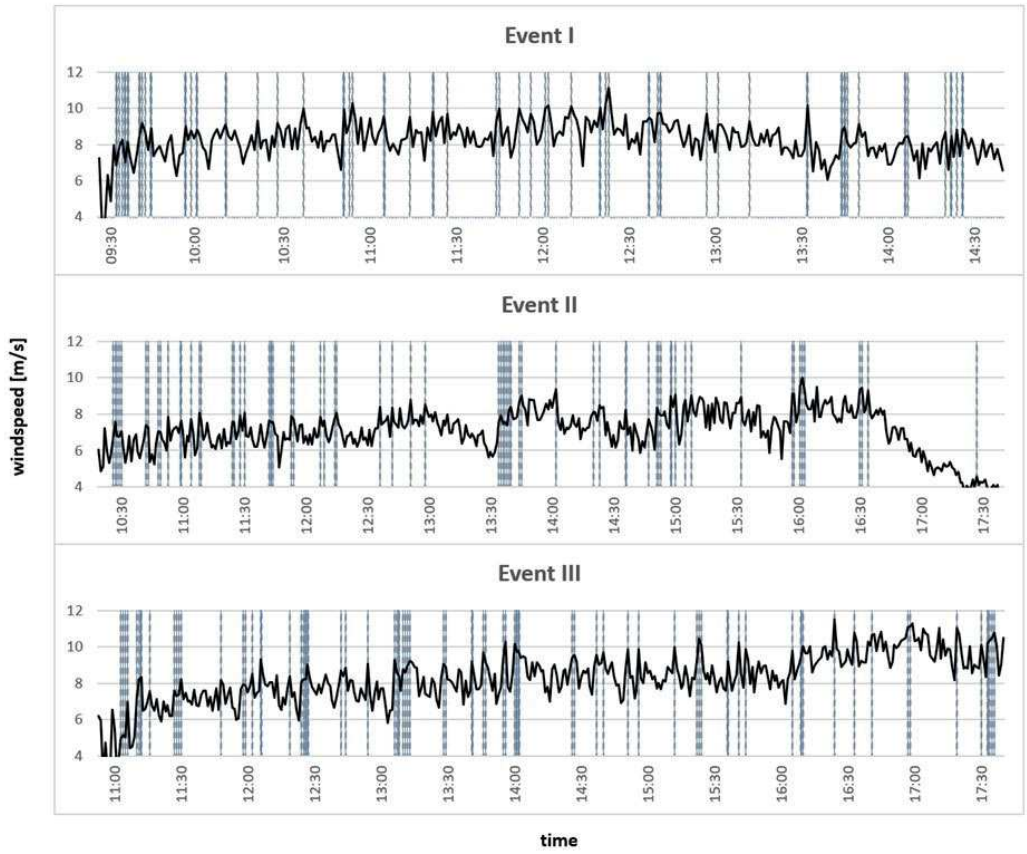

Figure 6. Wind speed during all three events. Grey bulks mark wind gusts following the gust definition described above.

This proposed definition of wind gusts has one sensitive parameter, and this is the chosen GIC value. In this study we chose a GIC value of 1.1 to make sure the events hit all the spikes in the wind time series, which can be seen as a more pragmatic approach. Moreover, this gust definition is only suitable for temporal sampling resolutions of 1 min and higher.

In Siegmund et al. (2022) [33] it was shown that the correlation strength between dust particles and wind velocity decreases with particle size. While in this former analysis only three particle size classes (PM_{10}, $PM_{2.5}$ and PM_1) were investigated, we here increase the resolution of this analysis to the whole spectrum of the EDM. Figure 7 illustrates the linear Pearson correlation coefficients between wind speed and particle concentration of all 31 particle size classes of the EDM. For this analysis, we use the linear correlation for illustration purposes only, leading into the following analyses of wind gust impact. Yet, the assumption of a linear relationship between wind speed and particle uptake cannot be used for quantitative analyses. Siegmund et al. (2022) [33] investigated particulate matter classes, representing clustered particle number concentrations; here, we work with the separated particle counts of each class. A correlation analysis can nevertheless directly be compared because both show a certain measure of dust intensity.

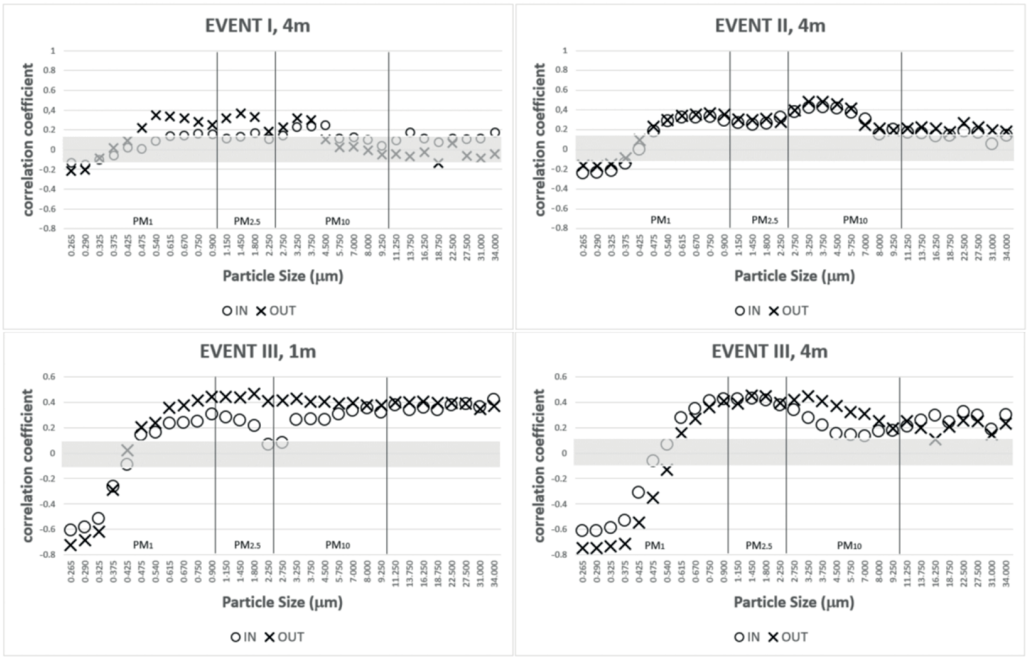

Figure 7. Linear Pearson correlation coefficients for the 1 min measurements between wind speed and particle counts for 31 particle size classes. The grey shadow indicates non-significant correlation coefficients ($\alpha = 0.05$). At Event I and II the 1 m particle count data were lost during the field campaign and cannot be shown here. For comparison reasons, the respective particulate matter classes are also displayed.

Figure 7 resembles the general findings of [33], but here for each individual particle class: bigger dust particles show a mainly strong positive correlation with wind speed; smaller particles show a lower, non-significant, or negative correlation. The detailed view on the particulate matter classes shows that particles in the PM_{10} and $PM_{2.5}$ classes have quite consistent signals. In contrast, the particles smaller than 1 µm diameter (PM_1 class) can further be subdivided into particles with positive or negative correlations, separated at the particle diameter of around 0.5 µm. Only particles smaller than 0.5 µm have non-significant or negative correlations, so that this particle diameter can be seen as a kind of threshold value. At Event III these were very strong, reaching up to −0.8. This event was the strongest of the three considered, and consequently more of the very small particles (PM_1) were already released outside of our measuring plot. These particle sizes are known to stay in suspension for very long times and are removable only by wash out by rain or if they adhere at surfaces by direct contacts. The latter also concerns larger particles in suspension together with these fine fractions, collecting them and depositing together. Because all three events were only relatively weak wind erosion events, the emission of larger particles were also low. Therefore, the very fine particle classes can accumulate along the travelled path in the atmospheric boundary layer (<10 m) even during short calming phases of the wind speed. In these times, they are still present at unchanged concentration, leading to the negative correlation shown in Figure 7. As PM_1 is almost not present in the soil as isolated particles, it needs a releasing process as wind erosion, tillage, or traffic to be dispersed in the air. However, these particles can be rapidly entrained and vertically transported out from the sampling height. There is a significant knowledge gap regarding the interplay between different releasing processes and particle composition at the landscape scale that shall be further addressed in future experiments.

Nevertheless, the correlation pattern as shown in Figure 7 can thus only be found in gusty wind conditions (i.e., high variance in wind speed), and hence, the following chapter discusses the impact of gusts on the particle uptake.

3.3. Wind Speed Variation and Its Impact on Particle Uptake

In Figure 8 the results of the calculations of the Gust uptake Efficiency (GuE) for the three particulate matter classes and for both "IN" and "OUT" stations are shown. At 1 m height, the values generally show larger differences, both between the particulate matter classes and the "IN" and "OUT" positions, whereas the values are generally more balanced in 4 m height. The GuE for all events is clearly over 100% on the 1 m height measurements (except for Event I, "IN") and closer to, yet still over 100% on the 4 m height measurements. This clearly shows that the transports at a height of 1 m can be assigned to the processes of erosion or sedimentation of the measurement field, whereas the particles at the height of 4 m rather originate from sources outside. It is also possible that particles are carried out of the sampling space by turbulent, vertical movement, see [40]. Regarding the particle sizes, a tendency for higher values for bigger particles can be seen, specifically at Events II and III.

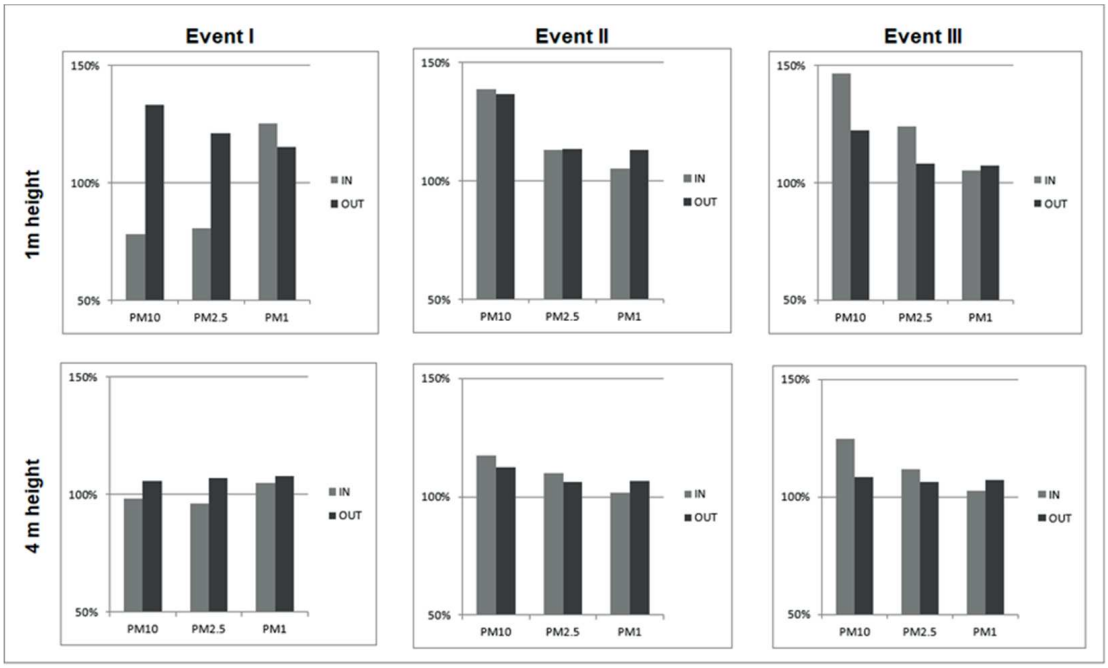

Figure 8. Gust update Efficiency (GuE) for all three events and for the heights of 1 and 4 m, calculated for the three particulate matter classes PM_{10}, $PM_{2.5}$, and PM_1.

A systematic difference between the values for "IN" and "OUT" cannot be seen, this seems to vary among the three events. Other studies such as [41] demonstrated that the total amount of saltating material transported along wind direction continuously increases with field length. In our study, station "OUT" is 160 m further along wind direction than station "IN", being a comparable setting to the setup of sand traps described by [41]. While [41] focused on particle sizes > 62 µm, the EDM devices of this study measured much smaller particles (<32 µm). Hence, from our results we cannot conclude that this effect also propagates through smaller particle sizes, at least not at this spatial scale.

Because the results of Figure 8 are quite heterogeneous between the three events, we increased the temporal resolution of the analysis for Figure 9 and calculated the GuE for 30 min time windows. Since the events occurred over different time spans, this results in 11–15 time windows per event.

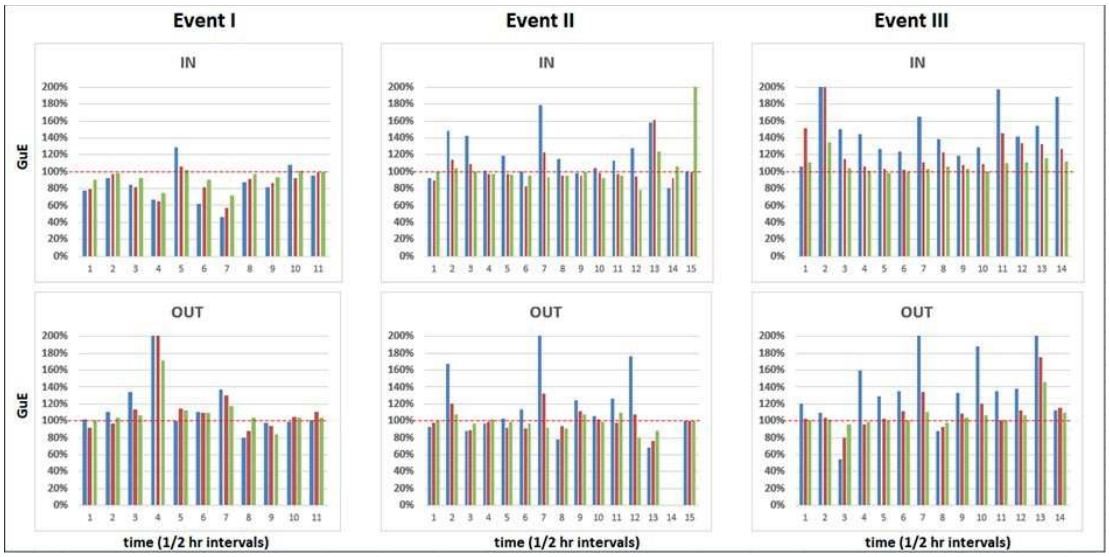

Figure 9. GuE for the three wind events at "IN" and "OUT" in 30 min temporal resolution for PM_{10} (blue), $PM_{2.5}$ (red), and PM_1 (green). The y-axis was limited to 200% for visibility purposes, resulting in sporadic overflows. This has no impact on the general interpretation of the results.

Figure 9 illustrates that the level of GuE is not constantly distributed over an event, but rather fluctuates in wave-like patterns. These wave patterns are equally expressed in the three particle classes. During periods where the GuE is generally above 100%, the coarser particles (PM_{10}) are always more affected by the gusts than the smaller particles. One feature of Figure 9 specifically points out: the dominance of PM_{10} GuE during Event, I. "OUT" ends after three hours (six half-hours intervals). Interval 7–11 PM_{10} has mainly a smaller GuE than the other particle size classes. The general periodicity of particle concentrations in all particle size classes results from the gusty wind conditions.

4. Discussion

In our analyses we found a 20% up to 50% increased particle uptake by gusts over the average emissions for PM_{10}, a 5–25% increase for $PM_{2.5}$, and an up to 10% increase for PM_1 particle concentrations at 1 m height. At the 4 m height this increased gust-induced particle uptake was less expressed. This is because dust in this height is already better sorted than in 1 m height, where saltation and suspension transports superimpose.

When determining the erodible fraction of soils, often wind tunnel experiments and rotary sieves are applied. When comparing the results of these two techniques against field experiments, Ref. [41] found good concordance in quality (positive correlation) but not in quantity. In other words, the erodible fraction was systematically higher at field experiments [42] than in laboratory settings. One reason for that can be observed in Figure 6, the gusty nature of "real" wind. Mostly, in wind tunnel experiments uniform or cascades of incrementally increasing wind speed are used [43–46]. Such approaches are more comparable to conditions with a very constant wind speed, we propose that gusty wind conditions can be considered to obtain comparable outcomes; one option would be wind tunnel experiments with gust simulation (frequently altering wind speeds).

In this study, we could not see a systematically higher dust activity at the "OUT" versus the "IN" station. A previous study [10] proved such an increasing cascade for saltating material. In our setup the distance between our two dust monitors, "IN" and "OUT" was not long enough to also capture that effect in the fine dust particles. Theoretically only emissions from the first third of the measuring field could reach the 4 m height at the "OUT" position 160 m away downwind. Topography was also previously shown to influence the spatial variability of sediment transport [11].

Also, we found the systematic change in dust uptake activity only during Event I where the wind direction is almost perfectly parallel to the plot. These findings lead to the conclusion that for future field experiments, it would be preferable to work on circular fields that have a large enough extension to be able to rotate the orientation of the measurement points according to each wind direction.

Our analyses as well as other studies such as [40] revealed different results for different particle size classes. While these differences were only slightly discussed in this manuscript, we propose to start further investigation on these systematic differences and their implications in future studies. One specific suggestion would be to analyze the proportion of big versus small particles in high resolution, i.e., in addition to the $PM_{10}/PM_{2.5}$ ratio which was suggested by [33], a $PM_1/PM_{0.5}$ ratio can be used because in this study the 0.5 µm threshold was found to separate negative from positive correlation with wind speed.

Finally, we constitute that the Gust uptake Efficiency (GuE) defined in this study is an appropriate measure to quantify the impact of wind gusts on the aerosol uptake during wind events with a high wind speed variability.

Limitations of the New Approach and Scope of Further Investigations

The variable parameter of how exactly a wind gust is defined (in our study as provided at the beginning of Section 3.2) needs to be carefully considered. The problem of a concrete event definition in continuous environmental data was comprehensively discussed in [47], where one possible approach was demonstrated to cover these uncertainties. Although possible, it is beyond the scope of this work to also perform such an extensive data approach which will be part of future investigations, possibly using the CoinCalc R package specifically designed for such purposes (see [48]).

For future studies we also recommend to further investigate how a gust can optimally be defined to best quantify the gust impact on soil erosion, how dust plumes can best be defined from time series, and to possibly apply event synchronization approached (such as, e.g., [49]) between gusts and dust plumes.

A concrete data analytics problem with the suggested approach on event definition is a scenario where the windspeed decreases abruptly and then starts accelerating again. In such a case a possibly evident wind gust directly after this pattern would not be identified as a gust. This happened a couple of times during our experiment, e.g., visible in Figure 6, Event II between 16:00 and 16:30. The same issue can be seen during tendentially decreasing wind velocities, e.g., Event III, between 13:00 and 13:30. The reason for this behavior is that the previously high wind velocities are also part of the mean calculation provided in Equation (3). In order to also capture those events, the average period (here set to $t-10$) would need to be decreased to, e.g., $t-5$. Yet for a data-driven automated approach, this cannot be performed manually and hence a mechanism must be defined to detect these events and automatically adopt the averaging period. In general, an approach making use of an auto-adoptive averaging period can be very promising. One possible approach can be classification methods screening the entire time series for clusters of specific patterns such as "decreasing tendency", "increasing tendency", "mixed", and others. Then, the averaging period for the gust definition can be adopted accordingly.

From a pure data-driven standpoint, combining the two major uncertainties of the suggested approach, the GIC value and the average period for gust definition to define a gust can comprehensively be investigated through the following setup: an analysis looping the entire sequence of analytics (event definition + GuE calculation) through a two-dimensional parameter set, using a range of GIC values and a range of average periods. This would result in a multi-dimensional GuE matrix. An interpretation of this matrix would lead to an "optimal" parameter set to defines maximal GuE. It can be assumed that this optimal set varies for changing meteorological conditions as well as for different soil types, SOM concentrations, and so on.

Author Contributions: Data curation, J.E.P.; Funding acquisition, M.S., D.E.B. and R.F.; Investigation, N.S., J.E.P., F.A., L.A.I. and R.F.; Project administration, M.S., D.E.B. and R.F.; Software, N.S.; Supervision, D.E.B.; Writing-original draft, N.S.; Writing-review and editing, J.E.P., F.A., L.A.I., M.S., D.E.B. and R.F. All authors have read and agreed to the published version of the manuscript.

Funding: This study was supported by the joint project "Multiscale analysis of quantitative and qualitative fine particulate matter emissions from agricultural soils of La Pampa, Argentina" funded by the Deutsche Forschungsgemeinschaft (DFG) of Germany (DFG-GZ: Fu 247/10-1) and the National Council for Research and Technology of Argentina (CONICET).

Data Availability Statement: Not applicable.

Conflicts of Interest: The authors declare no conflict of interest.

References

1. Shukla, P.R.; Skea, J.; Buendia, E.C.; Masson-Delmotte, V.; Pörtner, H.-O.; Roberts, D.C.; Zhai, P.; Slade, R.; Connors, S.; van Diemen, R.; et al. (Eds.) Summary for policymakers. In *Climate Change and Land: An IPCC Special Report on Climate Change, Desertification, Land Degradation, Sustainable Land Management, Food Security, and Greenhouse Gas Fluxes in Terrestrial Ecosystems*; Cambridge University Press: Cambridge, UK, 2019.
2. Knippertz, P.; Stuut, J.-B. *Mineral Dust: A Key Player in the Earth System*; Springer: Berlin/Heidelberg, Germany, 2014; 509p.
3. Steinke, I.; Funk, R.; Busse, J.; Iturri, A.; Kirchen, S.; Leue, M. Ice nucleation activity of agricultural soil dust aerosols from Mongolia, Argentina, and Germany. *J. Geophys. Res. Atmos.* **2016**, *121*, 13559–13576. [CrossRef]
4. Testa, B.; Hill, T.C.J.; Marsden, N.A.; Barry, K.R.; Hume, C.C.; Bian, Q.; Uetake, J.; Hare, H.; Perkins, R.J.; Möhler, O.; et al. Ice nucleating particle connections to regional Argentinian land surface emissions and weather during the Cloud, Aerosol, and Complex Terrain Interactions experiment. *J. Geophys. Res. Atmos.* **2021**, *126*, e2021JD035186. [CrossRef]
5. Goossens, D.; Riksen, M. (Eds.) Wind erosion and dust dynamics at the commencement of the 21th century. In *Wind Erosion and Dust Dynamics: Observations, Simulations, Modeling*; ESW Publications: Wageningen, The Netherlands, 2004; pp. 7–13.
6. Nerger, R.; Funk, R.; Cordsen, E.; Fohrer, N. Application of a modeling approach to designate soil and soil organic carbon loss to wind erosion on long-term monitoring sites (BDF) in Northern Germany. *Aeolian Res.* **2017**, *25*, 135–147. [CrossRef]
7. Iturri, L.A.; Funk, R.; Leue, M.; Sommer, M.; Buschiazzo, D.E. Wind sorting affects differently the organo-mineral composition of saltating and particulate materials in contrasting texture agricultural soils. *Aeolian Res.* **2017**, *28*, 39–49. [CrossRef]
8. Buschiazzo, D.; Zobeck, T.M.; Abascal, S.A. Wind erosion quantity and quality of an Entic Haplustoll of the semi-arid pampas of Argentina. *J. Arid Environ.* **2007**, *69*, 29–39. [CrossRef]
9. Zárate, M.A.; Tripaldi, A. The aeolian system of central Argentina. *Aeolian Res.* **2012**, *3*, 401–417. [CrossRef]
10. Avecilla, F.; Panebianco, J.E.; Buschiazzo, D.E.; De Oro, L.A. A study on the fragmentation of saltating particles along the fetch distance during wind erosion. *Aeolian Res.* **2018**, *35*, 85–93. [CrossRef]
11. Siegmund, N.; Funk, R.; Koszinsky, S.; Buschiazzo, D.; Sommer, M. Effects of low-scale landscape structures on aeolian transport processes on arable land. *Aeolian Res.* **2018**, *32*, 181–191. [CrossRef]
12. Suomi, I.; Lüpkes, C.; Hartmann, J.; Vihma, T.; Gryning, S.-E.; Fortelius, C. Gust factor based on research aircraft measurements: A new methodology applied to the Arctic marine boundary layer. *Q. J. R. Meteorol. Soc.* **2016**, *142*, 2985–3000. [CrossRef]
13. WMO. *Guide to Instruments and Methods of Observation, Volume I—Measurements of Meteorological Variables*; World Meteorological Organization: Geneva, Switzerland, 2018.
14. Harper, B.; Kepert, J.; Ginger, J. Wind speed time averaging conversions for tropical cyclone conditions. In Proceedings of the 28th Conference Hurricanes and Tropical Meteorology, AMS, Orlando, FL, USA, 28 April 2008.
15. Lee, J.A. A field experiment on the role of small scale wind gustiness in Aeolian sand transport. *Earth Surf. Processes Landf.* **1987**, *12*, 331–335. [CrossRef]
16. Durán, O.; Claudin, P.; Andreotti, B. On aeolian transport: Grain-scale interactions, dynamical mechanisms and scaling laws. *Aeolian Res.* **2011**, *3*, 243–270. [CrossRef]
17. Pfeifer, S.; Schönfeld, H.-J. The response of saltation to wind speed fluctuations. *Earth Surf. Processes Landf.* **2012**, *37*, 1056–1064. [CrossRef]
18. Martin, R.L.; Kok, J.F.; Hugenholtz, C.H.; Barchyn, T.E.; Chamecki, M.; Ellis, J.T. High-frequency measurements of Aeolian saltation flux: Field-based methodology and applications. *Aeolian Res.* **2018**, *30*, 97–114. [CrossRef]
19. Comola, F.; Kok, J.F.; Chamecki, M.; Martin, R.L. The intermittency of wind-driven sand transport. *Geophys. Res. Lett.* **2019**, *46*, 13430–13440. [CrossRef]
20. Sterk, G.; Jacobs, A.F.G.; van Boxel, J.H. The effect of turbulent flow structures on saltation sand transport in the atmospheric boundary layer. *Earth Surf. Processes Landf.* **1998**, *23*, 877–887. [CrossRef]
21. Stout, J.E.; Zobeck, T.M. Intermittent saltation. *Sedimentology* **1997**, *44*, 959–970. [CrossRef]
22. Baas, A. Evaluation of Saltation Flux Impact Responders (Safires) for measuring instantaneous aeolian sand transport rates. *Geomorphology* **2004**, *59*, 99–118. [CrossRef]

23. Bauer, B.O.; Yi, J.; Namikas, S.L.; Sherman, D.J. Event detection and conditional averaging in unsteady aeolian systems. *J. Arid. Environ.* **1998**, *39*, 345–375. [CrossRef]
24. Zanke, U. *Grundlagen der Sedimentbewegung (Basics of Sediment Transport), in German*; Springer: Berlin/Heidelberg, Germany; New York, NY, USA, 1982.
25. Stull, R.B. *An Introduction to Boundary Layer Meteorology*; Kluwer Academic Publishers: Dordrecht, The Netherlands; Boston, MA, USA; London, UK, 1988; 666p.
26. Shao, Y. *Physics and Modelling Wind Erosion*; Springer Science & Business Media: New York, NY, USA, 2008.
27. Dupont, S.; Rajot, J.-L.; Labiadh, M.; Bergametti, G.; Alfaro, S.C.; Lamaud, E.; Irvine, M.R.; Bouet, C.; Fernandes, R.; Khalfallah, B.; et al. Dissimilarity between dust, heat, and momentum turbulent transports during aeolian soil erosion. *J. Geophys. Res. Atmos.* **2019**, *124*, 1064–1089. [CrossRef]
28. Schmid, H.; Oke, T. A model to estimate the source area contributing to turbulent exchange in the surface layer over patchy terrain. *Q. J. R. Meteorol. Soc.* **2006**, *116*, 965–988. [CrossRef]
29. Horst, T.W.; Weil, J.C. Footprint estimation for scalar flux measurements in the atmospheric surface layer. *Bound. Layer Meteorol.* **1992**, *59*, 279–296. [CrossRef]
30. Horst, T.W.; Weil, J.C. How far is far enough?: The fetch requirements for micrometeorological measurement of surface fluxes. *J. Atmos. Ocean. Technol.* **1994**, *11*, 1018–1025. [CrossRef]
31. Horst, T.W. The footprint for estimation of atmosphere-surface exchange fluxes by profile techniques. *Bound. Layer Meteorol.* **1999**, *90*, 171–188. [CrossRef]
32. Foken, T. *Micrometeorology*; Springer: Berlin/Heidelberg, Germany, 2008; 328p.
33. Siegmund, N.; Funk, R.; Sommer, M.; Panebianco, J.; Avecilla, F.; Iturri, L.; Buschiazzo, D. Horizontal and vertical fluxes of particulate matter during wind erosion on arable land in the province La Pampa, Argentina. *Int. J. Sediment Res.* **2022**, *37*, 539–552. [CrossRef]
34. de Oro, L.; Buschiazzo, D. Threshold wind velocity as an index of soil susceptibility to wind erosion under variable climatic conditions. *Land Degrad. Dev.* **2018**, *20*, 14–21. [CrossRef]
35. Fryrear, D.W.; Saleh, A.; Bilbro, J.D.; Schomberg, H.M.; Stout, J.E.; Zobeck, T.M. *Revised Wind Erosion Equation (RWEQ)*; Technical Bulletin 1; Southern Plains Area Cropping Systems Research Laboratory, Wind Erosion and Water Conservation Research Unit: Lafayette, LA, USA, 1998.
36. WMO. *Challenges in the Transition from Conventional to Automatic Meteorological Observing Networks for Long-Term Climate Records*; World Meteorological Organization: Geneva, Switzerland, 2017.
37. Harper, B.A.; Kepert, J.D.; Ginger, J.D. *Guidelines for Converting between Various Wind Averaging Periods in Tropical Cyclone Conditions*; World Meteorological Organization: Geneva, Switzerland, 2010.
38. Saxton, K.; Chandler, D.; Stetler, L.; Lamb, B.; Claiborn, C.; Lee, B.-H. Wind erosion and fugitive dust fluxes on agricultural lands in the Pacific Northwest. *Trans. ASAE* **2000**, *43*, 623–630. [CrossRef]
39. Panebianco, J.E.; Buschiazzo, D.E. Effect of temporal resolution of wind data on wind erosion prediction with the Revised Wind Erosion Equation (RWEQ). *Cienc. Del. Suelo* **2013**, *31*, 189–199.
40. Hu, F.; Cheng, X.; Zeng, Q. The Mechanism of Dust Entrainment under Strong Wind with Gustiness. *Procedia IUTAM* **2015**, *17*, 20–28. [CrossRef]
41. Avecilla, F.; Panebianco, J.E.; Mendez, M.J.; Buschiazzo, D.E. PM_{10} emission efficiency for agricultural soils: Comparing a wind tunnel, a dust generator, and the open-air plot. *Aeolian Res.* **2018**, *32*, 116–123. [CrossRef]
42. Zeng, Q.; Cheng, X.; Hu, F.; Peng, Z. Gustiness and coherent structure of strong winds and their role in dust emission and entrainment. *Adv. Atmos. Sci.* **2010**, *27*, 1–13. [CrossRef]
43. Dong, Z.; Liu, X.; Wang, H.; Zhao, A.; Wang, X. The flux profile of a blowing sand cloud: A wind tunnel investigation. *Geomorphology* **2003**, *49*, 219–230. [CrossRef]
44. Avecilla, F.; Panebianco, J.; Buschiazzo, D. A wind-tunnel study on saltation and PM10 emission from agricultural soils. *Aeolian Res.* **2016**, *22*, 73–83. [CrossRef]
45. Panebianco, J.E.; Mendez, M.J.; Buschiazzo, D.E. PM10 Emission, sandblasting efficiency and vertical entrainment during successive wind erosion events: A wind-tunnel approach. *Bound.-Layer Meteorol.* **2016**, *161*, 335–353. [CrossRef]
46. Funk, R.; Papke, N.; Hör, B. Wind tunnel tests to estimate PM10 and PM2.5-emissions from complex substrates of open-cast strip mines in Germany. *Aeolian Res.* **2019**, *39*, 23–32. [CrossRef]
47. Siegmund, J.; Wiedermann, M.; Donges, J.; Donner, R. Impact of temperature and precipitation extremes on the flowering dates of four German wildlife shrub species. *Biogeosciences* **2016**, *13*, 5541–5555. [CrossRef]
48. Siegmund, J.; Siegmund, N.; Donner, R. CoinCalc—A new R package for quantifying simultaneities of event series. *Comput. Geosci.* **2017**, *98*, 64–72. [CrossRef]
49. Donges, J.; Schleussner, C.F.; Siegmund, J.; Donner, R. Event coincidence analysis for quantifying statistical interrelationships between events time series. *Eur. Phys. J. Spec. Top.* **2016**, *225*, 471–487. [CrossRef]

3. Discussion

The combined consideration the of the above chapters brings us back to the original research question stated in the introduction of this thesis:

How do the small-scale geomorphological characteristics of a location, as well as the highly dynamic parameters of a wind event, determine the wind erosion processes across various soil particle size classes, ranging from coarse sand to ultra-fine dust aerosols?

Not surprisingly, this very broad question cannot easily be answered, but we can try to discuss it by addressing the more specific questions and how they were approached by the analyses provided in the contributing publications:

- *Which specific topology parameters are crucial for the saltation processes?*

  With the dense net of measurement equipment to quantify saltation (see Siegmund et al. 2018), it was possible to derive a high-resolution map of erosion and deposition on the study area. It could be shown that areas of erosion and deposition alternate in complex patterns where the change areas of erosion and deposition are closely neighbored on a very small scale. It could be shown that specifically the relative slope direction in terms of "windward" or "leeward" has a clear impact on where soil material is eroded or deposited. To be highlighted here: this happened on a very small vertical scale, the slopes considered here are in a range around 1.2%. And that is how this analysis differs to many others working on aeolian transport and how the latter is influenced by topography where mostly dunes and other geomorphological structures are investigated on a very different (i.e., much higher) scale.

  The other topological features investigated in this analysis, namely slope percentage and the topographic position index did not show statistically robust impacts on the erosion or deposition patterns on that small scale.

- *Can small-scale erosion and deposition patterns originating from saltation be explained by the land surface topology?*

  Making use of the above-described findings, a multiple regression model was setup to try to statistically explain the erosion or deposition patterns. Using the slope direction as sole predictor did not bring statistically significant explanation, and hence other soil factors were added to the model. Finally, a regression model was setup using four

predictors, namely topsoil thickness, topsoil carbon content, total elevation, and slope direction. The combination of those four led to significant correlation coefficients throughout all events, mostly higher than 0.7.

There have been plenty of other attempts to model erosion and deposition patterns, often focusing predictors from pedological parameters only (see e.g., Hong et al. 2014 or Zobek et al. 2013). These studies show explained variances in a similar range to this thesis' results where one important factor often highlighted is the soil water content. This factor was left out in our analysis, because soil water content was considered to be relatively constant over the small plot. Hence, with leaving out this important factor, the presented statistical model gains even more importance because it produces similarly good results like models not leaving out soil water content. This underlines the importance of slope direction to be implemented in other models to explain the variance of erosion and deposition.

Therefore, the answer to this research question is partly "no" because the erosion and deposition patterns could not be explained using only the topology as only predictor.

- *How are the small-scale erosion and deposition patterns linked to the physical and chemical soil parameters?*

  In Siegmund et al., 2018 it was also investigated whether the soil parameters topsoil thickness, carbon content, Nitrogen content and pH value would be linked to the erosion and deposition patterns. Of these, only the topsoil thickness and the carbon content showed significant correlations with the erosion/deposition patterns. The soil texture could not be used for meaningful statistical analyses because the soil grain sizes only varied marginally throughout the plot. The two parameters topsoil thickness and carbon content play an antagonistic role on the investigated plot. While topsoil thickness is statistically linked to higher erosion rates, carbon content rather shows higher deposition rates. This could be interpreted that especially the carbon content is not a driver, but rather a result of ongoing erosion processes. On those parts of the plot where a relatively high carbon content can be found, this carbon may be a result from deposition processes. This could only be the case, if the erosion process would selectively erode and deposit material with higher carbon content, a hypothesis that could not be investigated during this study, because the related laboratory work was not conducted.

Yet, our results show a clear indication and therefore invite future studies to include such laboratory work into the study design.

- *In how far do the horizontal and vertical dust fluxes differ between the different partitions PM_{10}, $PM_{2.5}$ and $PM_{1.0}$?*

  In Siegmund et al., 2022a it could be shown that the horizontal flux of dust is linearly increasing with increasing wind velocity – over all three fractions PM_{10}, $PM_{2.5}$ and $PM_{1.0.}$ The vertical flux, however, showed exponential increase (upward flux) with increasing wind speed for PM_{10} values. This effect yet is already lower for $PM_{2.5}$. And the $PM_{1.0}$ measurements show a decreasing correlation with wind speed, giving evidence for downward directed fluxes of this fraction of dust. This finding was also supported by Siegmund et al., 2022b where an even finer distinguishing between the fractions (32 fractions ranging from 0.26µm to 34µm, i.e., $PM_{0.2}$ to PM_{34}) was performed to derive correlation coefficients between air
  dust and wind speed. Here all partitions smaller than $PM_{0.4}$ showed negative correlations, supporting the interpretation of a downwards flux of these particles with increasing wind speed.
  This finding leads to the conclusion that the contribution of partitions to the total dust load must vary between different heights. Consequently, we calculated the $PM_{2.5}/PM_{10}$ ratio for the two measurement heights of our experiment and showed the typical relative increase of the finer fraction with increasing height, which was already found earlier by, e.g., Carvacho et al. 2004 or Funk et al. 2008.
  Further investigations of the vertical variation of dust composition, especially also taking into account the very find dust $PM_{1.0}$ (which showed the opposite correlation with wind speed) would be of high interest for future experiments. Such experiments then should possibly include a higher vertical measurement resolution, for example installing several sets of measuring equipment at 1m distance between 1m and 6m above ground. The expected findings could then be used to extrapolate the findings of so many wind-tunnel experiments that only consider the immediate above-ground processes.
  Overall, the contribution of the measuring field to the total dust load measured in the lower atmosphere over the plot was very low. This could be shown by calculating the balances of incoming and outgoing fluxes (see Siegmund et al. 2022a). Hence, the

measured total PM concentrations are rather a composition of dust from various sources such as dust from windward plots but also from traffic on unpaved roads, cattle drives or close-by tillage operations. In other words, the dust represents all components the surrounding landscape structure.

This consideration is clearly opposite to what was found for the erosion and deposition patterns investigated in Siegmund et al. 2018, where even small-scale changes in topology and physical soil parameters had strong impact on where the wind process leads to erosion or deposition. These processes are related to the coarser soil fractions - sand and coarser silt.

We can, hence, conclude that the scale of the landscape processes that are related to wind erosion is smaller with coarser soil material, and larger with finer particles. And the finer the particles of interest are, the more we must consider rather the landscape.

- *How should a new statistical measure be defined to quantify the "gust create dust" effect that is observable in situ with a data driven approach?*

When working on the field in La Pampa, taking soil samples, installing measuring equipment and the like, one characteristic of the soil erosion process in that region was omnipresent: dust plumes. Once a wind gust blows across a field, a well visible plume of dust is built and travels across the plot. While this process is well explainable by the given knowledge of how particle uptake is generated (the saltation-induced cascade of fine particle uptake, see, e.g., Houser & Nickling 2001, note that the visible part dust plume mainly consists of the coarser soil fraction, while the actual "dust" consists of the finer particles that are partly not visible by the human eye), a quantitative measure or evidence is still missing in the wider literature. In Siegmund et al. 2022b we introduced a simple novel measure as a first attempt to quantify this process under the given measurement setup. Quantifying gust contribution needs to address two elements: How to define a gust and how does it contribute to the overall dust uptake? The first question had widely been discussed, merely in meteorological literature. These are, yet, widely based on a certain exceedance of a static threshold, such as exceedance of a threshold in comparison to the average wind speed. The limitation of such approaches is that on the one hand, they can only be used for stationary wind speed scenarios without evident mid-term trends and on the other hand they are not suitable for comparisons between events with different absolute levels of average wind speed. Both - non-

stationarity and differing absolute wind speed averages - were evident at the series of events measured in the campaign of this thesis. Also, both these conditions can be assumed to be evident at most other wind events that are investigated in the wind erosion literature. This leads to the necessity of a new, data driven, dynamic and adaptive approach to define *local* wind speed peaks in timeseries of wind speed measurements. We chose the very straightforward technique of a moving average (or "sliding window"), where each value in the time series that exceeds a relative threshold over the precursing moving average is defined as gust. This leads to events in the time series, that may overall seem very different (especially regarding their total value), but are similar in their local setting, i.e., their individual position in the time series (see Siegmund et al. 2022b, equation 3). Similar approaches have earlier been applied in other areas of geosciences, e.g., by Baumbach et al. 2017 and others. The effect of such an event definition for gusts can be well seen in Figure 6 of Siegmund et al. 2022b: sometimes data points are defined as gusts that have wind speeds of over 10m/s, sometimes events with only 5m/s. But what they all have in common is, that they denote clear peaks in their utter surrounding. The mentioned figure, yet also shows one weakness of the approach: not all peaks in the time series that maybe should be classified as event, are captured. One example is a scenario where the wind speed decreases and then quickly starts accelerating again. In such a case a possibly evident wind gust directly after this pattern would not be identified as a gust (a possible approach how to cope with such a problem is suggested in Siegmund et al. 2022b, page 12. Another, even more important limitation of the proposed gust definition is the arbitrarily changeable relative threshold. In our study, we set it to 10%, because empirical tests yielded the "best" results regarding capture of the most peaks in the time series. This problem has already been addressed earlier publications (see, e.g., Siegmund et al. 2016) where the robustness of the results could be shown by applying a range of differing threshold to the same analysis, giving (qualitatively) very similar results.

- *Do gusts extraordinarily contribute to soil particle uptake?*

The answer to this question is clearly "yes", and in Siegmund at al. 2022b it could also empirically be proven and quantified. We introduced the "Gust uptake Efficiency", measure for how much a data point classified as gust event over-proportionally contributes to the total

dust uptake (see Siegmund et al. 2022b, equation 4). Applying this approach to the time series of this field campaign resulted to 20% up to 50% higher dust uptake during gust events in comparison to all other points in time of the respective event. Hence, the new approach not only delivered a quantitative measure for a quantitatively observable phenomenon, but also delivered a new challenge to future studies: the often-conducted wind tunnel experiments largely simulate stepwise increasing wind speeds. Yet (considering what was found in Siegmund et al. 2022) transferring these results to real-life scenarios or even using them for statistical or dynamic modelling must be considered carefully.

4. Summary

Summarizing the considerations and findings of this thesis brings us back to the overarching research question:

How do the small-scale geomorphological characteristics of a location, as well as the highly dynamic parameters of a wind event, determine the wind erosion processes across various soil particle size classes, ranging from coarse sand to ultra-fine dust aerosols?

The contributing publications considered the landscapes as well as soil physical parameters' influence on the erosion processes of the coarse soil partition (Siegmund et al. 2018), the influence of wind speed on the horizontal and vertical fluxes of three different partitions of the fine soil particles in the air (Siegmund et al. 2022a) and the influence of the dynamic patterns of wind events on the temporal variability of dust uptake for a wide range of very fine soil particles (Siegmund et al. 2022b).

All these analyses with their findings and considerations shed more light on how our soils are built and what dynamic aeolian processes shape them. Even if not all questions could be answered and suggested approaches have their limitations, this thesis adds additional pieces to the big puzzle of "how the world works" - hopefully inspires and support other researchers to add on top of these analyses and even more contribute to our understanding of aeolian soil processes.

5. Bibliography

Acosta-Martínez, V., Van Pelt, S., Moore-Kucera, J., Baddock, M. C., & Zobeck, T. M. (2015): Microbiology of wind-eroded sediments: Current knowledge and future research directions. Aeolian Research, 18, 99-113.

Aimar, S. B., Mendez, M. J., Funk, R., & Buschiazzo, D. E. (2012): Soil properties related to potential particulate matter emissions (PM10) of sandy soils. Aeolian Research, 3, 437-443.

Aliaga, V. S., Ferrelli, F., Alberdi-Alganaraz, E. D., Bohn, V. Y., & Piccolo, M. C. (2016): Distribucion y variabilidad de la precipitacionen la region Pampeana, Argentina. Cuadernos de Investigación Geografica, 42(1), 261e280. (In Spanish)

Baumbach, L., Siegmund, J., Mittermeier, M. and R. Donner (2017): Impacts of temperature extremes on European vegetation during the growing season. Biogeosciences, 14, 4891-4903.

Bubenzer, O. (2007): Formbildung durch äolische Prozesse. In: Gebhard, H., Glaser, R., Radtke, U. and Reuber, P. (Eds.): Geographie. Spektrum Akademischer Verlag, Heidelberg 2007. (In German)

Carvacho, O. F., Ashbaugh, L. L., Brown, M. S., & Flocchini, R. G. (2004): Measurement of PM2.5 emission potential from soil using the UC Davis resuspension test chamber. Geomorphology, 59, 75-80.

Casagrande, G., & Vergara, G. (1996): Características climatica de la region. In: D. E. Buschiazzo, J. L. Panigatti, & F. J. Babinec (Eds.), Labranzas en la region semiarida Argentina (pp. 11e19). Instituto Nacional de Tecnologia Agropecuaria (INTA). (In Spanish)

Conen, F., & Leifeld, J. (2014): A new facet of soil organic matter. Agriculture, Ecosystems & Environment, 185, 186-187.

Funk, R., Reuter, H. I., Hoffmann, C., Engel, W. and Öttl, D. (2008): Effect of moisture on fine dust emission from tillage operations on agricultural soils. Earth Surface Processes and Landforms, 33, 1851-1863.

Hong, S.-W., Lee, I.-B., Seo, I.-H., Kwon, K.-S., Kim, T.-W., Son, Y.-H., Kim, M. (2014): Measurement and prediction of soil erosion in dry field using portable wind erosion tunnel. Biosyst. Eng. 118, 68-82.

Houser, C. & Nickling, W. G. (2001): The emission and vertical flux of particulate matter <10 mm from a disturbed clay-crusted surface. Sedimentology, 48, 255-267.

Knippertz, P., & Stuut, J.-B. (2014): Mineral dust. A key player in the earth system. Dordrocht, The Netherlands, Springer Science/Business.

Kuntze, H., Beinhauer, R., Tetzlaff, G. (1990): Quantification of Soil Erosion by Wind: I. Final Report of the BMFT Project. Project No. 0339058 A, B, C. Institute of Meteorology and Climatology, University of Hannover, Germany.

Li, H., Tatarko, J., Kucharski, M., & Dong, Z. (2015): PM2.5 and PM10 emissions from agricultural soils by wind erosion. Aeolian Research, 19, 171-182.

Mendez, M. J., Aimar, S. B., Aparicio, V. C., Ramirez Haberkon, N. B., Buschiazzo, D. E., De Geronimo, E., & Costa, J. L. (2017): Glyphosate and aminomethylphosphonic acid (AMPA) contents in the respirable dust emitted by an agricultural soil of the central semiarid region of Argentina. Aeolian Research, 29, 23-29.

Mirzamostafa, N., Hagen, L. J., Stone, L. R., & Skidmore, E. L. (1998): Soil aggregate and texture effects on suspension components from wind erosion. Soil Science Society of America Journal, 62, 1351-1361.

Panebianco, J. E., Mendez, M. J., & Buschiazzo, D. E. (2016): PM10 emission, sandblasting efficiency and vertical entrainment during successive wind-erosion events: A wind tunnel approach. Boundary-Layer Meteorology, 161, 335-353.

Rezaei, M., Riksen, M. J. P. M., Sirjani, E., Sameni, A., & Geissen, V. (2019): Wind erosion as a driver for transport of light density microplastics. Science of the Total Environment, 669, 273-281.

Shao, Y. (2001): A model for mineral dust emission. Journal of Geophysical Research, 106(D17), 20239-20254.

Siegmund, J., Wiedermann, M., Donges, J. and Donner, R. (2016): Impact of temperature and precipitation extremes on the flowering dates of four German wildlife shrub species. Biogeosciences, 13, 55415555, doi: 10.5194/bg-13-5541-2016.

Siegmund, N., Funk, R., Koszinsky, S., Buschiaazzo, D. E. and Sommer, M. (2018): Effects of low-scale landscape structures on aeolian transport processes on arable land. *Aeolean Research*, 32, 181-191.

Siegmund, N., Funk, R., Sommer, M., Avecilla, F., Panebiaco, J. E., Itturi, L. A., and Buschiazzo, D. E. (2022a): Horizontal and vertical fluxes of particulate matter during wind erosion on arable land in the province La Pampa, Argentina. *International Journal of Sediment Research*, 37, 539-552.

Siegmund, N., Panebiaco, J. E., Avecilla, F., Itturi, L. A., Sommer, M., Buschiazzo, D. E. and Funk, R. (2022b): From Gustiness to Dustiness - The Impact of Wind Gusts on Particulate Matter Emissions in Field Experiments in La Pampa, Argentina. *Atmoshpere*, 13, 1173.

Steinke, I., Hiranuma, N., Funk, R., Höhler, K., Tüllmann, N., Umo, N. S., …Leisner, T. (2020): Complex plant- derived organic aerosol as ice-nucleating particles - more than a sum of their parts? Atmospheric Chemistry and Physics, 20(14), 11387-11397.

Zobeck, T.M., Baddock, M., Van Pelt, R.S., Tatarko, J., Acosta-Martinez, V. (2013): Soil property effects on wind erosion of organic soils. Aeolian Res. 10, 43-51.